Sprouty2 Expression Controls Endothelial Monolayer Integrity and Quiescence

---

Dissertation

zur

Erlangung der naturwissenschaftlichen Doktorwürde (Dr. sc. nat.)

vorgelegt der

Mathematisch-naturwissenschaftlichen Fakultät

der

Universität Zürich

Von

Martin Anton Peier

von

Lostorf, SO

Promotionskomitee

Prof. Dr. Roland Wenger (Vorsitz)

Dr. Rok Humar (Leitung der Dissertation)

Prof. Dr. Edouard Battegay

Prof. Dr. Michael Hall

Zürich, 2012

ACKNOWLEDGEMENTS

It would not have been possible to write this thesis without the help and support of the kind people around me.

First of all, I would like to thank Professor Edouard Battegay for giving me the opportunity to carry out my thesis in his laboratory. His enthusiasm and generosity encouraged me to work hard and creatively.

I owe many thanks to my supervisor Dr. Rok Humar for supporting me scientifically during my thesis and for being a good friend throughout the years.

My sincere thanks go to Gerhard Christofori and Miguel Cabrita who provided helpful inputs to my thesis work.

Professor Roland Wenger deserves special thanks for critical and helpful discussions and for being my faculty representative. I would also like to thank Professor Patrick Küry for being the external expert and Professor Michael Hall for being a member of my thesis committee. I am grateful to Professor Christian Grimm for participating in my thesis defense.

Many thanks go to all the former and present lab members and the administrative staff of the Vascular Biology Laboratory for all kinds of support, advice and discussions. Special thanks go to Ina Kalus and Marlen Damjanovic for many creative coffee breaks, to Ana Isabel Perez Dominguez for technical assistance, to Elvira Haas for scientific discussions and to Mirjam Sollberger and Claudia Weiss for their administrative support.

Particular thanks are devoted to Indranil Bhattacharya who supported and motivated me during the final spurt of my thesis.

I deeply thank Thomas Walpen for his friendship, and the good time we spent together during and after the work. A problem shared is a problem halved!

I am grateful to all my friends who make my life splendid outside working.

My sincere love goes to Monika Güntensperger for her friendship and patience, and for bringing a lot of sunshine into my life.

Finally, I am deeply grateful to my parents and to Monika’s parents for their continuous support. At the same time, I feel very grateful to my sister and my brother and all the people I know who supported me during my time as a PhD student.

TABLE OF CONTENTS

1 ZUSAMMENFASSUNG

Gefässwandzellen, auch bekannt als Endothelzellen, kleiden die innere Wand aller Lymph- und Blutgefässe aus und bilden dabei eine äusserst kompakte Einzelzellschicht (auch Monolayer genannt). In gesunden Erwachsenen teilen sich nur gerade 0.01 % der Endothelzellen, während sich die anderen 99.99 % in einer Ruhephase (auch Quiescence genannt) befinden. Dabei sind die Zellen äusserst resistent, sowohl gegen den programmierten Zelltod (Apoptose) wie auch gegen Einflüsse wachstumsfördernder Faktoren [1]. Dieser physiologische Zustand der Endothelzellen ist von zentraler Bedeutung für die gesamte Blutversorgung und muss ständig vom Körper überwacht und aufrechterhalten werden [2, 3]. Störungen dieser endothelialen Barriere stehen dann auch in Verbindung mit verschiedenen Krankheiten wie Arteriosklerose und Krebs [4].

Man nimmt an, dass Zell-Zellkontakt-Moleküle das Wachstum inhibieren wenn die Zellen dicht sind und sich berühren. Wahrscheinlich werden dadurch Signalkaskaden reguliert, wie zum Beispiel die Rezeptor-Tyrosinkinasen (RTK) [5].

Die Sprouty (SPRY) Proteine sind wichtige Hemmproteine von RTK-induzierten Signalkaskaden, die unter anderem die MAPKinase ERK1/2 aktivieren. Das in Blutgefässen stark exprimierte SPRY2 Protein reguliert MAPK Signalkaskaden in der embryonalen Entwicklung [6, 7], in der Organ Bildung [8] und auch während der Angiogenese [9]. In Endothelzellen wird SPRY2 durch FGF2 induziert und wirkt danach als Feedbackinhibitor von derselben Signalkaskade [10]. Es ist aber unbekannt, ob SPRY2 und seine Funktion in die Zellkontakt-Inhibition involviert sind.

In dieser Doktorarbeit untersuchen wir daher den potentiellen Einfluss von SPRY2 auf die Bildung eines funktionellen Monolayers, welcher aus primären Mäuseaorta Endothelzellen (MAECs) besteht. Insbesondere haben wir uns für den Mechanismus interessiert, der es den Endothelzellen erlaubt, eine erhöhte Dichte an Zellen wahrzunehmen und darauf adäquat zu reagieren. Das heisst, die Zellen stoppen die Proliferation/Migration und bilden stattdessen einen kompakten Monolayer.

Mit einer Serie von Experimenten versuchten wir herauszufinden, ob die Expression vom SPRY2 von der Zelldichte beeinflusst wird. Dafür wurden MAECs zuerst dünn ausgesät und so lange kultiviert, bis sie schliesslich nach vier Tagen einen dichten Monolayer gebildet hatten. Nach einem Tag zeigten die Zellen eine dünn besiedelte

Kultur, die kaum SPRY2 Proteine produzierte. Nach 48 Stunden wiesen die Zellen eine erhöhte Zelldichte auf und exprimierten eine beachtliche Menge an SPRY2. Schliesslich, nach 72 bis 96 Stunden, waren die Zellen grösstenteils dicht und stellten grosse Mengen an SPRY2 her. Diese stark erhöhte SPRY2 Proteinmenge korrelierte mit reduzierter ERK1/2 Phosphorylierung.

Insbesondere nach 48 Stunden war der Anstieg von SPRY2 von einer erhöhten Expression des Hypoxie-Induzierbaren Faktors 1α (HIF-1α) begleitet. Eine Echtzeitmessung des Sauerstoffgehalts bestätigte, dass die Kultur von dicht wachsenden Zellen einen erhöhten Sauerstoffverbrauch vorwies, der nach 48 Stunden sein Maximum erreichte. Weitere Experimente zeigten dann, dass SPRY2 Protein (nicht die *Spry2* mRNA) durch künstlich herbeigeführte Hypoxie erhöht werden konnte. Wurden dichte Endothelzellen in einer Hungerlösung (Medium ohne Kälberserum) kultiviert, senkte sich der Sauerstoffverbrauch der Kultur wodurch die Hypoxie verschwand. Interessanterweise blieben die Mengen an SPRY2 Protein auch in einer dichten und normoxischen Kultur stark erhöht (75-mal mehr SPRY2 Protein als in einer dünnen Kultur). Diese Resultate wiesen auf einen zusätzlichen, Hypoxie-unabhängigen Mechanismus hin, der für die Stabilisierung von SPRY2 in dichten Zellkulturen mitverantwortlich sein muss, nämlich Zell-Zellkontakte. Tatsächlich, wenn die Kalzium abhängige Zell-Zellkontakte durch EGTA aufgebrochen wurden, verschwand die SPRY2 Proteine (nicht die *Spry2* mRNA) innerhalb von 30 Minuten. Umgekehrt, beim Austausch der EGTA Lösung durch normales Medium, bildeten sich neue Zell-Zellkontakte und SPRY2 konnte wieder nachgewiesen werden.

In einem nächsten Schritt verglichen wir die Fähigkeit von SPRY2-exprimierenden MAECs (*Spry2*$^{fl/fl}$) mit solchen die kein SPRY2 Protein vorwiesen (*Spry2*$^{-/-}$). Wir konnten zeigen, dass in Anwesenheit des Wachstumsfaktors FGF2, die *Spry*$^{-/-}$ MAECs keinen funktionellen Monolayer bilden können. Diese Zellen wiesen eine erhöhte ERK1/2 Aktivität auf, teilten sich unkontrolliert und nahmen eine spindelähnliche Form an. Die normale Morphologie des Monolayers konnte schliesslich durch eine Inhibierung der ERK1/2 Aktivität wiederhergestellt werden.

Mit dieser Dissertation zeigen wir einen neuartigen Mechanismus, durch welchen die monozelluläre Endothelschicht in Blutgefässen stabil wird und bleibt. Dabei wird das SPRY2 Protein benötigt, um die Zellteilung zu stoppen wenn die Endothelzellen hohe Dichten erreichen. Durch die Inhibierung der FGF2-ERK1/2 Signalkaskade trägt SPRY2 dazu bei die endotheliale Barriere zu bilden und aufrechtzuerhalten.

2 SUMMARY

Arranged in a tight monolayer, endothelial cells line the inner wall of all blood and lymphatic vessels. In the healthy adult, only 0.01% of the endothelial cells are dividing. The other 99.99 % endothelial cells show a physiological state, where they resist apoptosis and remain quiescent even in the presence of angiogenic factors [1]. This highly functional endothelial monolayer allows mature blood vessels to control vessel wall permeability and supply the organs with oxygen and nutrients [2, 3]. However, this physiological state (defined as vascular integrity) needs to be actively maintained [3]. Disturbed integrity of the endothelial monolayer contributes to the pathogenesis of several diseases including atherosclerosis and cancer [4].

Several surface molecules associated with adherens and tight junctions have been implicated in mediating cell-contact inhibition (cells undergo growth arrest when they come into contact with each other) and vascular integrity through the regulation of intracellular signaling cascades such as receptor tyrosine kinase (RTK) signaling [5].

The Sprouty (SPRY) family of proteins is an important class of negative regulators of RTK dependent MAPK activation. Sprouty2 (SPRY2), the SPRY family member with high expression in endothelial cells [9], modulates MAPK-signaling in embryogenesis [6, 7], organ development [8], and angiogenesis [9]. In endothelial cells, SPRY2 is induced by FGF2 and inhibits FGF2-stimulated growth and sprouting by inhibiting the MAPK extracellular signal-regulated kinase 1/2 (ERK1/2) [10]. However, it remains unknown whether contact inhibition involves SPRY2 function.

In this thesis, we have therefore examined the potential role of Sprouty2 (SPRY2) in the formation maintenance of a functional, quiescent monolayer in mouse aortic endothelial cells (MAECs) in vitro. We were particularly interested of how endothelial cells process signals arising from increasing cell density to allow a switch from a proliferative, migratory phenotype to a quiescent, impermeable monolayer.

To investigate whether cell density affects SPRY2 expression, we have monitored the protein expression levels of SPRY2 in MAECs growing from an initially sparse culture to a confluent monolayer over a time period of four days. Nearly absent in sparse cells (24 hours after plating), SPRY2 protein expression markedly increased when cells were sub-confluent (after 48 hours) and peaked when cells showed confluence (72 to 96 hours after plating). Cell density induced SPRY2 also correlated

with decreased FGF2-induced ERK1/2 phosphorylation. The increase in SPRY2 protein expression was accompanied by elevated hypoxia-inducible factor 1α (Hif-1α) expression when cells were growing to confluency. Real-time measurement of oxygen levels in MAECs confirmed that the O_2 consumption peaked after 48 hours creating local hypoxia in the endothelial layer. SPRY2 protein but not mRNA levels increased when cells were grown in hypoxia (1% O_2). Thus, hypoxia drives SPRY2 protein induction on a posttranscriptional level.

However, when serum starvation of the MAECs restored normal oxygen levels, SPRY2 expression remained at high levels (~75 fold induction) in confluent compared to sparsely plated cells. These observations pointed to an additional mechanism which stabilized SPRY2 protein expression at high cell densities: intact cell-cell contacts. Indeed, SPRY2 protein but not mRNA expression vanished when Ca^{2+}-dependent cell-cell contacts were disrupted by ethylene glycol tetraacetic acid (EGTA). Conversely, removing EGTA restored cell-cell contacts and SPRY2 protein expression.

Finally, we demonstrate that dense *SPRY2*$^{-/-}$ MAECs were incapable of forming a functional endothelial monolayer in the presence of FGF2: *SPRY2*$^{-/-}$ MAECs exhibited spindle-like shapes and generated a highly permeable cell layer with a ~4 fold increase in permeability compared to wild type cells. In addition, dense *SPRY2*$^{-/-}$ MAECs exhibited a twofold increase in ERK1/2 activity, did not become quiescent and continued to proliferate at confluence. As a consequence, when inhibiting ERK1/2 activity by UO126, *SPRY2*$^{-/-}$ cells regained the capacity of forming a wild type cobblestone shaped endothelial monolayer.

Thus, with this PhD thesis we show a novel mechanism how vessels achieve and maintain vascular stabilization , specifically that cell density-induced SPRY2 is required to establish endothelial quiescence and barrier integrity through the inhibition of FGF2-ERK1/2 signaling.

3 INTRODUCTION

3.1 Vascularization of the embryo

In early embryonal development, oxygenation of a cell aggregate can be maintained by diffusion of molecular oxygen (O_2) [11]. At a critical tissue size a vascular system has to be created to keep up O_2 supply for each cell and forming tissue. Therefore the growth of the vascular tree tightly accompanies embryonic development. The newly formed vessels provide oxygen, nutrients and growth factors and thereby promote growth and morphogenic maturation of the developing organs [11].

Vasculogenesis, the formation of new blood vessels when there are no pre-existing ones, initiates embryonic vascular growth. During vasculogenesis endothelial progenitors (angioblasts) are recruited from various embryonic regions. These angioblasts proliferate, migrate and differentiate into endothelial cells, which eventually give rise to a primitive vascular network composed of small capillaries [12, 13].

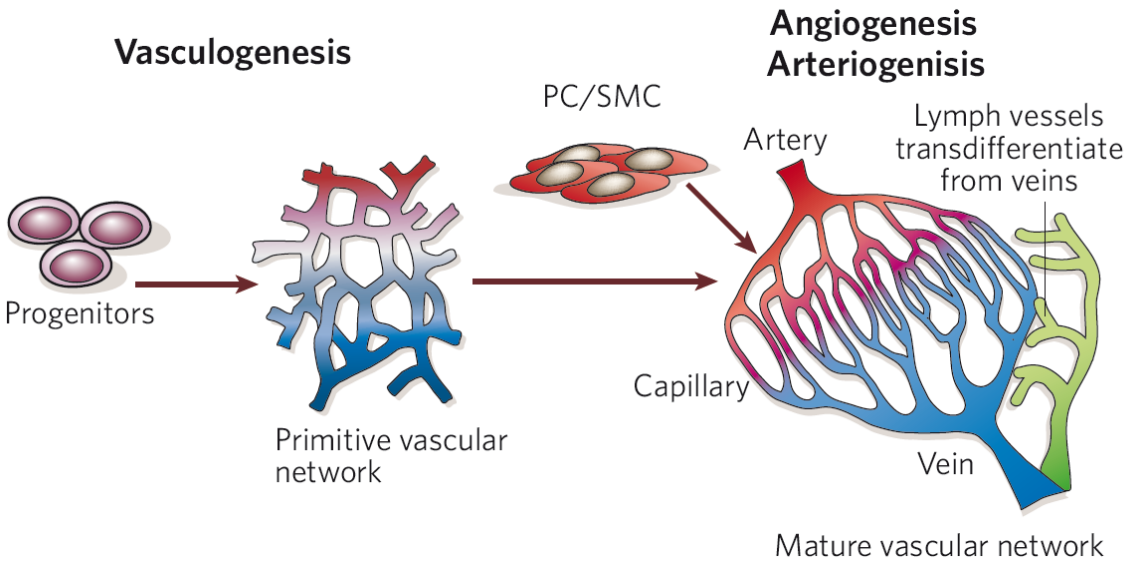

Figure 1. Vascular development in the embryo. Development of the vascular systems: during vasculogenesis, endothelial progenitors give rise to a primitive vascular labyrinth of arteries and veins; during subsequent angiogenesis, the network expands, pericytes (PCs) and smooth muscle cells (SMCs) cover nascent endothelial channels, and a stereotypically organized vascular network emerges. Lymph vessels develop via trans-differentiation from veins [11, 14].

Distinct signals specify arterial or venous differentiation [15]. Angiogenesis, the sprouting of preexisting vessels, ensures expansion of the vascular network [16-18]. Attracted mesenchymal stem cells and neurocrest cells differentiate into vascular smooth muscle cells (VSMCs) and pericytes (VSMCs like cells) and stabilize the developing vessels [14] (Fig. 1).

3.2 Angiogenesis in adults

In the adult, most vessels remain quiescent and only 0.01 % of the endothelial cells are dividing. Angiogenesis occurs regularly only during wound healing, in the buildup of the endometrium during the ovarian cycle and in the placenta during pregnancy [11]. However, ECs keep their ability to divide rapidly in response to a physiological stimulus and are able to revascularize the damaged tissue after an injury. Angiogenesis begins when a quiescent microvessel is activated by angiogenic stimului, such as VEGF, Ang-2, FGFs or hypoxia [11]. The activated vessel eventually dilates, endothelial cells loosen their junctions and pericytes detach from the vessel wall. Matrix metalloproteinases (MMPs) degrade the basement membrane allowing ECs to migrate in response to chemotactic signal. VEGF increases the permeability of the endothelial cell layer and allows the plasma proteins to extravasate form the vessel. The resulting provisional extracellular matrix provides a scaffold for the endothelial migration columns [16]. A concentration gradient of VEGF selects a tip cell which then leads the way of the migrating column. To prevent endothelial cells from moving en masse towards the angiogenic stimulus, the tip cell immediately inhibits tip cell phenotype of its neighboring cells predominantly via DLL4-Notch signaling converting them to stalk cells. The main task of the stalk cells is to elongate the sprout by proliferation and to finally form a lumen [16]. A basement membrane forms and pericytes as well as smooth muscle cells attach to newly formed vessel. Blood-vessel sprouts will then fuse with other sprouts to build on new circulatory systems. In contrast to tip and stalk cells, phalanx cells increase quiescence in the presence of VEGF [19]. They express a soluble form of the VEGF receptor 1 (sFLT1). sFLT1 acts as a VEGF trap to counteract the tip cell-inducing activity of VEGF, thereby preventing the formation of excessive branches [20, 21] (Fig. 2).

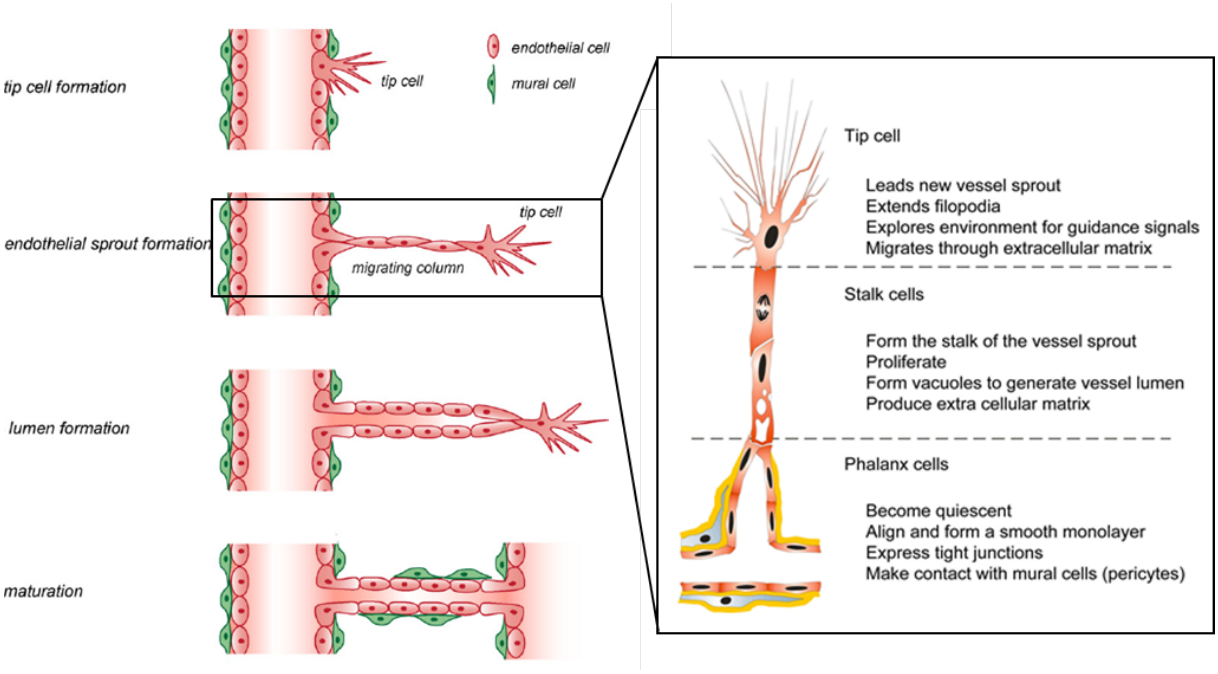

Figure 2. Schematic representation of the angiogenic process. Angiogenesis starts from pre-existing vessels with the conversion of a previously quiescent EC into a tip cell. The tip cell forms filopodia to probe the surrounding environment and to migrate towards the angiogenic stimulus. Stalk cells proliferate to prolong the column, merge and form vacuoles to give rise to the vascular lumen. The newly formed vessel finally undergoes stabilization and maturation via intercellular adhesion and mural cell coverage. The phalanx cells remain quiescent and prevent the formation of supernumerary branches (adapted from [22]).

3.3 Maturation and stabilization of newly formed blood vessels

Vessel maturation – the stepwise transition from an actively growing vascular bed to a quiescent, mature network – involves suppression of endothelial proliferation, migration and sprouting, and stabilization of the nascent vascular tubes via incorporation of mural cells into the vessel wall [23, 24].

Sprouting endothelial cells release platelet-derived growth factor-B (PDGFB) that attract co-migrating pericytes (smooth muscle-like cells), which in turn express PDGFBR. Pericytes establish direct cell–cell contact with ECs to cover capillaries and immature blood vessels and regulate morphology and function of the vessels [25, 26]. Endothelial cells (ECs) release transforming growth factor-β1 (TGFβ1) to promote the differentiation of progenitor cells into VSMCs [40, 41]. VSMCs form layers around mature and larger diameter vessels, such as arteries and veins, and are separated from the endothelium by a basement-membrane layer [14, 27].

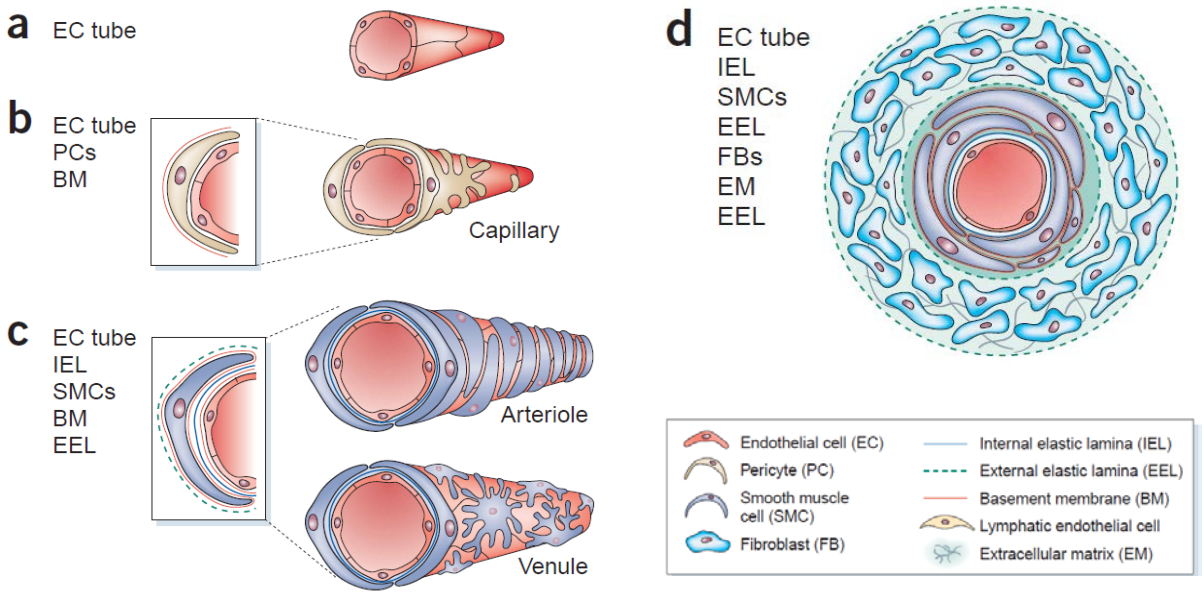

Figure 3. Wall composition of nascent versus mature vessels. (**a**) Nascent vessels consist of a tube of ECs. These mature into the specialized structures of capillaries, arteries and veins. (**b**) Capillaries consist of ECs surrounded by basement membrane and a sparse layer of pericytes embedded within the EC basement membrane. (**c**) Arterioles and venules have an increased coverage of mural cells compared with capillaries. Pre-capillary arterioles are completely invested with vascular SMCs that form their own basement membrane and are closely packed and tightly associated with the endothelium. (**d**) The walls of larger vessels consist of three specialized layers: an intima composed of endothelial cells, a media of VSMCs and an adventitia of fibroblasts, together with matrix and elastic laminae. VSMCs and elastic laminae contribute to the vessel tone and mediate the control of vessel diameter and blood flow [23].

3.4 Arteriogenesis – vessels adapt to their requirements

The complexity of our cardiovascular system calls for a variety of different vessels. Starting from the capillaries that reach every single cell and are so tiny, only one blood cell can move through them at a time, and ending up with the aorta which allows the heart to pump 5-6 liters of blood every minute into the systemic circuit [1]. The cardiovascular system is composed of the heart and circulatory system which can be divided into the pulmonary circuit and the systemic circuit. In the pulmonary circuit, the right ventricle pumps oxygen-poor blood through the pulmonary artery to the lungs. The pulmonary vein returns the oxygen-rich blood to the left ventricle. The large, highly pressurized system is responsible for the systemic distribution. It starts with the left ventricle, pumping oxygenated blood through the aorta, large arteries,

small arteries, arterioles, and the capillary system where the gas and metabolic exchanges take place, then venules, small veins, and large veins ending with the right heart completing the circulatory system [1].

Arteriogenesis describes the remodeling adaption of pre-existing vessels to the corresponding requirements. Physical forces such as blood flow, blood pressure and shear stress stimulate arteries to increase their luminal diameter. Smooth muscle cells proliferate and surround the vessels in several layers to increase their stability necessary to withstand the blood pressure [28, 29].

Venules have irregularly arranged pericytes and are composed of thinner EC walls with valves to prevent backflow of blood. Capillaries are the most abundant vessels in our body and are covered by a sparse layer of pericytes. Because of their wall structure and large surface-area-to-volume ratio, these vessels form the main site of exchange of nutrients between blood and tissue [23]. Depending upon the organ or tissue, the capillary endothelial layer is continuous (as in muscle), fenestrated (as in kidney or endocrine glands) or discontinuous (as in liver sinusoids). The endothelium of the blood-brain barrier or and the blood-retina barrier are further specialized to include high numbers of tight junctions, and are thus virtually impermeable to various molecules [1, 23].

3.5 The hypoxic response via HIF-1α

Oxygen-sensing mechanisms help mammals to quickly adapt to hypoxia, by increasing respiration, blood flow, erythrocyte count and angiogenesis [30]. During normoxic conditions, prolyl hydroxylases (PHDs) hydroxylate specific proline residues in HIF target proteins, marking them for recognition by the von Hippel-Lindau (VHL) E3 ubiquitin ligase complex, which subsequently leads to proteasomal degradation of the HIF-1α subunit. Three prolyl hydroxylases (PHD1, PHD2 and PHD3) have been identified, but PHD2 predominantly regulates basal HIF-1α levels under normoxic conditions [31].

Under aerobic conditions the dioxygenases utilize O_2 as substrate. One oxygen atom is inserted into the HIF-1α prolyl residue to form 4-hydroxyl group and the other oxygen atom is inserted into the co-substrate α-ketoglutarate, forming succinate and CO_2 as side products [31]. Low O_2 levels inactivate PHD and therefore stabilize HIFs [32]. The stabilized HIF-1α subunits form heterodimers with the constitutively ex-

pressed and oxygen independent HIF-1β subunit. The heterodimeric transcription factor activates the expression of many angiogenic genes and thereby initiates angiogenesis (Fig. 4).

Under normoxic conditions, HIF proactively increases in response to growth stimuli, since enhanced proliferation eventually leads to higher oxygen consumption [33]. The growing cell thus profits from an anticipatory increases in HIF-dependent target gene expression.

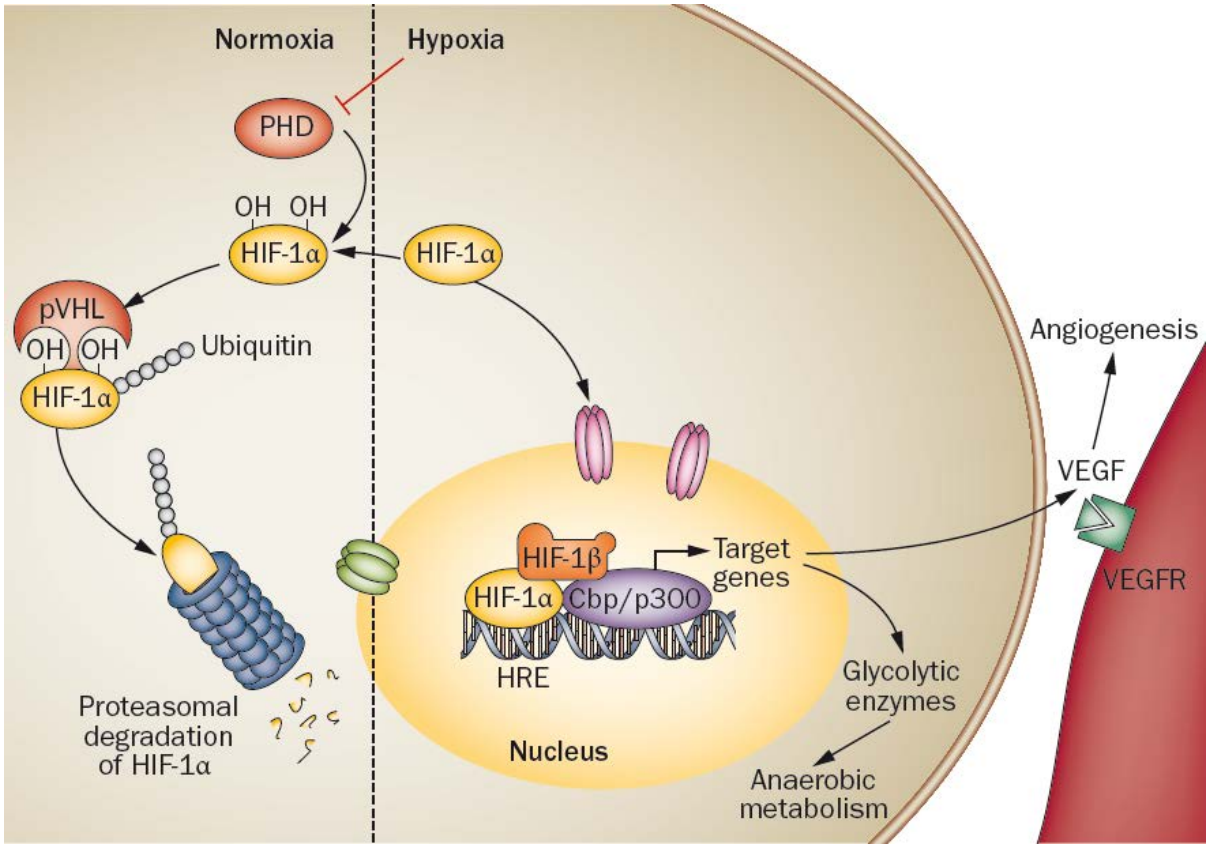

Figure 4. Molecular mechanisms of HIF-1α regulation. In normoxia, the cellular oxygen sensors (PHDs) hydroxylate specific proline residues (Pro402 and Pro564) of HIF-1α, leading to its proteasomal degradation mediated by pVHL, an E3 ubiquitin ligase. During hypoxia, HIF-1α is not ubiquitinylated or degraded, and acts as a transcription factor that binds to HREs to induce expression of a plethora of target genes, including VEGF, which promotes angiogenesis, and genes involved in anaerobic metabolism [34].

3.6 Physiological, pathological and therapeutic angiogenesis

Physiological angiogenesis is temporally limited, and exclusively occurs when needed. By contrast, tumors angiogenesis can persist for years and is morphologically and functionally abnormal. The tumor vasculature for example is characterized by dilated and elongated vessel shapes, leaky sprouts, and decreased vessel density. This abnormal vessel architecture is due to the continuous and excessive release of growth factors in solid tumors [11]. In age-related macular degeneration, abnormal growth of leaky blood vessel causes loss of vision due to bleeding which irreversibly damages photoreceptors. In atherosclerosis, uncontrolled neovascularization in plaques promotes growth and destabilizes plaque structure [35]. Several drugs have been designed that counteract excessive pathological angiogenesis: the most famous drugs Avastin® and Lucentis® target the VEGF system and are successfully used to treat cancer and certain retinopathies such as age-related macular degeneration [36]. Insufficient vessel growth and abnormal vessel regression on the other hand not only cause heart and brain ischemia, but can also lead to neurodegeneration, hypertension, respiratory distress, osteoporosis and other disorders. Pro-angiogenic molecules such VEGF and FGF are still considered as potential drugs to treat ischemia with therapeutic angiogenesis [37, 38], in spite of disappointing early clinical trials results.

3.7 In-vitro angiogenesis

Studying angiogenesis in-vitro reduces the number of animals used for in-vivo experiments. Capillary-like sprouts emerging in these cultures represent early to midterm steps of angiogenesis and can be quantified to study potential angiogenic compounds and underlying mechanisms [39]. Nicosia et al. embedded rat aortic rings in fibrin or collagen gels supplemented with an optimized endothelial growth medium. The endothelial cells generated branching microvessels in the absence of serum or other soluble protein supplements. The angiogenic response was quantitated by counting the newly formed microvessels in the living cultures [40]. Also little squares of thoracic aortas can be placed onto the gels endothelium facing down and covered with collagen or fibrinogen [41]. Furthermore, small pieces of left ventricular myocardium can be cultured in three-dimensional fibrin gels and emerging endothelial

sprouts studied by morphometry [42] (Fig. 5A). Instead of tissue pieces, endothelial cell spheroids embedded in collagen matrix can also be used to investigate emerging capillary-like structures [43-45] (Fig. 5B).

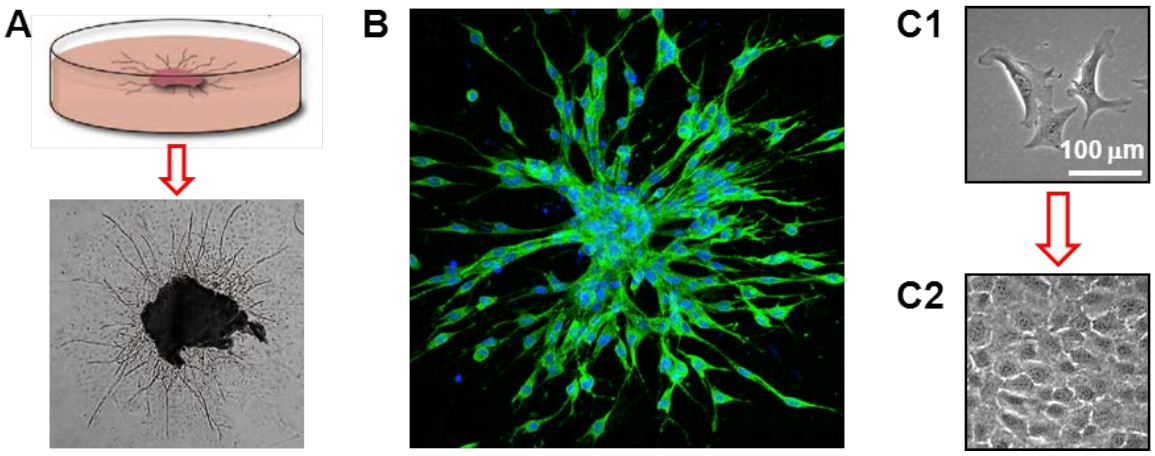

Figure 5. In vitro angiogenesis. (A) Three-dimensional *in vitro* angiogenesis assay using heart or aortic tissue in fibrin gels. Capillary tubes bifurcate and give rise to a primitive capillary tube network. (A, lower panel) (adapted from [39]). (B) Sprouting angiogenesis. Spheroids of ca. 400 endothelial cells were mixed with collagen and stimulated with growth factors to obtain outgrowth of endothelial sprouts. (C1,C2) Endothelial cells in culture display both the 'activated' and 'quiescent' endothelial phenotype [2]. The behaviour of growing 'angiogenic' cells compares to that of an in vitro sparse culture (C1), whereas a tight monolayer of cultured endothelial cells arranged in a cobblestone morphology demonstrates quiescence (C2).

3.8 The Endothelial monolayer

The endothelium is a monolayer of cells that form a continuous layer on the intimal surface of the entire cardiovascular system, including the arteries, veins, and chambers of the heart (endocardium) [46].

Interendothelial junction structures maintain the integrity [2] of the endothelium but also allow the endothelial layer to act as a selective barrier controlling permeability and transport of solutes and macromolecules across the vascular wall [47]. Beside its barrier function, the endothelium helps to control the maintenance of a non-thrombogenic surface, leukocyte adhesion, and angiogenesis. Furthermore, the endothelial cells control the proliferation and the contraction of the underlying vascular smooth muscle cells by producing nitric oxide and other regulatory factors, thereby contributing to the local regulation of the vasomotor tone [48].

The observation that endothelial cells line the inner wall of all blood and lymph vessels as a tight monolayer led to the view that endothelial monolayers can be studied in-vitro in two-dimensional systems. When plated at sparse conditions, endothelial cells behave like growing ‘angiogenic’ cells when stimulated with growth factors (Fig. 5C1). Plated at confluence, endothelial cells form a tight monolayer arranged in a cobblestone like morphology comparable to quiescent endothelial cells in a mature vessel [2] (Fig. 5C2).

Endothelial cultures are used to study many different vascular functions such as vascular integrity and permeability [49-51], responses to all kinds of physiological stimuli, functions related to vessel remodeling and angiogenesis, and interactions with other cells such as smooth muscle cells, pericytes, leukocytes and tumor cells (summarized in [52]).

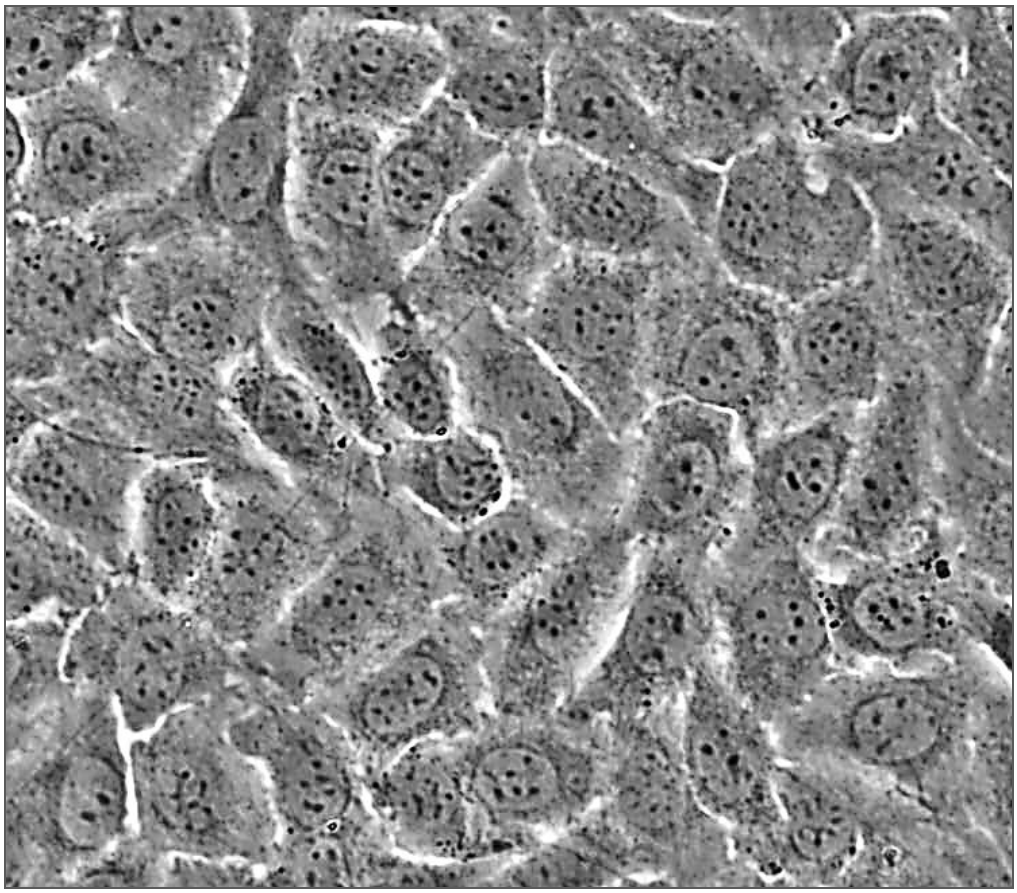

Figure 6. Top view of a confluent endothelial monolayer. The figure shows a confluent monolayer composed of primary mouse aortic endothelial cells. At this stage, the endothelial cells display a quiescent phenotype (defined as reversible cell growth / proliferation arrest).

3.8.1 Endothelial cell-cell contacts

As a gatekeeper the endothelium controls the penetration of blood proteins and cells through the vessel wall [2]. Cell-cell adhesive structures such as adherens and tight junctions maintain endothelial integrity, and at the same time, allow a dynamic regulation of leukocyte transmigration during the inflammatory response and cellular remodeling during angiogenesis [53].

In endothelial cells three types of intercellular junctions, namely adherens, tight, and gap junctions contribute to the structural integrity of the endothelium. Tight and adherens junctions establish and maintain cell-to-cell adhesion, gap junctions control the passage of water, ions, and other small molecules from one cell to another. All three junctions are formed by distinct transmembrane proteins that undergo homophilic cell-cell interactions and promote the transfer of intracellular signals [54].

3.8.2 Endothelial adherens junctions

Adherens junctions are protein complexes that occur at cell–cell junctions in epithelial and endothelial tissues. Cadherins are the central part of endothelial adherens junctions and form zipper-like structures along intercellular contacts. Beside promoting cell-cell adhesion, cadherins transfer various signals and are implicated in mediating contact inhibition [55].

In endothelial cells, adherens junctions consist of the calcium dependent N-cadherin and the endothelial specific VE-cadherins (cadherin-5) which localizes at sites of cellular contacts [56], connecting the site of the junction to the actin cytoskeleton. VE-cadherins connect adjacent cells by forming hexamers [57, 58]. VE-cadherins form trimers in *cis* at the cell surface and interact in *trans* with a trimer of a neighboring cell. This adhesive interaction of two cadherin trimers strictly depends on extracellular calcium [59]. VE-cadherin binds β-catenin, plakoglobin, and p120 through its cytoplasmic tail. β-Catenin and plakoglobin in turn link to α-catenin, which binds vinculin, α-actin, and zonula occludens protein 1 (ZO-1). These interactions mediate the anchorage to actin microfilaments [54]. VE-cadherin also regulates vascular permeability and leukocyte transmigration besides maintaining integrity of the endothelium [60]. VEGF induces tyrosine phosphorylation of VE-cadherin, β-Catenin and plakoglobin thereby decreasing the association of VE-cadherin with the cytoskeleton [61, 62].

3.8.3 Endothelial tight junctions

Tight junctions (TJ) localizes to the zonula occludens, the area where the membranes of adjacent cells meet and form an almost impermeable endothelial monolayer. Tight junctions are distributed heterogeneously across the vascular tree and show variations in number and composition. Endothelial cells of the large arteries and the blood brain barrier (BBB) show a well-developed TJ-system whereas capillaries ECs contain few and rudimentary organized TJs [47].

Claudins form the major adhesive components of tight junctions. Beside claudin-3 and -11, endothelial cells specifically express Claudin-5 [63, 64]. Occludin, another transmembrane component requires the co-expression of junctional protein zona occludins-1 (ZO-1) for cell surface expression. The ZO proteins link claudins and occludins to the actin cytoskeleton [54]. Occludin is predominately expressed at cell-cell contacts in brain endothelial cells and only rarely in endothelial cells of non-neural tissue [65]. Accordingly, occludin downregulation associates with various disease states involving BBB or BRB disruption [47].

The junctional adhesion molecules A (JAM-A) colocalize with TJs and support cell-cell adhesion via homophilic interactions [47, 66], mediate monocyte transmigration through the endothelial cell monolayer [67, 68], and participates in FGF2-induced angiogenesis [69]. As opposed to JAM-A, junctional localization of JAM-C increases paracellular permeability, possibly by modulating VE–cadherin cell–cell contacts [70]. At interendothelial junctions, JAM-C may also interact with JAM-B [71]. The JAM related transmembrane molecule ESAM [72] is implicate in tumor angiogenesis [73], and participates in neutrophil extravasation [74]. Nectins form another group of cell–cell adhesion molecules [75, 76], associate with TJ and AJ proteins, and participate in the initial step of junction formation [47]. Endothelial cells express only nectin-2 (α-herpes receptor) and Necl-5 (poliovirus receptor) [77, 78] (Fig. 7).

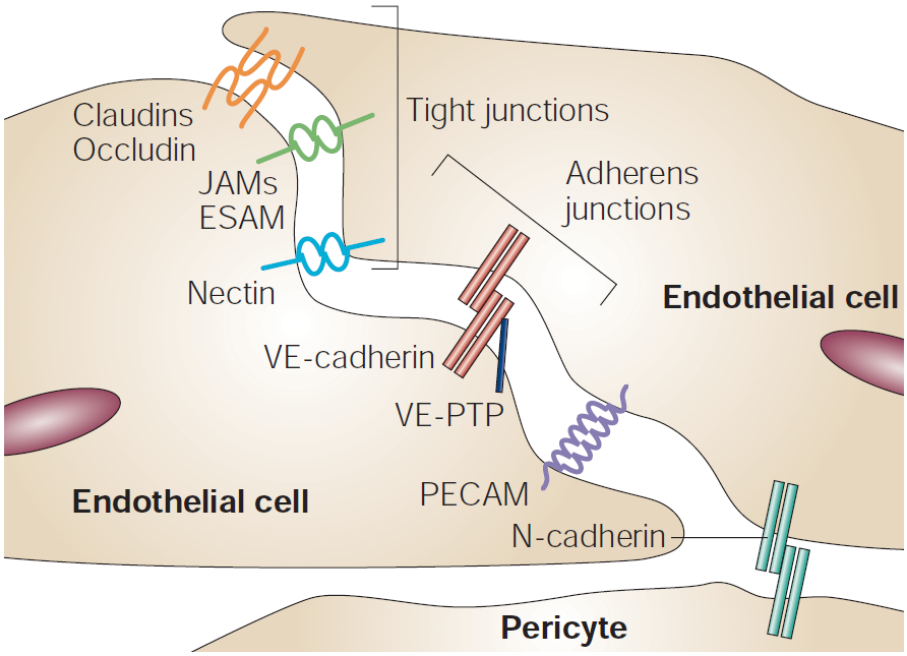

Figure 7. Schematic representation of tight and adherens junctions in endothelial cells. At tight junctions, adhesion is mediated by claudins, occludin, members of the junctional adhesion molecule (JAM) family and endothelial cell selective adhesion molecule (ESAM). At adherens junctions, adhesion is mostly promoted by vascular endothelial cadherin (VE-cadherin), which, through its extracellular domain, is associated with vascular endothelial protein tyrosine phosphatase (VE-PTP). Nectin participates in the organization of both tight junctions and adherens junctions. Outside these junctional structures, platelet endothelial cell adhesion molecule (PECAM) contributes to endothelial cell–cell adhesion. In endothelial cells, neuronal cadherin (N-cadherin) is not concentrated at adherens junctions, but instead probably induces the adhesion of endothelial cells to pericytes and smooth muscle cells [2, 4].

3.8.4 Contact inhibition and mitogenic quiescence

The capacity for cells to regulate their proliferative responses in the context of cell-cell contact is a fundamental requirement for the organization and maintenance of specialized tissues in multicellular organisms. Indeed, contact-mediated inhibition of growth is not restricted to cells in tissues but is a general property displayed by cultured primary cells of many types, including endothelial, smooth muscle, epithelial, and other lineages [79]. Increasing cell-cell contacts in adherent cells eventually block the growth factor stimuli to proliferate in vitro. This density or contact-dependent inhibition of cell proliferation (also known as cellular quiescence) is achieved at a specific saturation density [5, 80].

In endothelial cells, it is likely that the establishment of intercellular contacts transfers negative intracellular signals, which restrains the capacity of quiescent cells to respond to proliferative signals such as VEGF, FGF and angiopoietin (ANG) [2]. Indeed, contact inhibition is at least partially mediated by the establishment of cadherin-based junctions, since cell division is inhibited when cells are plated onto a substrate containing VE-cadherin extracellular domains [81]. Accordingly, VE-cadherin-deficient endothelial cells loose contact inhibition and display increased cell densities in response to VEGF stimulation. The VE-cadherin null cells show increased VEGF-induced VEGFR-2 tyrosine phosphorylation, MAPK activity and enhanced cell proliferation [82]. How endothelial cell keep quiescence in the presence of FGF is less understood. On the one hand, physiological FGF signaling is necessary for the maintenance of vascular integrity [83] and, on the other hand, FGF induces angiogenesis [84]. Although cell confluence inhibits FGF induced p42/p44 MAPK (ERK1/2) activity in mouse vascular endothelial cells, it remains elusive whether VE-cadherins or other cell-cell contact molecules participate in this process [5]. Like the FGF-system, the ANG1-Tie2 ligand-receptor system is in involved in vascular angiogenesis as well as in vascular stabilization [85]. In migrating endothelial cells, Ang1 induces motility and Tie2 activation in cell-matrix contacts. In contrast, in contacting cells Ang1 induces Tie2 translocation to cell-cell contacts, promotes the formation of mature pericyte-covered vessels with tight cell-cell junctions [86], and further stabilizes the vasculature by enhancing Dll4/Notch signaling [87]. In contrast to Ang-1, Ang-2 destabilizes the quiescent endothelium and primes it to respond to inflammatory (tumor necrosis factor and interleukin-1) and angiogenic (VEGF) cytokines [88, 89].

3.8.5 Endothelial quiescence and the cytoskeleton

Through their cytoplasmic tails, both adherens and tight junctions bind to cytoskeletal proteins that promote anchoring of junctions to actin microfilaments. Cytoskeletal association is required for stabilization of the junctions, but also for the dynamic regulation of junction opening and closing [90]. In endothelial cells, the process of actin polymerization is very dynamic, which allows for the rapid reorganization of actin structures and the transition from the quiescent phenotype, characterized by thick cortical actin ring and the absence of stress fibers, to the activated cell phenotype with thin or no cortical actin and abundant stress fibers [91]. Permeability-increasing

agonists such as LPS, thrombin and VEGF increase intracellular calcium levels and thereby activate the myosine light chain kinase MLCK allowing actin-myosin mediated EC contraction [92]. The contraction of the cytoskeleton and the loss of intercellular junctional organization lead to the appearance of paracellular gaps and eventually to the dysfunction of the endothelial barrier (Fig. 8).

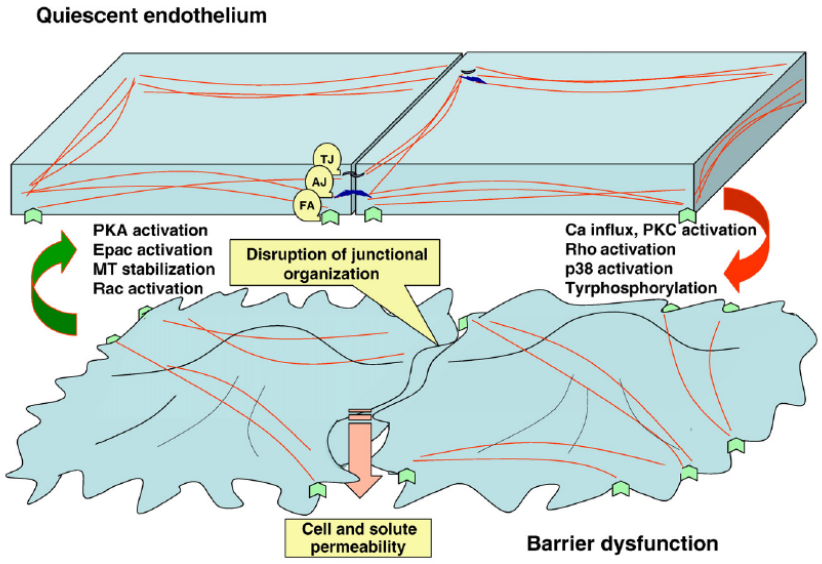

Figure 8. Cytoskeletal rearrangements in endothelial quiescence and barrier dysfunction. These transmembrane complexes are linked to microfilaments, ensuring the cell cytoskeleton architectural integrity. In an agonist-challenged monolayer, the induction of stress fiber formation and the development of acto-myosin-driven tension, together with the loss of intercellular junctional organization, lead to the appearance of paracellular gaps and the dysfunction of the endothelial barrier [91].

3.9 Altered vascular permeability and endothelial dysfunction

Selective regulation of vascular permeability is achieved by regulation of the size and state of paracellular gaps and control of the transcellular transport. The normal vasculature demonstrates a certain level of basal permeability that varies among different vascular beds [93]. Barrier hyperpermeability, necessary for example to provide the access of leukocytes to the pathogen is reversible and does not permanently disturb vascular integrity. In this way the control of vascular permeability may be restored once the triggering cause is removed [3, 93].

In extreme conditions, however, the integrity of the endothelial monolayer is severely affected and cell-to-cell junctions are disrupted. In pulmonary tissue, such vascular

leakage leads to subsequent liquid accumulation in the alveolar space and progressive pulmonary failure [91].

During ischemic stroke, emerging edema around the ischemic area extends brain damage [4]. Eventually, endothelial cells may detach from the vessel wall, creating areas of vascular damage and possibly small thrombi. In tumors, the vasculature is often fragile and exhibits altered permeability, leading to vessel leakage and hemorrhages [4]. High altitude cerebral edema (HACE) is a vasogenic edema characterized by the disruption of the blood–brain barrier by mechanical and biochemical factors. Cerebral capillary hypertension results from impairment of cerebral venous return during hypoxia-induced cerebral vasodilatation. HACE often occurs secondary to acute mountain sickness and or high altitude pulmonary edema due to thin air and resulting hypoxia. HACE causes disturbances of consciousness that may progress to deep coma, psychiatric changes of varying degree, confusion and ataxia of the way of walking. HACE may cause significant morbidity and occasionally death in otherwise perfectly healthy people [94]. Alternatively, several chemical compounds including bradykinin, histamine and VEGF [94-96] mediate BBB leakage and cerebral edema.

Endothelial cells normally maintain vascular hemostasis and prevent thrombotic complications. However, when affected by infection, stress, hypertension, dyslipidemia, or high homocysteine levels, endothelial cells undergo changes resulting in "endothelial dysfunction," characterized by decreased endothelial expression of nitric oxide, enhanced expression of proinflammatory adhesion molecules, and associated increased binding of circulating leukocytes to these cells [97]. Dysfunction is implicated as a key factor in the initiation and progression of inflammatory and atherogenic process that underlies coronary artery disease, peripheral ischemia, and stroke, and contributes to hypertension and heart failure [46, 98, 99].

3.9.1 The endothelial monolayer and Inflammation

Inflammation is an important component of host defense against pathogens; however, excessive or uncontrolled inflammation can disrupt normal tissue homeostasis. Inflammatory processes are characterized by an increase in microvascular permeability to macromolecules and immune cells [100]. Under normal conditions, circulating leukocytes adhere poorly to the endothelium. In response to inflammatory molecules

such TNF-α and IL-1 endothelial cells expresses adhesion molecules that bind cognate ligands on leukocytes. Leukocytes then roll on the activated endothelial cells via selectin interactions and later firmly attach by integrin binding. Chemokines finally direct their diapedesis and migration into the intima where they fight the pathogens [101]. If the innate immune response has successfully removed the pathogen, the endothelial cells restore barrier function and normal tissue architecture. However, when the stimulus is not eliminated then inflammatory process will persist and activates the adaptive immune response. Persistent hyperpermeability leads to the excessive swelling of the tissue due to the fluid extravasation from vascular lumen. If the adaptive immune system fails to eradicate the antigen, the inflammatory process evolves to a more and more chronic form.

3.9.2 Endothelial monolayer integrity in tumors

A growing tumor may not exceed the size of 0.2-2 mm (the limit of oxygen and nutrient diffusion) without acquiring an additional vasculature [102, 103]. When tumor cells get hypoxic they excessively produce VEGF, FGF and other growth factors to induce neovascularization of the hypoxic tumor area. Attracted inflammatory cells further release VEGF contributing to continuous vessel remodeling. The resulting imbalance of pro- and anti-angiogenic signaling within tumors creates an abnormal vascular network that is characterized by dilated, tortuous, and hyperpermeable vessels. The physiological consequences of these vascular abnormalities are irregular blood flow and impaired oxygen delivery [104] resulting in a reduction in the efficacy of chemo- and radiotherapy. Since cancer cells are more resistant to hypoxia than normal cells, they undergo epigenetic changes in hypoxic conditions that promote their malignant phenotype and the epithelial-to-mesenchymal transition (EMT) [105]. HIF-1α-mediated production of several growth factors in cancer cells and the activation of oncogenes promote invasive growth and metastasis [106].

At the cellular level, the endothelial cells lining tumor vessels have an irregular, disorganized morphology. Continuous VEGF-VEGFR2 signaling promotes contraction of the EC cytoskeleton and weakening of VE-cadherin junctions, and hence a loosening of EC associations [4]. Moreover, deregulated PDGFβ, Ang1/2, and TGF-β signaling in tumors impairs vessel coverage with perivascular cells and prevents a proper vessel maturation and stabilization [107].

A recent study revealed that PHD2 haplodeficiency induced tumor vessel normalization [20]. The ECs of the tumor vasculature in PHD2 haplodeficient mice were lined in a single, tight and regular monolayer. In contrast to the ECs of wild type tumor vessels, which were hyper-activated and exhibited loosened tight cell-cell contacts. These changes in EC shape in PHD2 haplodeficient mice did not affect primary tumor growth, but improved the tumor perfusion and oxygenation. Moreover, this normalized endothelial monolayer prevented a metastatic switch and prolonged the survival of PHD2 haplodeficient mice [20, 108].

3.10 Sprouty proteins

The founding member of the Sprouty (SPRY) protein family has been originally discovered in a screen for genes in Drosophila that were responsible for modulating the developing trachea [109]. Drosophila SPRY (DSPRY) inhibited the RTK/Ras/ERK signaling downstream of different growth factors [110]. Based on sequence homology to *Drosophila Spry*, orthologs were identified in the mouse, human, chicken, zebrafish and frog (*Xenopus laevis* and *Xenopus tropicalis*) [109, 111-116]. Compared to DSPRY (63kDa), the vertebrate SPRY proteins are considerably smaller than the *Drosophila* homolog, with predicted molecular masses of 32–35 kDa. Similarity to the fly protein is restricted primarily to the cysteine-rich region (44–52% identity) termed the SPRY domain. Of the 22 cysteine residues found in DSPRY, at least 18 are present in each vertebrate protein [8]. The SPRY domain also contains a highly conserved motif Raf1-binding domain (RBD). The N-terminal half of the SPRY proteins contains a highly invariant tyrosine residue (Y) located in a short, conserved motif.
Sprouty2 (SPRY2), one of four mammalian homologues, exhibits the highest sequence conservation across species; human SPRY2 is 97% homologous to mouse SPRY2, 85% to chick SPRY2 and 51%, in the cysteine-rich region, to DSPRY [111] (Fig. 9).
SPRY2 plays a comparable role to DSPRY in regulating branching of the mammalian lung [114]. SPRY2 thereby functions as a negative regulator of embryonic lung morphogenesis and growth downstream of FGF10 signaling [6].

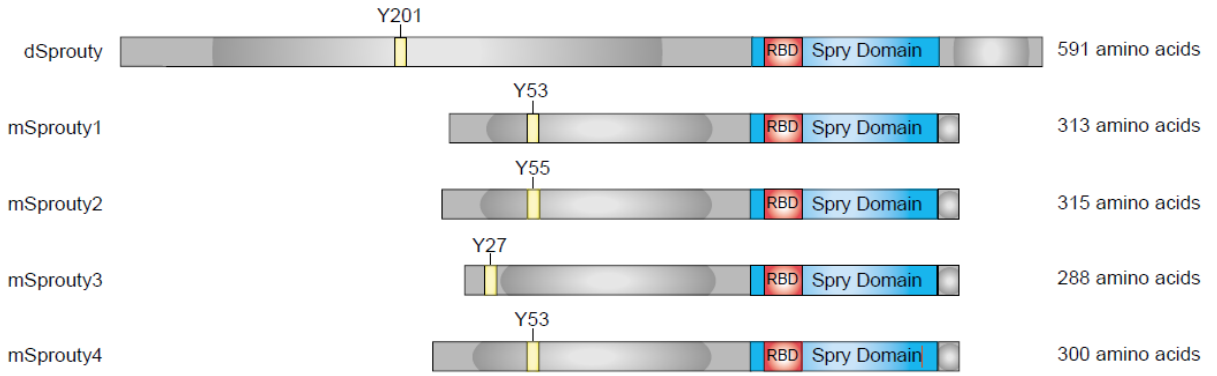

Figure 9. Structure of Drosophila and mouse Sprouty proteins. All Sprouty proteins contain a cysteine-rich SPRY2 domain at the C-terminus with a Raf1-binding domain RBD. The more divergent N-terminus harbors a highly invariant tyrosine residue located in a short conserved motif. The SPRY2 gene product exhibits the highest sequence similarities across species including Drosophila SPRY [8].

3.10.1 Sprouty proteins and RTK signaling

As negative-feedback loop regulator all Sprouty proteins are induced by the signaling cascade they target. Growth factor stimulation activates the Ras-ERK MAPK pathway, which ends in the translocation of phosphorylated ERK to the nucleus, where it activates the transcription of target genes, one of which is *Spry* [8]. SPRY proteins specifically inhibit Ras–ERK MAPK signaling by RTKs, leaving the phosphoinositide 3-kinase (PI3K) and other MAPK pathways unaffected [117, 118].

The conserved tyrosine residue of SPRY1 and SPRY2 is phosphorylated upon FGF and EGF signaling, SPRY4 phosphorylation is induced by FGF and insulin. The Src family of kinases is likely responsible for phosphorylation of SPRY at this conserved tyrosine, while Shp2 phosphatase is involved in dephosphorylating this critical residue [119-122] (Fig. 10).

Membrane localization of SPRY proteins is a conserved mechanism induced by RTK signaling. SPRY2 colocalized with microtubules and translocated to membrane ruffles upon growth factor stimulation [123]. A subset of growth factor-activated SPRY proteins localize to membrane structures and interact with target proteins via their C-terminus. Accordingly, SPRY2 harboring an R252D mutation fails to translocate to the plasma membrane [124], and ectopically-expressed C-terminal truncated versions of SPRY2 are unable to inhibit cell migration, cell proliferation and MAPK activation in response to diverse growth factors [125, 126].

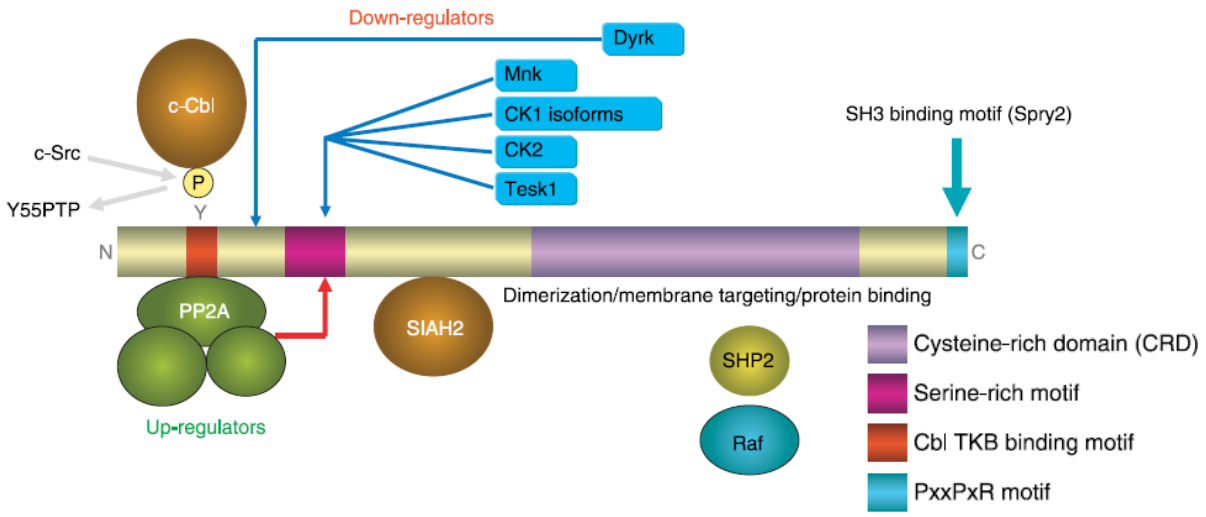

Figure 10. The covalent modifiers of SPRY proteins. Sprouty function is controlled by covalent modification: predominantly phosphorylation and ubiquitination. The location of the binding and targeting for the Ser/Thr kinases is indicated. Two ubiquitin E3 ligases, Cbl, and SIAH2, bind to the N-terminus of SPRY, whereas the SHP2 tyrosine phosphatase and Raf kinase bind to the cysteine-rich domain (CRD). It presently appears that covalent modifications that determine the activity and fate of SPRY localize to the N-terminus while the majority of binding localizes to the CRD [127].

3.10.2 Sprouty and FGF signaling

FGF stimulation induces SPRY2 phosphorylation on Tyr55 by a Src-like kinase and on Y227 by a yet unknown kinase [119, 122, 128, 129]. Simultaneously, SPRY2 is dephosphorylated on the serines 112 and 115 by PP2A [10, 130]. A subgroup of SPRY2 translocates to the plasma membrane [10] and interferes with the RTK cascade on several levels. Under certain conditions, SPRY binding to GRB2 is sufficient to inhibit FGF-induced activation of MAPK, while in others GRB2 association is not required [131, 132]. In addition, SPRY binding to SOS1 and potentially to Raf1 inhibits FGF-stimulated MAPK activation [8, 133]. SPRY binds RAF1, through its conserved RAF1-binding domain (RBD). This interaction inhibits the phosphorylation and activation of RAF1, and thus, the subsequent activation of ERK1/2. In ATDC5 chondrocytes, FGF2 induced *Spry* gene expression through Ca^{2+}- PLCγ dependent pathways [134]. Chelation of extra and intra-cellular calcium prevented SPRY1 induction, whereas SPRY2 expression exclusively depended on intra-cellular calcium. Furthermore, transfection of FGF-receptors lacking the PLCγ binding site only weakly induced *Spry1* and *2* expression. Finally inhibition of PLCγ repressed the activation of *Spry1* and *Spry2* expression [134].

3.10.3 Sprouty, EGF, VEGF and RTK independent signaling

In contrast to their canonical function as negative feedback loop regulators of RTK signaling cascades the Sprouty proteins enhances EGF signaling in certain cellular settings [8, 9]. Upon growth factor stimulation the E3 ubiquitin ligase c-Cbl usually terminates EGF signaling via binding and ubiquitination of the EGF receptor. SPRY2 interferes with this interaction and competes with the EGFR for c-Cbl-binding preventing receptor internalization, thereby sustaining EGFR signaling [135-138]. SPRY2 binds the endocytic adapter CIN85 and inhibits the clustering of c-Cbl that is required for EGFR endocytosis and degradation [138]. Since other RTKs, such as FGFR are degraded via c-Cbl interaction it remains uncertain how Sprouty proteins discriminate between EGF and FGF signaling. It is believed that both EGF and FGF stimulated phosphorylation of SPRY2 Tyr55 while, only FGF significantly phosphorylated a conserved tyrosine (Y227) in the C-terminus of SPRY2 [129]. In addition, SPRY2 interferes with trafficking of activated EGFR to late endosomes [139].

In endothelial cells, VEGF binds to VEGF receptor (VEGFR) and activates MAPK via the phospholipase C gamma (PLCγ) and protein kinase C (PKC) pathway where PKC phosphorylates Raf1, thereby activating ERK/MAPK in a Ras independent manner [140, 141]. Although all SPRY isoforms carry a Raf1-binding domain (RBD) in their highly conserved C-terminal domain, only SPRY4 has been shown to directly bind Raf1 in a VEGF dependent manner, thus interfering with VEGF signaling [142] (Fig. 11). Typically, the regulation of SPRY2 expression and activity depends on RTK-MAPK signaling [8]. However, more and more RTK independent mechanisms are being described. In Fibroblasts, TGFβ1 increased SPRY2 degradation, and at the same time, also decreased its transcription [143]. Furthermore, TNFα downregulated SPRY2 at the level of translation [144]. Conversely, SPRY2 overexpression inhibited TNFα mediated apoptosis, suggesting that SPRY2 plays a role in controlling apoptotic action of TNFα.

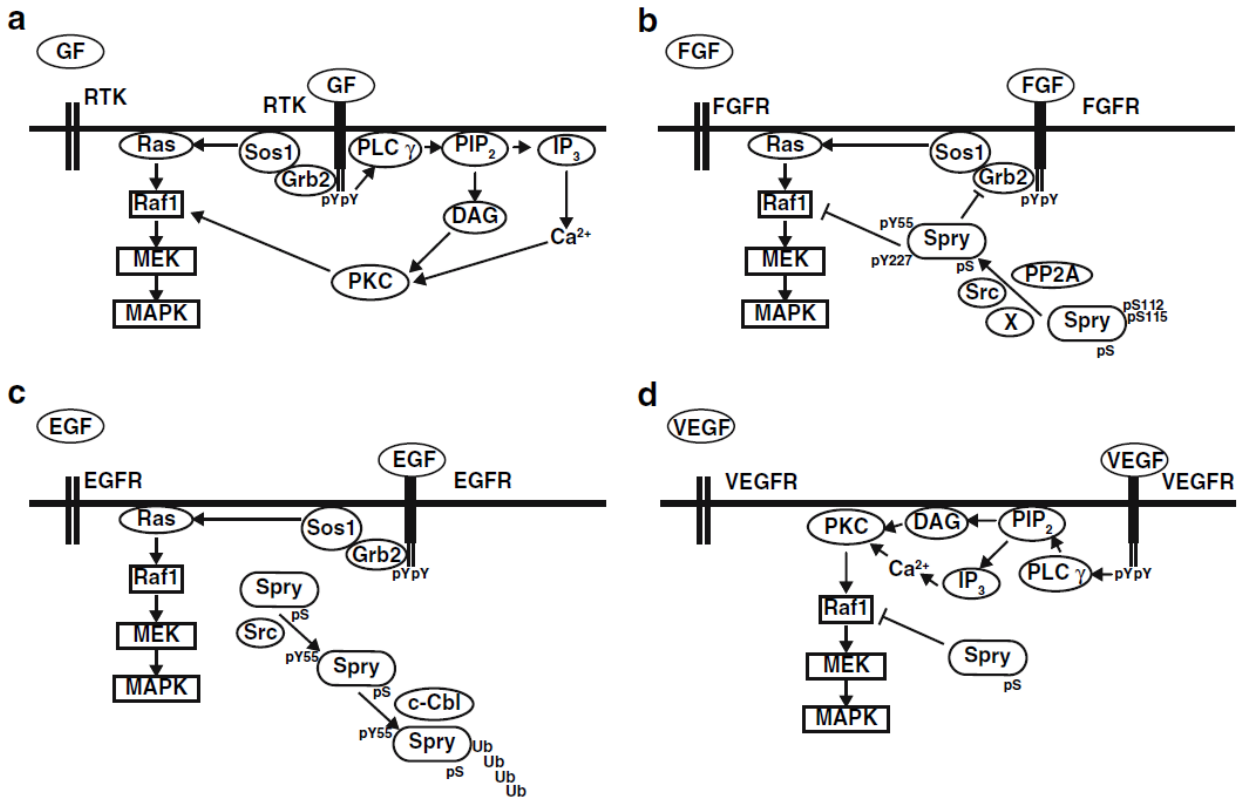

Figure 11. SPRY mechanisms of action in growth factor signaling pathways. (a) Signal transduction in the absence of SPRY. Upon ligand binding, RTKs can activate MAPK in a Ras-dependent manner via the adapter protein GRB2 and SOS1-mediated activation of Ras, Raf1, MEK, and eventually MAPK. Another conserved RTK pathway that can be activated is that mediated by PLCγ, which converts phosphatidylinositol [*4*, *5*]-bisphosphate (PIP_2) into two second messengers: inositol [*1*, *4*, *5*] trisphosphate (IP_3) and diacylglycerol (DAG), leading to calcium (Ca^{2+}) mobilization. Both DAG and Ca^{2+} activate PKC, which in turn phosphorylates Raf1, thus leading to MAPK activation. (**b**) SPRY-mediated inhibition of the FGF signaling pathway. SPRY is serine phosphorylated on multiple residues in unstimulated cells and at least serines 112 and 115 are dephosphorylated by PP2A upon FGF stimulation. Also, SPRY phosphorylation at Y55 by a Src-like kinase and by an unknown kinase (X) at Y227 is required for SPRY to inhibit FGF-induced activation of MAPK. Under some conditions, SPRY binding to GRB2 is sufficient to inhibit FGF-induced activation of MAPK, while in others GRB2 association is not required. Also, SPRY binding to SOS1 and potentially to Raf1 inhibits FGF-stimulated MAPK activity. (**c**) SPRY-mediated potentiation of the EGF signaling pathway. Upon EGF binding, SPRY is tyrosine phosphorylated and competes with EGFR for binding to c-Cbl. By interacting with c-Cbl, SPRY becomes ubiquitinylated and eventually degraded, allowing for sustained EGFR signaling. (**d**) SPRY-mediated inhibition of the VEGF signaling pathway. The VEGFR signals via the PLCγ/PKC pathway. Upon VEGF activation, SPRY interacts with Raf1 via its RBD and inhibits activation of MAPK. Tyrosine phosphorylation of SPRY is not required for this activity. pY and pS denote phosphorylated tyrosine and serine residues, respectively. In this schematic, using SPRY2 as the representative SPRY isoform, pY55 and pY227 represent the N- and C- terminal phospho-tyrosines [9].

3.10.4 Hypoxia and SPRY2

Hypoxia stabilizes Sprouty proteins in Hela cells and SPRY2 in colon carcinoma cells (LS174T). Under normoxic conditions SPRY2 is hydroxylated on proline residues 18,144 and 160 by prolyl hydroxylase domain proteins 1-3 (PHD1-3). Upon proline phosphorylation SPRY2 interacts with Von Hippel-Lindau protein (pVHL). pVHL subsequently ubiquitinates SPRY2 and targets it for degradation. Accordingly silencing of PHD1 or pVHL increase SPRY2 levels and its ability to inhibit FGF-induced ERK1/2 activity [145].

3.10.5 Sprouty proteins in the vasculature

A genetic screen has revealed enriched *SPRY2* mRNA in tube forming human microvascular endothelial cells (HMVECs) versus proliferating HMVECs [146]. In a subsequent study overexpression of Sprouty1 and 2 inhibited FGF, VEGF and EGF induced proliferation and differentiation of human umbilical endothelial (HUVEC) cells [10]. Expression of SPRY4 in endothelial cells inhibited FGF2- and VEGF-induced MAPK activity upstream of Ras. Furthermore, gene-transfer of *Spry4* in the mouse embryo inhibited sprouting and branch formation of the yolk sac vasculature [147].
The FoxO transcription factors are tumor suppressors and regulate endothelial cell homoeostasis. In liver endothelial cells *Spry2* is a direct target of the FoxO transcription factors. The *Spry2* promoter contains several FoxO binding elements. Accordingly, *Spry2* mRNA was significantly down regulated in FoxO knockout liver endothelial cells [148].
In the rat carotid artery, endogenous Sprouty2 decreased immediately after balloon induced injury and then increased between 7 and 14 days. Exogenously expressed human SPRY2 inhibited growth and migration of vascular smooth muscle cells in vitro and neointima formation after blood vessel injury in vivo [149]. Accordingly, suppression of SPRY2 and SPRY4 enhanced angiogenesis in a mouse model of hind limb ischemia [150].

3.10.6 *Spry2* knockout phenotypes

Despite the ubiquitous Sprouty expression in the vasculature, none of the Sprouty knockouts described exhibit an overt vascular phenotype.

Sprouty2 null mice have been generated by two different groups [151, 152] and investigated in several studies yielding new information about the function of Sprouty2. Overall, *Spry2* null mice show reduced body size and shortened life span. Loss of SPRY2 resulted in enteric nerve dysplasia leading to esophageal achalasia and intestinal pseudo-obstruction due to deregulated glial cell line-derived neurotropic factor (GDNF) resulting in ERK and AKT hyperactivation [152]. In another study, Sprouty2-deficient mice showed a higher incident of cleft palate than wild type mice. This process depended on increased palate mesenchymal cell proliferation via FGF signaling [153]. Shim et al. found that lack of Sprouty2 resulted in dramatic perturbations in the organ of Corti cytoarchitecture. The mice suffered of severe hearing loss due to an additional pillar cell layer. This postnatal cell fate transformation in the auditory epithelium was due to increased FGF8 signaling [151]. A further chapter was added by Klein et al. who discovered an additional tooth in the diastema of *Spry2*-null mice [154]. In subsequent study the authors showed that increased FGF signaling resulted in decreased apoptosis and increased proliferation [155]. Finally, loss of Sprouty2 partially rescues renal hypoplasia and stomach hypoganlionosis in Ret Y1062F mutant mice by regulating downstream signaling of the GDNF/RET complex [156].

4 RATIONALE AND AIMS

Over the last years, an enormous amount of knowledge with regard to formation of new vessels has been accumulated. However, the ultimate steps of angiogenesis, including tube stabilization and restoration of the barrier function, are still poorly understood. Furthermore, not only newly-formed vessels but also existing ones need to be actively maintained in order to preserve vascular integrity and tissue homeostasis [4, 47]. In that physiological situation, endothelial cells form a tight monolayer, resist apoptosis and remain quiescent (defined as reversible cell growth/proliferation arrest) even in the presence of angiogenic factors [2, 3].

Thus the question of how endothelial cells process signals arising from increasing cell density to allow a switch from a proliferative, migratory phenotype to a quiescent, impermeable monolayer remains largely unanswered.

Several surface molecules associated with adherens and tight junctions have been suggested to mediate cell-contact inhibition and vascular integrity via regulating intracellular signaling cascades and transcription [4]. Endothelial cells mediate contact inhibition of growth at least in part, by cell cycle exit via inhibition of the MAPK ERK1/2, a major downstream target of FGF, VEGF and other angiogenic growth factors [5]. Therefore, potential negative regulators of this growth promoting signaling cascades are likely to play a central role in this feedback inhibition of cell growth.

As potent antagonist of MAPK signaling, SPRY2 is a potential candidate for mediating endothelial cell quiescence. Several overexpressing studies [10, 126, 157] and SPRY2 knockout mice [151, 153-155] confirmed its potential as a negative regulator of several RTK-related signaling pathways. However, the endogenous expression pattern(s) of SPRY2 remain not well delineated, and it is unknown whether SPRY2 function regulates endothelial quiescence.

The major aims of this thesis are

(i) to assess regulation of SPRY2 expression in endothelial cells in vitro with respect to;

- **a.** cell-density
- **b.** hypoxia
- **c.** cell-cell contacts

(ii) the generation of *Spry2* knockout endothelial cells

- **a.** to investigate ERK1/2 phosphorylation in the presence and absence of SPRY2
- **b.** to investigate the potential role of SPRY2 in mediating contact inhibition during the formation and maintenance of the endothelial monolayer

5 MATERIALS AND METHODS

5.1 Isolation of mouse aortic endothelial cells

Mouse aortic endothelial cells (MAECs) were isolated from aortae of 8-10 weeks old C57BL/6 wild type male mice or Sprouty2 floxed female mice. Fibrin gels were prepared by mixing 3 mg / ml of fibrinogen (Sigma,F4883) with serumfree DMEM (500 ml DMEM (Biochrom AG, FG 0435) were complemented with 5 ml of non-essential amino acids (GIBCO®, 11140); 5 ml of Sodium Pyruvate (GIBCO® 11360), and 5 ml Pen-Strep (GIBCO® 15140)) and 300 μg / ml of thrombin (Sigma T4393) on ice. 24-well plates were coated with 400 μl / well of the prepared fibrin gel and incubated for about half an hour at 37°C to allow polymerization.

The excised aorta was cleaned by cutting off connective and fat tissue under the binocular. The Aorta was then cut in small rings by using sterile scalpels (Swann-Morton, 0501), and the pieces were placed on top of the gel. Then the aortic pieces were overlaid by using another portion of fibrin gel. After gel had polymerized at 37°C, 500 μl / well of pre-warmed EC growth media *(serumfree DMEM that contained 10 % FCS (Biochrom S0615), 100 μg / ml of ECGS (Millipore 02-102), and 0.1 u / ml of heparin (B. Braun 3511014))* was loaded to the wells. To protect the fibrin gel from degradation, 300 μg / ml of E-amino caproic acid (Sigma A-7824) diluted in PBS was added to all wells every other day. After 10 days of culturing, angiogenesis-like sprouts were observed under the microscope (Olympus1X71). The outgrown cells were harvested by pipetting up and down the fibrin gel. The gel-cell mixture was transferred to a six-well plate which had previously been coated with 0.1% gelatin gold (Carl Roth GmbH 4274.1), and 1 ml / well of EC growth media w/o Heparin was added. The next day, cells were washed once with warm PBS and new EC growth media was added. Confluent cells were split 1:2 by trypsinization by using TrypLE™-Express (GIBCO®, 12605) and characterized with endothelial cell specific immunofluorescent marker von Willebrand Factor (VWF, LabForce AG) (Fig. 12).

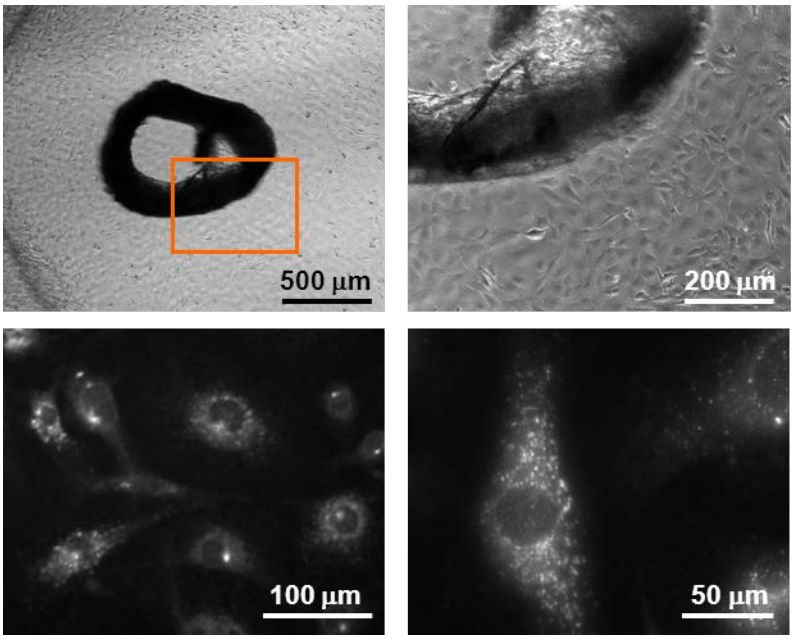

Figure 12. Isolation of mouse aortic endothelial cells (MAECs). The excised, cleaned aorta is cut in rings and placed on fibrin gel. The outgrown endothelial cells form a typical monolayer next to the aortic explant (upper panel). The subcultured cells express the endothelial specific von Willebrand Factor (lower panel).

5.2 Cell culture and treatments

For all experiments using MAECs, cell culture dishes were coated with 0.1% gelatin gold (Carl Roth GmbH 4274.1) for 20 minutes at 37°C. MAECs were maintained in DMEM (Biochrom FG435), complemented with 10% FCS (Biochrom S0615), 1% sodium pyruvate (GIBCO 15140), 1% non-essential amino acids (GIBCO 11140) and 1% penicillin-streptomycin (GIBCO 15140). Human breast carcinoma cell line (HBL-100) and human epithelial colorectal adenocarcinoma cells (Caco2) were cultured in RPMI 1640 (GIBCO 21875), complemented with 10% FCS (Biochrom S0615) and 1% penicillin-streptomycin (GIBCO 15140). Cell numbers were assessed with a NucleoCounter® NC-100™ (Chemometec). MAECs were treated with one or more of the following growth factors, reagents, and inhibitors: FGF2 25 ng / ml (R&D Systems 3139-FB/CF); recombinant mouse TNFα 10 ng / ml (RD 410-MT-010); MG132 5 µM (Calbiochem 474790), EGTA 2.5 mM (Calbiochem 324626), BAPTA-AM 10 µM (Molecular Probes B1205); human thrombin 1 u / ml (Sigma T4393); recombinant mouse VE-cadherin 2 µg / ml (RD 1002-VC); VE-cadherin blocking antibody 10 µg / ml (BD Pharmingen 555289); and U0126 5 µM (Promega V112A). To create a hypoxic envi-

ronment cells were placed in a hypoxia incubator (Thermo Scientific Hera Cell 150) with 1% oxygen for 24 hours. Micrograph pictures of cells were taken with a digital camera (Olympus F-viewXS) and an inverted microscope (Olympus1X71). GFP expression was monitored using a U-LH100HG light source with a U-MWB2 filter (Olympus).

5.3 Immunoblotting

To extract protein, cells were washed twice with ice cold PBS and then harvested by scraping with a cell scraper (BD Falcon 353089) into 1 ml of ice cold PBS. The cell suspension was collected with a 1 ml pipette, transferred to a 2 ml Eppendorf tube, and then centrifuged for 5 minutes at 14,000 rpm at 4°C. The pellet was resuspended in RIPA buffer that contained a complete mini protease inhibitor (Roche 11836153001) and a phosphatase inhibitor cocktail 2 (Sigma P5726) and then was lysed by using liquid nitrogen in four freeze-and-thaw-cycles. The sample was centrifuged for 15 minutes at 14,000 rpm at 4°C. The resulting supernatant was transferred to a new 1.5-ml Eppendorf tube and the protein concentration measured by using a BCA protein assay kit (Thermo scientific 23223). Equal amounts of protein were loaded on a 10% acrylamide-SDS gel. Separated proteins were transferred to a nitrocellulose membrane (Whatman BA85) by using a semidry blotting procedure, blocked for 1 hour at room temperature (RT) in Tris buffered saline (TBS) that contained 5% skim milk powder (Sigma 70166).

Membranes were washed once with TBS-tween (0.1%) and incubated overnight at 4°C with one of the following primary antibodies: rabbit anti Sprouty2 1:4,000 (H-120, Santa Cruz sc-30049), rabbit anti Sprouty2 1:1,000 (abcam ab50317), rabbit anti pospho-ERK1/2 1:1,000 (Cell Signaling 9101), rabbit anti total-ERK1/2 1:1,000 (Cell Signaling 9102), rabbit anti FoxO1 1:1,000 (Cell Signaling 9462), rabbit anti FoxO3a 1:1,000 (Cell Signaling 2497), rabbit anti phospho-FoxO1 (Thr24)/FoxO3a (Thr32) 1:1,000 (Cell Signaling 9464), rabbit anti HIF-1α 1:1000 (Novus Biologicals NB100-479) and mouse anti β-Actin 1:10,000 (Sigma A-5441).

The next day, the membrane was washed three times in TBS-0.1 % tween and incubated with a secondary antibody goat anti rabbit HRP 1:5,000 – 1:20,000 (Cell Signaling 7074) or anti mouse HRP 1:80,000 (Cell Signaling 7076) for 1 hour at room temperature (RT). After another wash step, a chemiluminescent substrate that is

used for the detection of HRP (Thermo Scientific 34080) was applied to the membrane, and then the membrane was incubated for 1 minute. The signal was detected with a CL-XPosure film (Thermo Scientific 34090), and the resulting bands were quantified by using ImageJ (Wayne Rasband, NIH, MD, USA).

5.4 Oxygen sensing

Changes in the oxygen saturation of cell cultures were measured in real time by using an SDR SensorDish reader (Presens). MAECs were plated on an Oxodish 24-well plate (OD24) with integrated oxygen sensors (Presens 200000430). Oxygen saturation of the media was measured every 30 minutes and data was collected and analyzed by using SDR_v38 software (Presens) on a personal computer.

5.5 mRNA extraction and quantitative real-time PCR

To isolate RNA, cells were first harvested by scraping by scraping with a cell scraper and the RNA then isolated by using RNeasy kit (Qiagen 74106) according to directions in the manufacturer's manual. The RNA was then reverse transcribed to cDNA by using the Taqman Kit (Roche Applied Biosystems N808-0234). The following primers were used for qRT-PCR:

Spry2-fwd (ATAATCCGAGTGCAGCCTAAATC)
Spry2-rev (CGCAGTCCTCACACCTGTAG)
GAPDH-fwd (TGTGTCCGTCGTGGATCTGA)
GAPDH-rev (CCTGCTTCACCACCTTCTTGA)

The cDNA samples and the forward and reverse primers for the endogenous control gene (GAPDH) and the target gene (*Spry2*), together with SYBR green PCR master mix (Applied Biosystems 4385612) were loaded on a 96-well PCR reaction plate. Data was collected and normalized to GAPDH by running the relative quantitation program with the 7500 real time PCR system (Applied Biosystems).

5.6 FoxO1/3 silencing

3 million cells were transfected with one 2 μl of the following siRNAs: FoxO1 siRNA, FoxO3 siRNA, and siRNA negative control (Stealth RNAi™ siRNA Invitrogen 1320003). Cell transfection was performed using a basic endothelial cells nucleofector kit in a Nucleofector II device (Lonza) according to the manufacturer's protocol.

5.7 Electric cell-substrate impedance sensing

Electrical resistance measurements were performed using an ECIS ZΘ apparatus (Applied Biopyhysics) in 8-well (0.8 cm^2 / well) arrays with 40 (8W10E+) gold electrodes with a diameter of 250 μm (Applied Biopyhysics). Each experiment was carried out in duplicates. Before seeding the cells, each well was pre-incubated with serum-free DMEM overnight. That was followed by a 20 minutes coating with 0.1% gelatin gold (Carl Roth GmbH 4274.1) and 0.9% sodium chloride in PBS followed by three wash steps with growth media. The arrays in the measurement station were then placed in an incubator (37°C, 5% CO_2) to allow real-time monitoring. Total resistance was measured at a frequency of 4 kHz. The initial baseline values were normalized to 1.

5.8 Generation of *Spry2* knockout cells

800,000 *Spry2* floxed MAECs were seeded on a 10 cm culture dish. The next day, the media was removed and a virus (100 MOI) that contained either Ade-CRE-GFP (Vector Biolabs 1045) or Ade-CMV-GFP (Vector Biolabs 1060) was added in 3 ml of growth media to the cells. After 6 hours, the media was removed, replaced by 10 ml of normal growth media, and then incubated at 37°C. Endothelial cells expressed GFP the following day. Down-regulation of *Spry2* was assessed by using qRT-PCR and Western blot (Fig. 13). Steps that involved handling viruses or virus-transfected cells were undertaken in a level-2 biosafety hood (Skan VSB 90) in a certified cell culture laboratory.

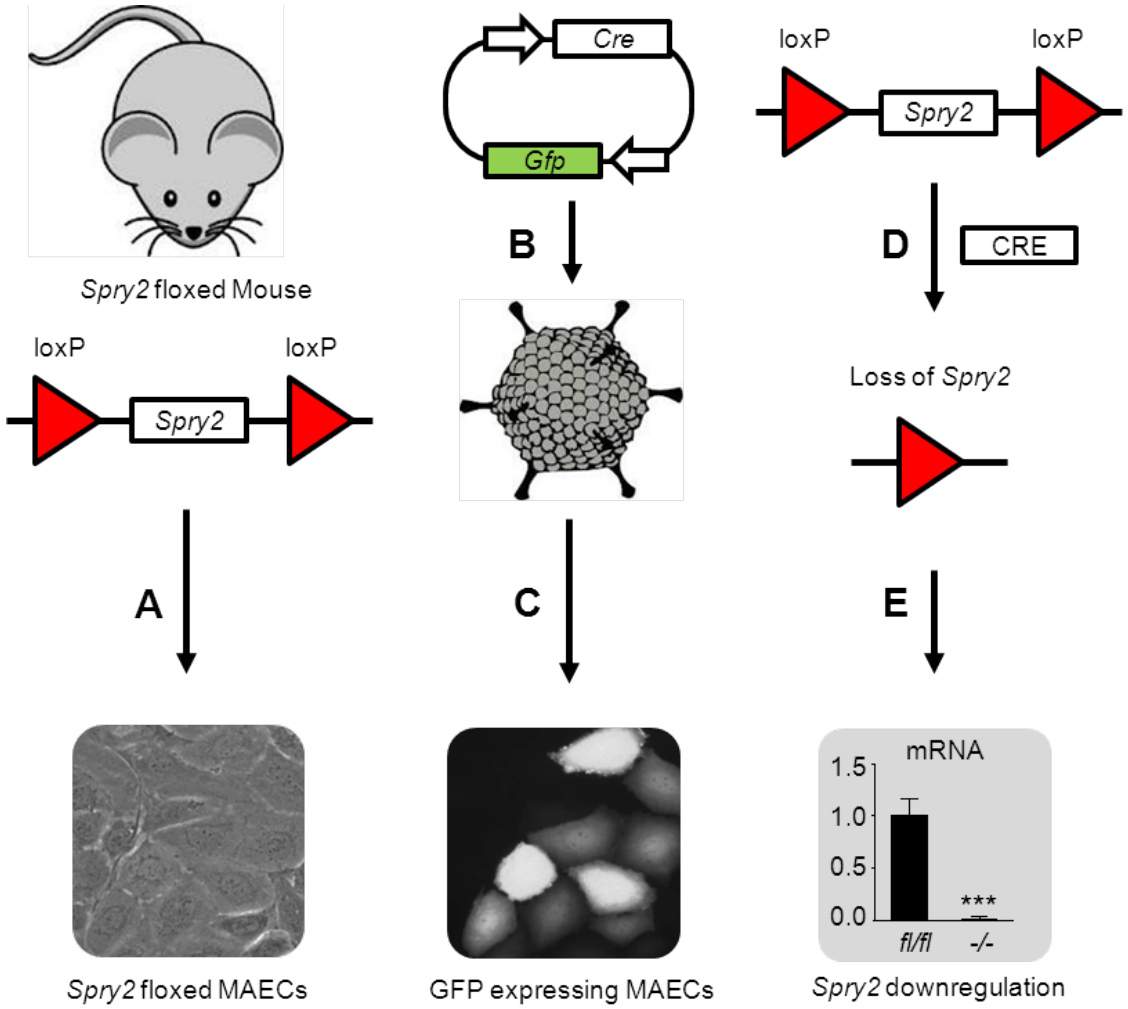

Figure 13. Generation of *Spry2* knockout MAECs(A) The aorta of floxed-*Spry2* mice is excised and MAECs are isolated. (B, C) Virus that contains either Ade-CRE-GFP or Ade-CMV-GFP vectors is added to MAECs. (D) The introduced CRE recombinase excises *Spry2* from the DNA. (E) qRT-PCR confirms efficient knockout of *spry2*.

5.9 Proliferation assay

20,000 cells per well were seeded in 6 replicates and then grown in 100 µl of growth media with 1% FCS in a 96-well plate both with and without 25 ng / ml of FGF2. After 48 hours, 10 µl of alamarBlue® solution (Invitrogen DAL1100) was added for 3 hours. Fluorescence was measured (Ex 560; Em 590) by using a Spectramax M2 reader (Molecular Devices).

5.10 Permeability assay

200,000 cells were re-suspended in 200 μl of complete growth medium supplemented with 1% FCS both with and without 25 ng / ml of FGF2. Cells were then seeded in triplicate on cell culture inserts (3-μm pore size, Falcon 353096) and placed in 24-well culture plates (Falcon 353047) that contained 600 μl of FGF2-free medium per well. After 48 hours, the inserts were moved to a new 24-well plate and 70 kDa FITC-dextran was added to all inserts for 10 minutes. Fluorescence at Ex 585 nm and Em 520 nm of the lower well was analyzed by using a Spectramax M2 reader.

5.11 Statistical analysis

All statistical tests were performed by using GraphPad Prism 5.04 for Windows® (GraphPad software, San Diego, CA, USA). We have used unpaired t-test to evaluate differences between two groups. If there were more than two groups, we used one-way ANOVA, followed by a Newman-Keuls post-test. $P<0.05$ was considered significant.

6 RESULTS

6.1 High cell density causes transient hypoxia and increases SPRY2 expression during the formation of the endothelial monolayer

To investigate whether high endothelial cell density affects SPRY2 protein expression, mouse aortic endothelial cells (MAECs) were plated sparsely and grew to high cell density and confluence over a time period of 24 to 96 hours (Fig. 14A). After 24, 48, 72 and 96 hours cells were analyzed for SPRY2 expression. SPRY2 protein levels were low after 24 hours of culturing. After 48 hours SPRY2 expression increased markedly and reached a maximum between 72 and 96 hours after seeding (Fig. 14B). Thus, SPRY2 protein expression increased with higher cell density.

Conventional monolayer cultures are often hypoxic when incubated in an air / 5% CO_2 atmosphere [158]. Thus, hypoxia that results from increased oxygen-consumption during endothelial monolayer formation may correlate with high cell density and may upregulate SPRY2 expression. To investigate this hypothesis, we analyzed the expression of the hypoxia marker HIF-1α over a time period of 24 to 96 hours. HIF-1α levels increased at 48 hours, dropped at 72 hours, and were undetectable after 96 hours of cell seeding (Fig. 14C). We then further substantiated these findings by measuring oxygen levels of sparsely-seeded cells directly and in real time over a period of 0-96 hours: Oxygen saturation decreased slightly after 24 hours (80% $O_{2\ saturation}$) and declined to a minimum between 48 and 72 hours after cell seeding (70% $O_{2\ saturation}$) compared to a control with no cells present (85% $O_{2\ saturation}$ throughout the experiment) (Fig. 14D). These results demonstrate that increased SPRY2 expression after 48 hours of endothelial cells growing to confluence is accompanied by hypoxia and elevated HIF-1α expression.

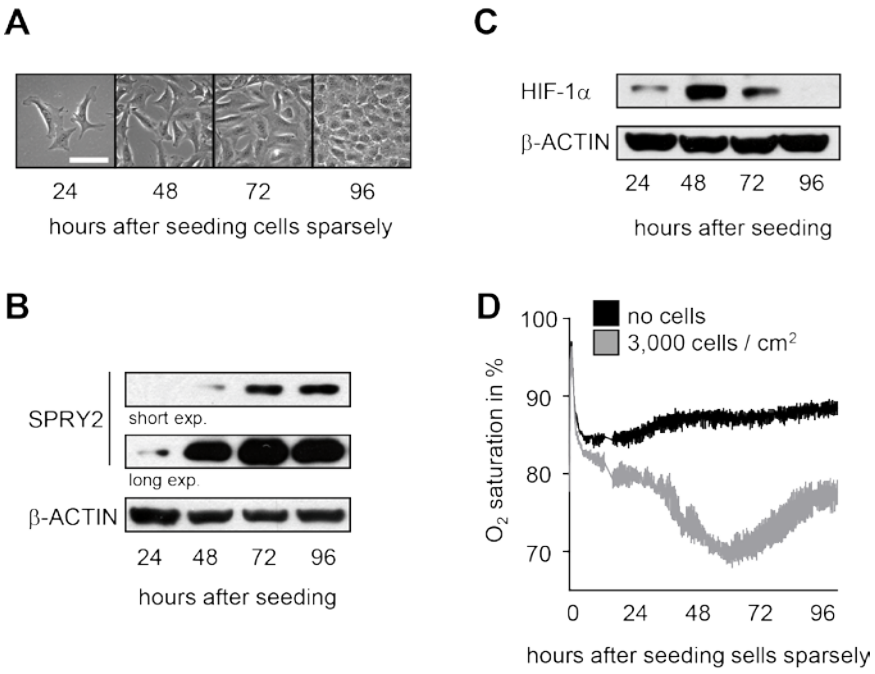

Figure 14. High cell density and hypoxia increase SPRY2 expression during the formation of the endothelial monolayer. (A) Micrographs (scale bar 100 μm) of mouse aortic endothelial cells (MAECs) plated at sparse condition (3,000 cells / cm^2) and grown for the indicated time. (B and C) Total SPRY2, HIF-1α, and β-Actin expression of samples collected at the indicated times were analyzed by Western blotting. (D) Real-time measurement of the oxygen consumption of MAECs growing to confluence (initially plated at sparse density; 3,000 cells / cm^2). Results show representative of two independent experiments performed in duplicates.

6.2 SPRY2 expression under normoxic and hypoxic conditions

To investigate whether hypoxia really induces SPRY2 protein expression, we reduced oxygen consumption by starving the cells to reduce metabolism [158]. Replacement of the growth media by serum-free media after 24 hours reduced the oxygen consumption of the endothelial cell cultures and restored basal oxygen levels after 48 hours. However, in the presence of serum, oxygen levels decreased further and reached a minimum level (65% $O_{2\ saturation}$) after 48 hours of cell seeding (Fig. 15A). In parallel experiments, HIF-1α protein levels were measured before and after serum starvation. Indeed, HIF-1α protein levels dropped and were undetectable after changing growth media to serum-free conditions (Fig. 15B). Similarly, SPRY2 protein levels decreased but were still detectable in starved cells (Fig. 15B).

To assess whether endothelial cells cultured in serum-free medium did not lose the potential to induce SPRY2 expression under hypoxia, cells were seeded at sparse or

confluent density, and serum-free endothelial cells were subjected to hypoxic (1% O_2) and normoxic conditions in a hypoxia incubator. After 24 hours, SPRY2 increased in cells under hypoxic conditions; this correlated with increased HIF-1α protein levels (Fig. 15C). Hypoxia, however, did not affect *Spry2* mRNA levels (Fig. 15D). Thus, it is likely that hypoxia regulates SPRY2 expression independent of HIF-1α on a post-transcriptional level.

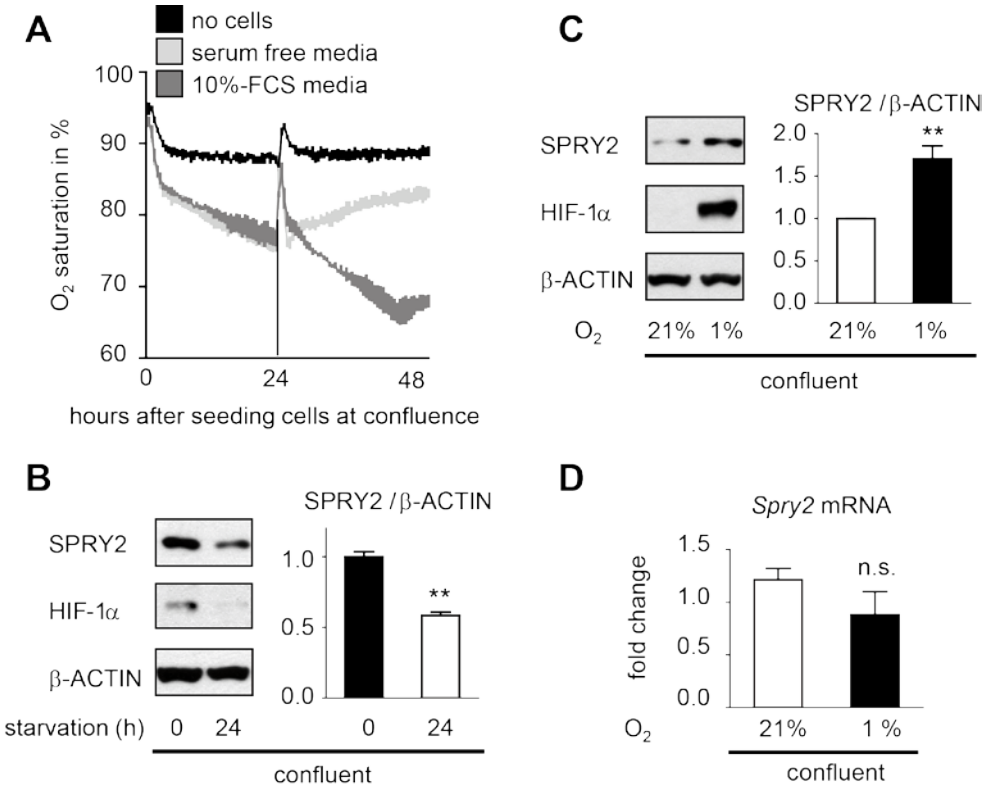

Figure 15. SPRY2 expression under normoxic and hypoxic conditions. (A) Real time oxygen consumption of growing and quiescent cells (cells plated at confluence; 50,000 cells / cm^2). After 24 hours, either serum free or media with 10 % FCS was added for additional 24 hours to the cells (indicated with a line). Results show representative of three independent experiments. (B) In parallel experiments, cells were grown in 10% FCS for 24 hours and then either collected (FCS+) or starved for 24 hours (FCS-). Total cell lysates were assessed for HIF-1α, SPRY2 and β-Actin expression. Three independent experiments, normalized to β-Actin expression, are summarized in a graph that shows densitometric quantification of the bands (***P*<0.01). (C) MAECs were grown for 24 hours and then starved and grown under either hypoxic (1% O_2) or normoxic (21 % O_2) conditions. Total lysates were analyzed for HIF-1α, SPRY2, and β-Actin expression. Three independent experiments, normalized to β-Actin expression, are summarized in a graph that shows densitometric quantification of the bands (***P*<0.01). (D) mRNA was collected from cells grown under either hypoxic (1% O_2) or normoxic (21 % O_2) conditions and analyzed for SPRY2 expression by using qRT-PCR. Values were normalized to GAPDH (n=4).

6.3 Density dependent SPRY2 expression in serum deprived MAECs

To investigate, whether SPRY2 protein levels remained elevated in dense compared to sparse starved cultures, we seeded cells at different cell numbers (Fig. 16A), starved for 24 hours and assessed for SPRY2 protein expression. Sparsely plated cells (1,500 – 6,000 cells / cm^2) expressed SPRY2 protein at very low levels. Sub-confluently plated cells (12,000 – 25,000 cells / cm^2) increased SPRY2 protein markedly (40 fold and 66 fold, respectively). Plating 50,000 cells / cm^2 lead to the formation of a confluent monolayer and induced SPRY2 protein 74 fold as compared to sparsely plated cells at 1,500 cells / cm^2 (Fig. 16B). We therefore hypothesized that in starved cells, SPRY2 might be stabilized at elevated level independent of hypoxia via another mechanism such as cell-cell contacts since SPRY2 protein levels remained elevated in dense serum-free but normoxic cultures (Fig. 16B).

Next we assessed, whether starved confluent cells exhibit increased *Spry2* mRNA transcription. Indeed, *Spry2* mRNA levels were moderately enhanced (two fold) in confluent (50,000 cells / cm^2) compared to sparse cells (3,000 cells / cm^2). (Fig. 16D). In order to directly compare the *Spry2* mRNA to the protein levels, we analyzed the same lysates for SPRY2 protein expression. The densitometric quantification of the Western Blot bands revealed a 70 fold increases of SPRY2 protein in confluent cells (50,000 cells / cm^2) as compared to sparsely plated cells (3,000 cells / cm^2) (Fig. 16D). Taken together, these results suggest that high cell density increases SPRY2 levels via transcriptional and post transcriptional mechanisms. The post transcriptional part thereby seems to be more prominent.

We then asked whether the observed cell-density-dependent regulation is restricted to MAECS. Therefore, we assessed SPRY2 expression in a human breast carcinoma cell line (HBL-100) and a human epithelial colorectal adenocarcinoma cells (Caco2), which were plated at different cell densities. Although, both cell lines exhibited a monolayer-like morphology and exhibited partial contact inhibition, they grew to very high densities (100,000 cells / cm^2). SPRY2 expression increased with higher cell density in both cell lines HBL-100 and Caco2 (Fig. 17), suggesting that density induced SPRY2 expression is a not a unique feature of MAECs.

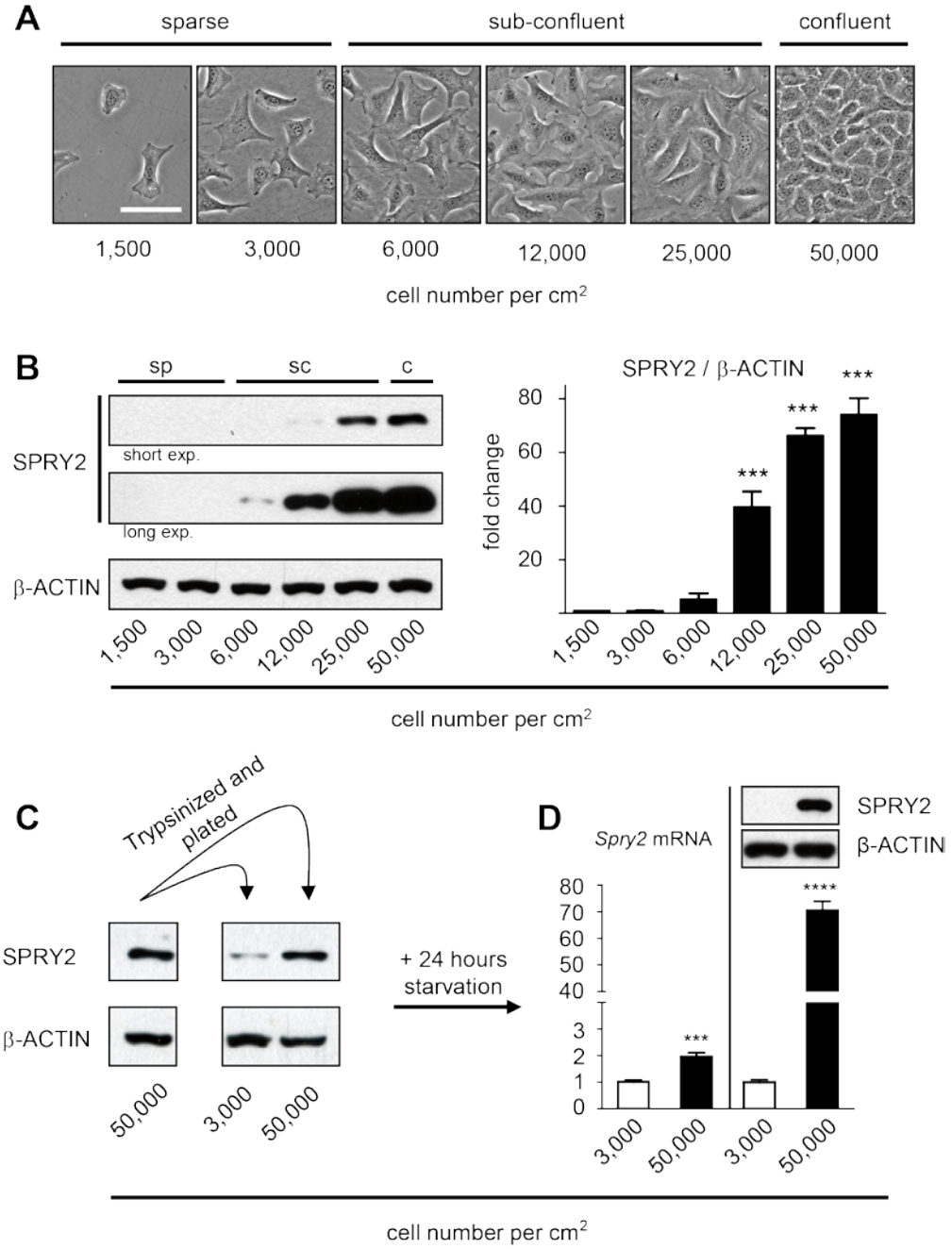

Figure 16. Starved confluent endothelial cells express high SPRY2 protein levels. (A) Micrographs (scale bar 100 μm) of MAECs plated at different cell numbers. (B) Western blot of SPRY2 total protein. Equal loading was confirmed by reprobing the membrane with the anti β-Actin antibody. Three independent experiments, normalized to β-Actin expression, are summarized in a graph that shows densitometric quantification of the bands. The values shown are means +/- s.e.m.; ****P*<0.001 vs. 1,500 cells / cm^2. (C, D) A confluent MAEC culture was analyzed for SPRY2 expression by immunoblotting (C, left column) before plating the cells at sparse or confluent conditions. After 24 hours, cells were lysed (C, right column) or starved for another 24 hours. (D) After starvation, cells were analyzed for SPRY2 expression by immuoblotting and qRT-PCR. The values were normalized to GAPDH +/- (qRT-PCR) or β-Actin (immunoblotting) s.e.m.; ****P*<0.001; *****P*<0.0001; n=3.

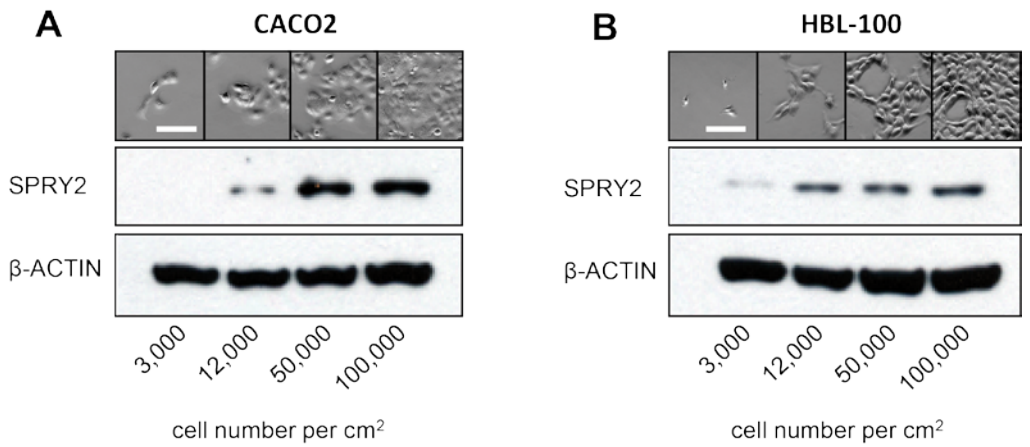

Figure 17. SPRY2 expression increases with higher cell density in tumor cell lines. Micrographs (scale bar 100 μm) of Caco2 (A) and HBL-100 cells (B) plated at different cell number. SPRY2 protein expression was analyzed by immunoblotting. Equal loading was confirmed by reprobing the membranes with the anti β-Actin antibody.

6.4 Cell density increases SPRY2 expression independent of the FoxO1/3 transcription factors

Cell confluence increased SPRY2 partly via transcription (Fig. 16B). Since the *Spry2* promoter contains several FoxO binding elements [148], we asked whether the FoxO transcription factors may upregulate *Spry2* transcription at high cell density. Dephosphorylated FoxO1 predominantly locates to the nucleus and shows increased transcriptional activity [159]. We therefore tested, whether the FoxO1 phosphorylation depended on cell density. Indeed, the relative FoxO1 phosphorylation levels decreased with higher cell density suggesting that confluent cell exhibited increased FoxO transcriptional activity (Fig. 18A). Silencing of FoxO1 and 3 mRNA effectively decreased FoxO1/3 protein levels (Fig. 18B). Surprisingly, FoxO1/3 knockdown did affect neither SPRY2 protein (Fig. 18B) nor *Spry2* mRNA levels (Fig. 18C) suggesting that transcription factors others than FoxO1/3 upregulated *Spry2* mRNA and SPRY2 protein levels at high cell density.

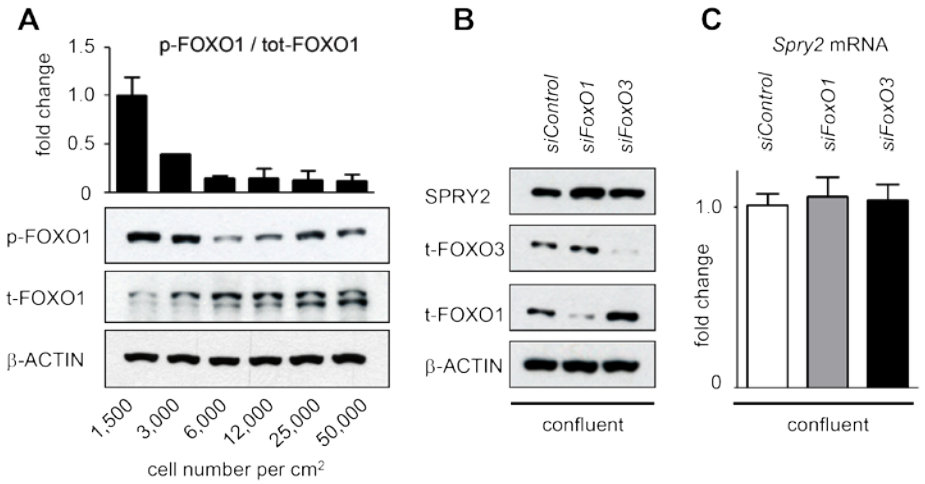

Figure 18. Cell density increases SPRY2 expression independent of the transcription factors FoxO1 and FoxO3. (A) MAECs were plated at different cell number and analyzed for Foxo1 phosphorylation and total protein expression. Equal loading was confirmed by re-probing the membranes with the anti β-Actin antibody. The relative FoxO phosphorylation levels were analyzed by densitometric quantification of the FoxO Western Blot bands of two independent experiments. (B, C) Immunoblotting (B) and qRT-PCR (C) revealed that SPRY2 expression was not affected by FoxO1/3 silencing.

6.5 Cell-cell contacts stabilize SPRY2 protein levels in confluent cells

To exclude the possibility that the increase in SPRY2 protein depends on factor(s) secreted by MAECs into the culture medium that would induce SPRY2 expression in an autocrine manner, conditioned medium from confluent MAECs cultures was supplied to a sparse culture of MAECs and vice versa. The amount of SPRY2 protein was compared after 6 h. Conditioned medium of confluent cells did not induce SPRY2 protein expression and vice versa (Fig. 19A).

Thrombin and TNFα both interfere with cell-cell contacts and increase endothelial permeability [160, 161]. We therefore tested, whether Thrombin and TNFα affect SPRY2 protein expression in confluent cells. A clear decrease in SPRY2 protein was detected after 6 hours treatment of confluent cells with Thrombin as well as with TNFα (Fig. 19B). In addition, TNFα reversibly decreased the total normalized electrical resistance of the confluent MAEC monolayer (Fig. 19C). Moreover, TNFα increased the permeability of the endothelial monolayer to 70 kDa FITC-Dextran confirming that TNFα disturbed cell-cell contacts (Fig. 19D). Taken together, these observations strongly support the perception that SPRY2 protein levels are positively regulated by cell-cell contacts.

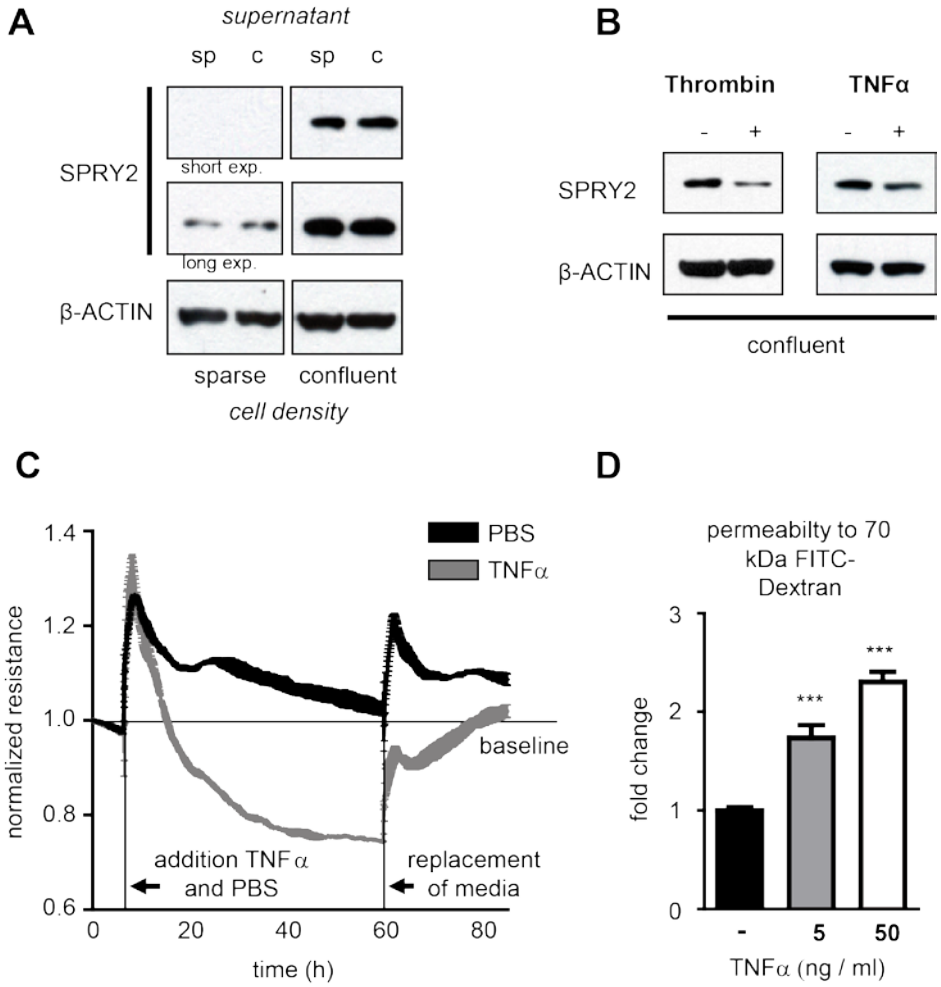

Figure 19. Confluency stabilizes SPRY2 protein via cell-cell contacts rather than by soluble factors. (A) The supernatant of a confluent cell cultures was collected 24 after starvation and added either to sparse or confluent cells. At the same time the supernatant of sparse cells was collected and added either to confluent or sparse cells. After 6 hours the cells were lysed and assessed for SPRY2 and β-Actin expression. (B) MAECs were plated at confluence, starved next day for 24 hours and then treated with thrombin (1 unit / ml) or TNFα (10 ng / ml) for 6 hours. The lysates were then analyzed by Western Blot for SPRY2 expression. Equal loading was confirmed by re-probing the membranes with the anti β-Actin antibody. (C) Cells were plated at confluence, and total resistance was measured in real time by ECIS. When cells reached a steady plateau in resistance (resistance = 1), either TNFα (10 ng / ml) or PBS was added to the cells. After 60 hours new media was added to all cells. (D) The change of the permeability of the monolayer in the presence of TNFα. Cells were seeded at confluence on a well insert. TNFα (5 and 50 ng / ml) or PBS was then added to the cells overnight. Next day, 70 kDa FITC-Dextran was added for another 24 hours. The permeability of the monolayer was then evaluated by measuring fluorescence of the lower well. The values obtained for the controls without TNFα were normalized to 1. Bars show values of triplicates as fold change of control +/- SD; ***=p<0.001.

6.6 Disruption of calcium dependent cell-cell contacts decreases SPRY2 protein expression

In order to further examine the kinetics of SPRY2 regulation by cell-cell contacts, we used ethylene glycol tetra acetic acid (EGTA) to chelate extracellular calcium and to disrupt calcium dependent cell-cell contacts [162].

The addition of EGTA to confluent MAECs resulted in the formation of gaps between cells after 30 minutes and in a complete detachment from each other after 3 hours (Fig. 20A). Replacement of EGTA with new media restored the monolayer after 24 hours of incubation. In parallel experiments, treatment with EGTA completely eliminated SPRY2 expression after 0.5 and 3 hours of EGTA treatment (Fig. 20B). The restoration of the monolayer by new media also restored SPRY2 protein to the levels seen prior to EGTA treatment. We then measured the electrical resistance of the confluent endothelial monolayer during EGTA treatment by electrical cell impedance sensing (ECIS). The electrical resistance dropped markedly after the addition of EGTA and then returned to basal levels (resistance prior the addition of EGTA) within 48 hours after the addition of new media. This result demonstrated that the effect of treatment with EGTA was reversible and did not damage endothelial cell viability (Fig. 20C). Of note, chelation of intracellular calcium with Bapta-AM did not affect SPRY2 protein levels (Fig. 20D), and neither EGTA nor Bapta-AM affected *Spry2* mRNA levels (Fig. 20E). These findings indicate that density-dependent SPRY2 protein expression depends on intact cell-cell contacts and is independent of the level of intracellular calcium.

VE-cadherins are the predominant components of endothelial adherens junctions [54, 56, 163] and interact with cadherins of neighboring cells in a homophilic manner [57]. These adhesive complexes strictly depend on extracellular calcium [59, 162]. Therefore, VE-cadherin is a candidate molecule for the regulation of SPRY2 protein expression in confluent cells. In order to investigate whether VE-cadherin directly modulates SPRY2 expression we used a VE-cadherin blocking antibody [164] and soluble recombinant mouse VE-cadherin. Interestingly, the VE-cadherin antibody (10 ug / ml) exclusively decreased SPRY2 protein levels when added to confluent cells, whereas in sparse cells no effect could be observed (Fig. 21A). In contrast, increased VE-cadherin blocking antibody concentration (100 μg / ml) seems to have a reverse effect: Preliminary experiments revealed that SPRY2 protein levels decreased when cells were plated in the presence of 100 μg / ml of the VE-cadherin blocking antibody

(results not shown). Finally, preliminary results revealed that the treatment of cells with soluble recombinant VE-cadherin decreased SPRY2 protein in both, sparse and dense cells. Taken together, these preliminary results suggest that VE-cadherin somehow modulates SPRY2 expression (Fig. 21B). However, the exact regulation mechanism remains elusive, since it is not clear how the VE-cadherin antibody and the soluble VE-cadherin protein interact with the endogenous VE-cadherin in reality.

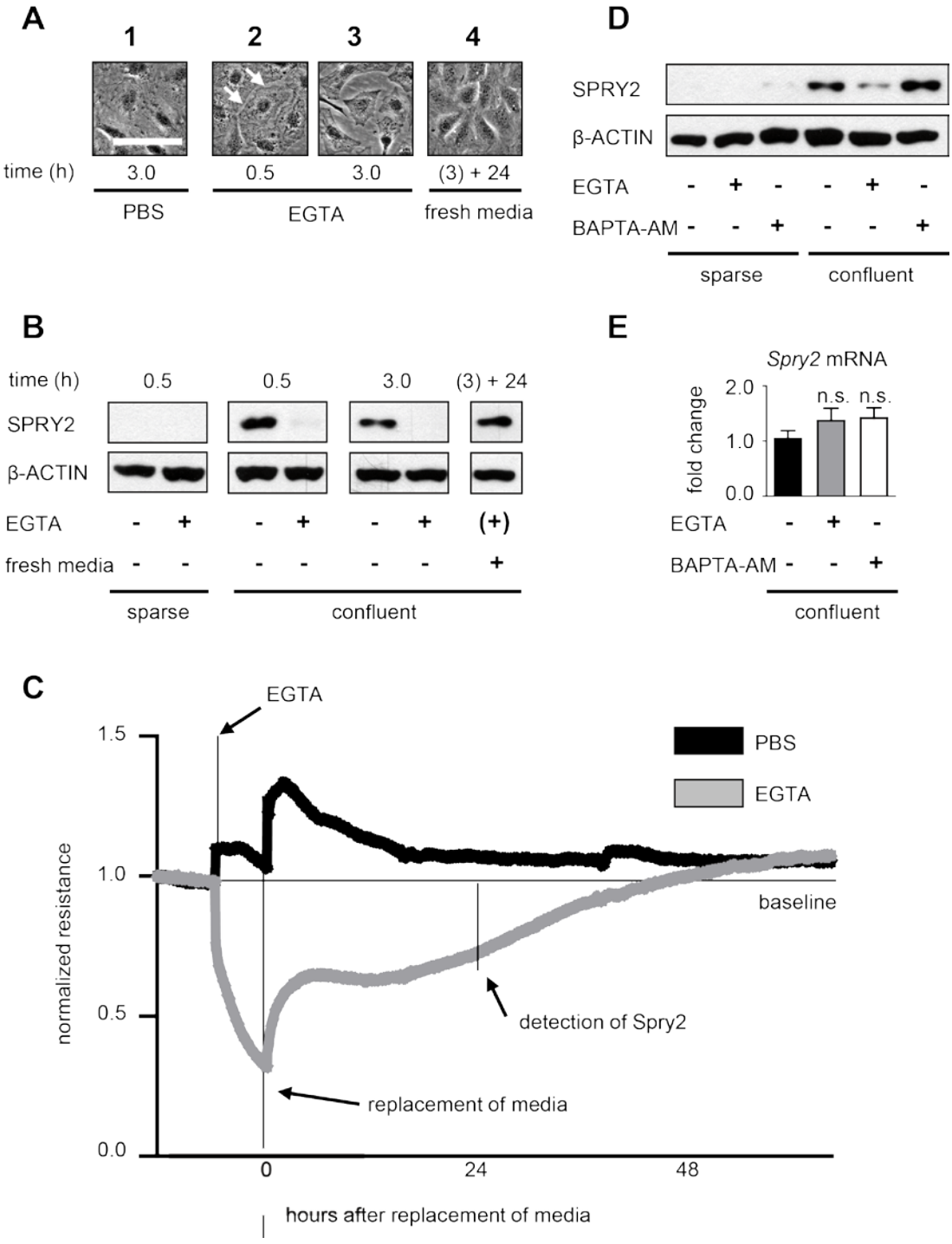

Figure 20. SPRY2 protein expression depends on an intact endothelial monolayer. (A, panels 1-3) Micrographs (scale bar 100 μm) of MAECs plated at confluence and treated with PBS (the control) or EGTA for the indicated time. (A, panel 3) After 3 hours, EGTA was replaced by fresh growth media, and cells were grown for an additional 24 hours. (B) SPRY2 expression after EGTA treatment. Cells were collected after the indicated incubation time with PBS or EGTA or 24 hours after replacement of EGTA with fresh media (3.0 + 24). The membranes were reprobed with β-Actin. (C) Cells were plated at confluence, and total resistance was measured in real time by ECIS. When cells reached a steady plateau in resistance (baseline), either EGTA or PBS was added to the cells. After 8 hours new media was added to all cells and the time point was set to zero. (D) Cells were treated with either EGTA or BAPTA-AM for 3 hours and analyzed for SPRY2 expression and β-Actin. (E) In parallel experiments, total RNA was isolated from cells that had been treated with EGTA, BAPTA-AM, or PBS. *Spry2* mRNA levels then were determined by using qRT-PCR and normalized to GAPDH. The values shown are means +/- s.e.m.; n=3.

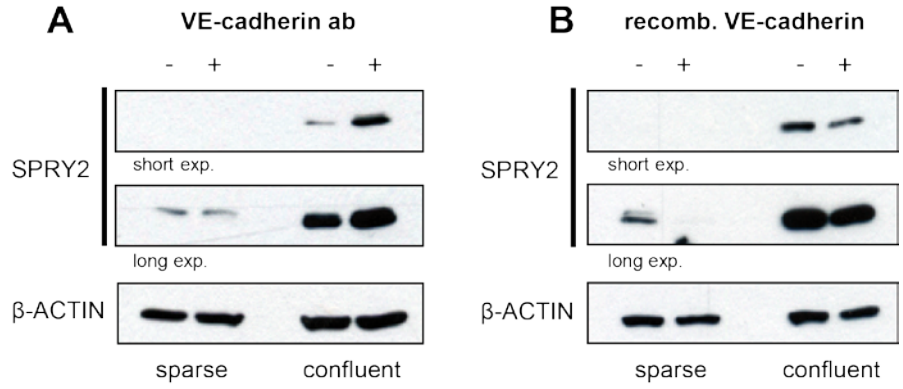

Figure 21. VE-cadherin affects SPRY2 protein levels. (A) Sparse and confluent cells were incubated with anti-VE-cadherin antibody (10 μg / ml) for 6 hours and analyzed for SPRY2 protein expression by immunoblotting. (B) Recombinant VE-cadherin protein (+; 2.5 μg / ml) or BSA (-; 2.5 μg / ml) was added to sparse or confluent cells for 6 hours prior toSPRY2 detection by Western blotting. Both membranes were reprobed with β-Actin.

6.7 High cell density induces SPRY2 and correlates with decreased ERK1/2 phosphorylation

To monitor whether ERK1/2 activity is affected by confluence in MAECS, we compared ERK1/2 phosphorylation in sparse and confluent cells in response to FGF2 stimulation. Sparse and confluent un-stimulated cells displayed no ERK1/2 activity. Stimulation of sparse cells with FGF2 for 3, 9 and 24 hours induced MAPK phosphorylation at the time points measured. Stimulation of confluent cells with FGF2 strongly increased ERK1/2 phosphorylation after 3 and 9 hours (Fig. 22A1). However

after 24 h, the activity decreased markedly and was significantly lower in confluent compared to sparse cells (Fig. 22A2). These expected observations are in line with the results of Vinals et al. obtained in murine lung endothelial cells [5]. SPRY2 is a well-established modulator of MAPK activity [10, 117] and might therefore inhibit ERK1/2 activity in confluent cells. As expected, FGF2 treatment also increased SPRY2 protein levels. It was interesting to see that this increase in SPRY2 protein expression was much more prominent in confluent cells than in sparse cells (Fig. 22B). To point out the reverse correlation of SPRY2 expression and ERK1/2 phosphorylation, we compared SPRY2 protein expression and ERK1/2 phosphorylation after 24 hours of FGF2 stimulation. In sparse cells, high ERK1/2 phosphorylation levels were detected along with low SPRY2 protein levels. Vice versa, confluent cells expressing SPRY2 at high levels displayed low ERK1/2 phosphorylation levels (Fig. 22C). Of note, FGF2-increased SPRY2 protein expression in confluent cells and to a lesser amount also in sparse cells, suggesting that cell density augmented FGF2-induced SPRY2 expression in confluent cells.

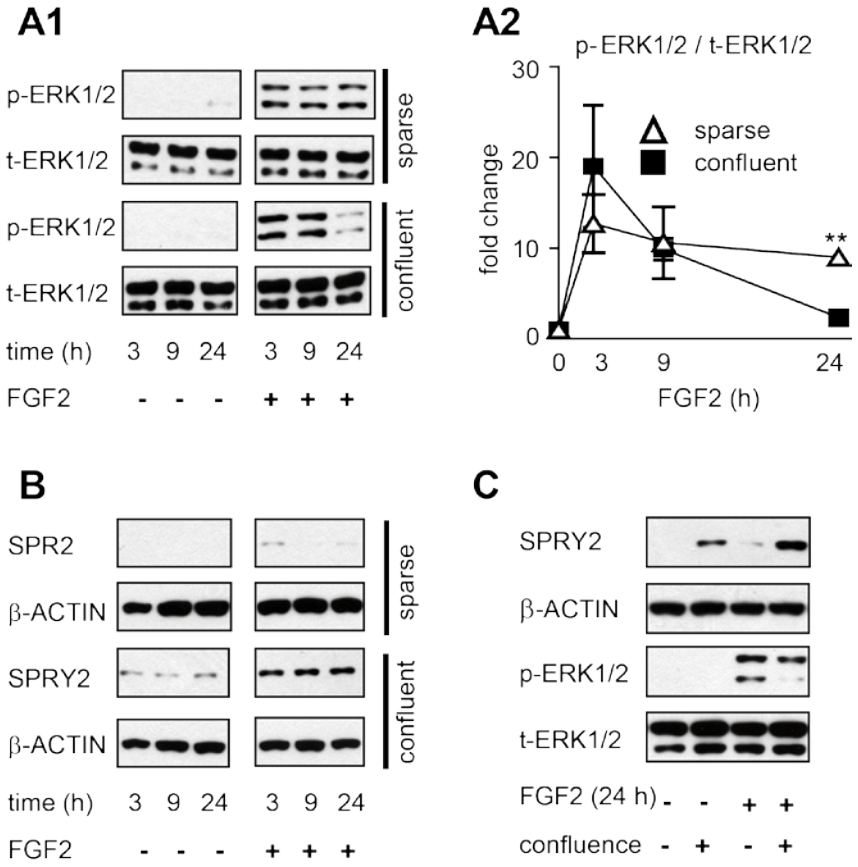

Figure 22. In confluent endothelial cell cultures SPRY2 inhibits ERK1/2 activity. (A1) Cells were plated at sparse or confluent conditions, starved for 24 hours and then stimulated with FGF2 (25 ng / ml) or PBS for the indicated time. Cell lysates were analyzed for ERK1/2 phosphorylation and total protein expression. (A2) Relative phosphorylation levels of ERK1/2 were measured in sparse and confluent cells that had been treated with FGF2 for the indicated amount of time. Values were normalized to the corresponding control at 3 hours. The values shown are means +/- s.e.m.; ** P<0.01; n=3. (B) We analyzed SPRY2 expression in sparse or confluent cells that had been treated with FGF2 (25 ng / ml) or PBS for 3, 9 and 24 hours. (C) Reverse correlation between SPRY2 expression and ERK1/2 phosphorylation after 24 hours of FGF2 stimulation.

6.8 *Spry2* knockout increases FGF2-induced ERK1/2 signaling

We then used *Spry2*$^{fl/fl}$ MAECs to generate *Spry2* knockout cells to further explore the role of SPRY2 and MAPK activity in confluent endothelial cells. *Spry2*$^{-/-}$ and *Spry2*$^{fl/fl}$ showed equal GFP expression 24 hours after adenoviral transfection with Ade-CRE-GFP and Ade-CMV-GFP vectors (Fig. 23A). *Spry2* mRNA knockout was efficient and stable for at least 5 passages after the transfection with Ade-CRE-GFP (Fig. 23B). Immunoblotting confirmed that SPRY2 protein could not be detected in the CRE-transfected cells (Fig. 23C). No evident phenotypic differences could be observed between *Spry2*$^{-/-}$ and *Spry2*$^{fl/fl}$ MAECS during the normal culturing procedure. *Spry2*$^{-/-}$ and *Spry2*$^{fl/fl}$ MAECs were then plated at confluence, starved, and stimulated with FGF2 for 24 hours. The cells were then lysed and assessed for ERK1/2 phosphorylation and SPRY2 protein expression (Fig. 24A).

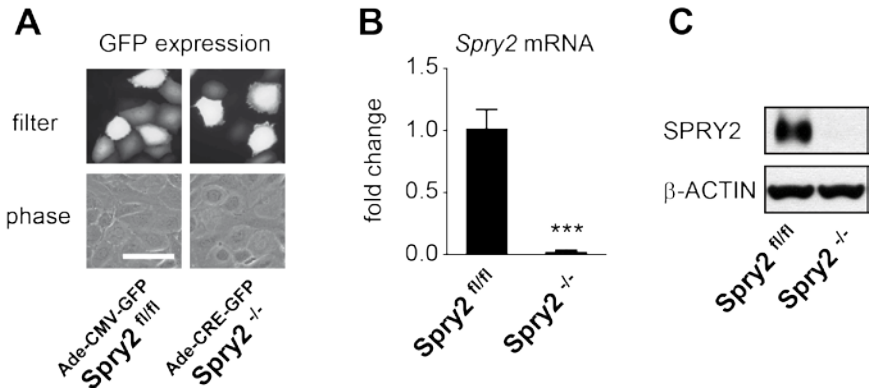

Figure 23. *Spry2* knockout MAECs. (A) GFP expression 24 hours after transfection with either Ade-CRE-GFP (*Spry2*$^{-/-}$) or the corresponding control virus Ade-CMV-GFP (*Spry2*$^{fl/fl}$) (scale bar 100 μm). (B, C) Efficient knockout of *Spry2* was confirmed by using qRT-PCR (Error bars show mean +/- s.e.m.; ***P<0.001; n=3) (B), and immunoblotting (C).

SPRY2 protein was absent in *Spry2*$^{-/-}$ cells. *Spry2*$^{fl/fl}$ cells expressed SPRY2 both with and without FGF2 stimulation. However, after 24 hours of FGF2 stimulation, SPRY2 significantly increased in *Spry2*$^{fl/fl}$ cells. Next we asked, whether *Spry2*$^{-/-}$ MAECs exhibited increased ERK1/2 phosphorylation. Indeed, in *Spry2*$^{-/-}$ cells, FGF2-induced ERK1/2 phosphorylation levels doubled compared to those in *Spry2*$^{fl/fl}$ cells, while ERK1/2 phosphorylation was absent without stimuli in both cell types (Fig. 24B). These results validate that knockout of *Spry2* increased FGF2-mediated ERK1/2 phosphorylation and that SPRY2 inhibits FGF2-induced ERK1/2 activity in confluent *Spry2*$^{fl/fl}$ MAECs. Although the *Spry2*$^{-/-}$ cells exhibited increased ERK1/2 signaling upon FGF2 treatment, the cells did not show any phenotypic alterations. This observation might be due to the fact that the cells were able to form a mature monolayer prior the angiogenic stimulus.

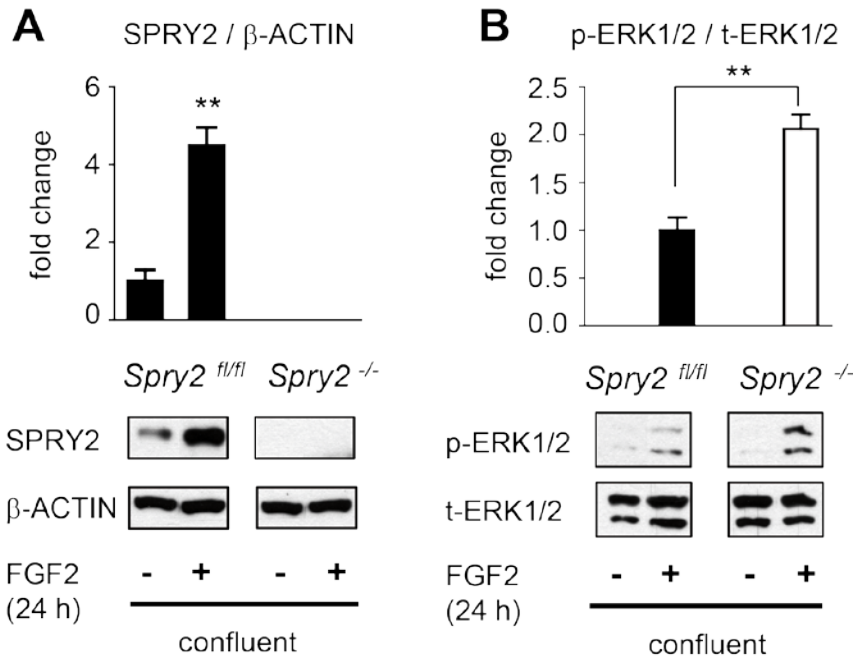

Figure 24. Loss of SPRY2 increases FGF2-induced ERK1/2 phosphorylation. *Spry2*$^{fl/fl}$ and *Spry2*$^{-/-}$ MAECs were seeded at confluence, starved for 24 hours and then stimulated with FGF2 (25 ng / ml) or PBS for 24 hours before lysis and immunoblotting. (A) Densitometric quantification of SPRY2 levels of *Spry2*$^{fl/fl}$ MAECs were normalized to β-Actin. Bars show values +/- s.e.m; ** = p<0.01; n=3. (B) Phosphorylation of ERK1/2 in *Spry2*$^{fl/fl}$ and *Spry2*$^{-/-}$ MAECs with and without FGF2 (25 ng / ml). The membrane was reprobed for total-ERK1/2. Phosphorylation levels were quantified after 24 hours of FGF2 stimulation of *Spry2*$^{fl/fl}$ and *Spry2*$^{-/-}$ MAECs. Bars show values as fold change of FGF2-stimulated *Spry2*$^{fl/fl}$ cells. +/- s.e.m.; ***P*<0.01; n=3.

We therefor decided to plate the cells together with FGF2. To provoke FGF2 specific effects on the endothelial cells we used serum reduced growth media with 1% instead of 10 % FCS. We then analyzed SPRY2 protein expression under these conditions. As expected, reducing the serum content of the growth media also decreased SPRY2 protein expression. This reduction in SPRY2 protein expression, however, was not observed when the cells were cultured with 1% FCS in the presence of FGF2 (Fig. 25).

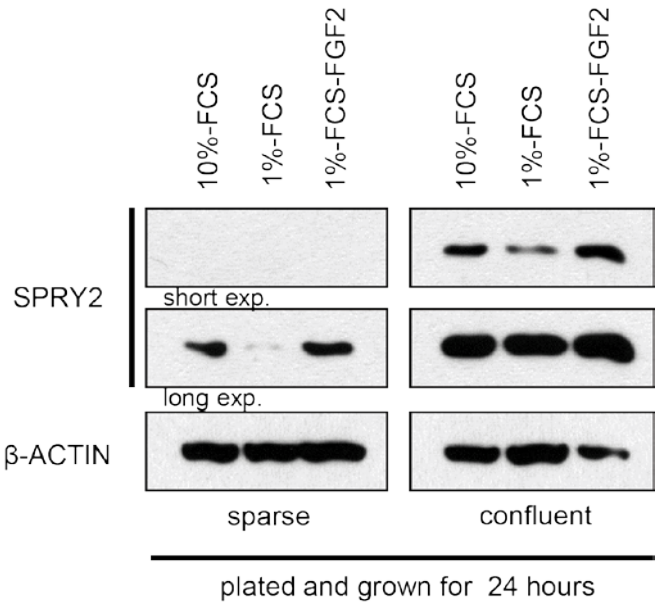

Figure 25. SPRY2 expression of serum reduced cultures in the presence and absence of FGF2. Cells were plated at sparse or confluent conditions in the presence of 1% and 10 % serum without FGF2 and 1% serum with FGF2 (25 ng / ml) and then grown for 24 h. SPRY2 protein expression was analyzed by immunoblotting. Equal loading was confirmed by reprobing the membranes with the anti β-Actin antibody.

6.9 *Spry2* knockout results in loss of contact inhibition and endothelial monolayer integrity in the presence of FGF2

To evaluate the role of SPRY2 in the formation of the endothelial monolayer, we seed *Spry2*$^{-/-}$ (knockout) and *Spry2*$^{fl/fl}$ (wild type) MAECs at confluence in the presence or absence of FGF2. We observed that *Spry2*$^{-/-}$ MAECs grown for 48 hours in the presence of FGF2, were incapable of forming a mature monolayer and displayed an elongated, angiogenic phenotype with longitudinal gaps between the cells and little cell-cell contacts (Fig. 26B). In contrast to the latter results, *Spry2*$^{fl/fl}$ MAECs

formed a regular cobblestone-type cell monolayer with only a few elongated cells (Fig. 26A). FGF2 was required to disturb layer formation in *Spry2*$^{-/-}$ MAECs, because without FGF2 inclusion, *Spry2*$^{-/-}$ and *Spry2*$^{fl/fl}$ cells both formed a regular mature monolayer (Fig. 26A, B).

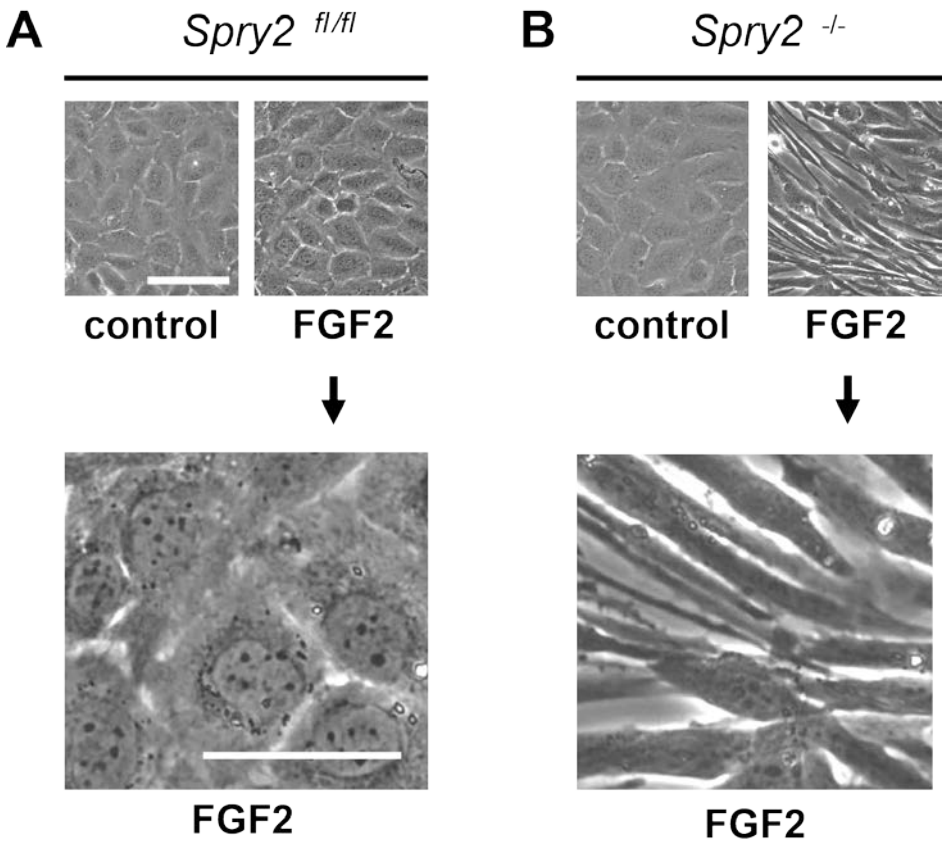

Figure 26. *Spry2*$^{-/-}$ MAECs grown to high cell densities are incapable of forming a cobblestone shaped monolayer. (A and B) Micrographs (scale bar 100 μm) that show *Spry2*$^{fl/fl}$ (A) and *Spry2*$^{-/-}$ (B) cells plated at confluence and then grown for 48 hours in the presence of 1% FCS both with and without FGF2 (25 ng / ml). Magnification (scale bar 50 μm) of the FGF2-treated *Spry2*$^{fl/fl}$ and *Spry2*$^{-/-}$ cells is also shown.

To further characterize the perturbed endothelial monolayer formation by *Spry2*$^{-/-}$ cells, we analyzed proliferation and permeability. Cell numbers increased significantly in *Spry2*$^{-/-}$ MAECs as compared to *Spry2*$^{fl/fl}$ MAECs after 48 hours of FGF2-stimulation (Fig. 27A). Again, no difference was observed between *Spry2*$^{-/-}$ and *Spry2*$^{fl/fl}$ when cells were grown without FGF2. Importantly, the monolayer formed by *Spry2*$^{-/-}$ cells exhibited significantly increased permeability against 70 kDa FITC-Dextran in the presence of FGF2, while no difference was observed in cells without FGF2 (Fig. 27B).

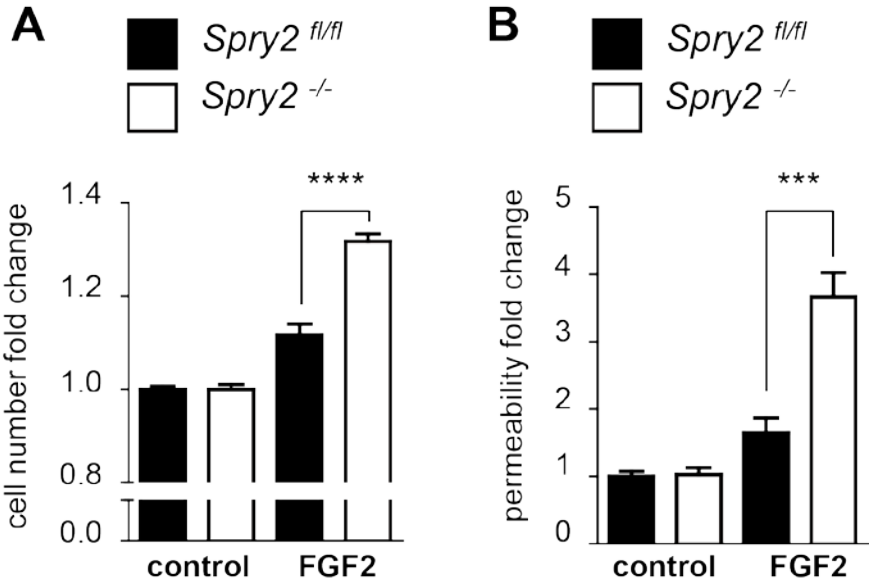

Figure 27. *Spry2*$^{-/-}$ MAECs show increased proliferation and are incapable of forming a functional and impermeable endothelial monolayer in the presence of FGF2. (A) Changes in the numbers of *Spry2*$^{fl/fl}$ and *Spry2*$^{-/-}$ cells were measured by using alamarBlue assay. Cells were plated at 90% confluence and grown for 48 hours in the presence of 1% FCS both with and without FGF2 (25 ng / ml). Then alamarBlue was added and the change in fluorescence measured after 3 hours. The values obtained for the controls without FGF were normalized to 1. Bars show values as fold change of control +/- s.e.m; **** = p<0.0001; n=4. (B) The change of the permeability of *Spry2*$^{fl/fl}$ and *Spry2*$^{-/-}$ monolayer in the presence of FGF2. Cells were seeded at confluence on a well insert in the presence of 1% FCS with and without FGF2 (25 ng / ml). The permeability of the monolayer to 70 kDa FITC-Dextran after 10 min was evaluated by measuring fluorescence of the lower well. The values obtained for the controls without FGF were normalized to 1. Bars show values as fold change of control +/- s.e.m; ***=p<0.001; n=4.

6.10 Inhibition of ERK1/2 signaling restores the wild type monolayer morphology of *Spry2*$^{-/-}$ MAECs

Next we asked whether inhibiting the MAPK ERK1/2 pathway could rescue disturbed endothelial monolayer formation of *Spry2*$^{-/-}$ cells. We therefore plated *Spry2*$^{fl/fl}$ MAECs and *Spry2*$^{-/-}$ MAECs in the presence or absence of U0126. After 1 hour, FGF2 or PBS (control) was added and cells were grown for 48 hours. Again, *Spry2*$^{-/-}$ MAECs showed a highly angiogenic phenotype in the presence of FGF2. However, when cells were pre-incubated with U0126 before adding FGF2, the wild type cobblestone phenotype was restored (Fig. 28A).

To demonstrate the efficacy of ERK1/2 inhibition by U0126, samples were collected 4 hours after addition of the inhibitor and analyzed by immunoblotting. In the absence of U0126, FGF2 induced ERK1/2 phosphorylation in *Spry2*$^{fl/fl}$ and *Spry2*$^{-/-}$ MAECs (Fig 28B1). Again, the FGF2-induced ERK1/2 phosphorylation was more prominent in *Spry2*$^{-/-}$ MAECs (Fig. 28B2). When cells were grown in the presence of U0126, ERK1/2 activity was efficiently inhibited in *Spry2*$^{fl/fl}$ and *Spry2*$^{-/-}$ MAECs. Interestingly, SPRY2 expression depended on ERK1/2 activity, since in *Spry2*$^{fl/fl}$ MAECs, U0126 reduced SPRY2 protein expression (Fig. 28B1).

HIF-1α expression increases endothelial barrier permeability [165] and interferes with tight- and adherens junctions [166]. Since HIF-1α expression can be regulated by growth factors independent of hypoxia [167], we asked whether *Spry2*$^{-/-}$ MAECs showed enhanced HIF-1α expression in the presence of FGF2. FGF2 markedly increased HIF-1α expression (Fig. 28C). However, no significant difference could be observed between *Spry2*$^{fl/fl}$ and *Spry2*$^{-/-}$ MAECs, suggesting that FGF2-induced HIF-1α expression is not affected by SPRY2. Of note, pretreatment of the cells with the ERK1/2 inhibitor U0126 prevented FGF2-induced HIF-1α expression in *Spry2*$^{fl/fl}$ and *Spry2*$^{-/-}$ MAECs, suggesting that FGF2 increased HIF-1α expression via ERK1/2 (Fig. 28C). Although the overall expression of HIF-1α was not affected by *Spry2* knockout, we cannot rule out that SPRY2 controls HIF-1α activity and thereby maintains vascular integrity.

Altogether these findings show that SPRY2, as a regulator of ERK1/2 activity, is indispensable for endothelial cells to properly form a monolayer and maintain barrier integrity in the presence of FGF2. We feel that expression SPRY2 is especially important in the early phase of the monolayer formation.

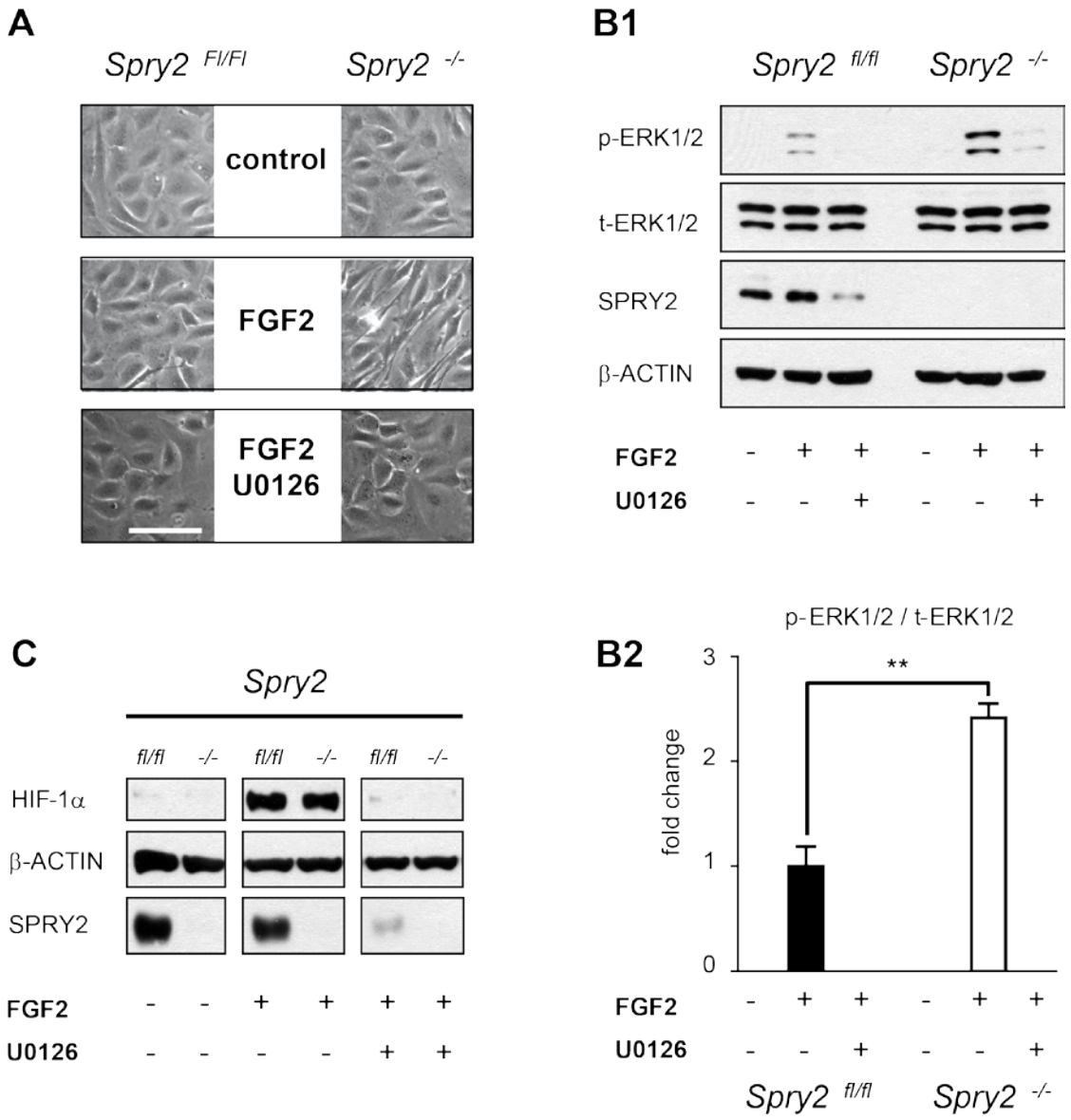

Figure 28. Inhibition of ERK1/2 rescues the wild type endothelial monolayer morphology. (A) Micrographs that show *Spry2*$^{fl/fl}$ and *Spry2*$^{-/-}$ cells plated at confluence in the absence or presence of FGF2 (25 ng / ml) and then grown for 48 hours. Where indicated, cells were incubated with U0126 (5 μM) 1 hour prior the addition of FGF2 (scale bar 100 μm). (B1) MAECs were plated at confluence in the presence or absence of FGF2 both with and without pre-incubation with U0126 (5 μM). Cells were collected 4 hours after seeding and then analyzed by immunoblotting. (B2) Densitometric quantification of the ERK1/2 phosphorylation levels of B1. Bars show values as fold change of FGF2-stimulated *Spry2*$^{fl/fl}$ cells. +/- s.e.m.; ***P*<0.01; n=3. (C) MAECs were plated at confluence in the presence or absence of FGF2 both with and without 1 hour pre-incubation with U0126 (5 μM). Cells were collected 4 hours after seeding and then analyzed by immunoblotting.

7 DISCUSSION

The establishment of a mature, organized vascular network is fundamental for tissue homeostasis. Therefore, the formation of new vessels (angiogenesis) is an essential physiological process for embryologic development, organ growth, and tissue repair. During angiogenesis, a concerted action of hypoxia and growth factors induce vascular cell proliferation, migration and lumen formation [11, 19, 24, 84]. Once primary vessels have formed, endothelial cells shift their response from proliferation and migration to vessel maturation and stabilization giving rise to new, functional blood vessels that are able to control permeability and supply the newly vascularized areas with oxygen and nutrients. In this state, endothelial cells form a tight monolayer, resist apoptosis and remain quiescent even in the presence of pro angiogenic factors [2, 3]. The balance between quiescence and angiogenesis is tightly regulated at the molecular level and results in a tissue-specific, structured, hierarchically organized and functional vascular tree [105]. Loss of vascular integrity and dysregulated angiogenesis is a hallmark of various pathologies including cancer, inflammatory disorders, atherosclerosis and age-related macular degeneration [168, 169].

It is therefore important to understand how cells precisely control and restrict signaling events when vascular integrity has to be maintained. On the other hand endothelial cells need to keep the capability to proliferate and migrate in situations, where neovascularization is urgently needed. This thesis adds to the understanding of how endothelial cells can react to growth factor stimuli in respect to their current situation (sparse vs. confluent), and provide new insights into one of the last steps of angiogenesis: the formation and maintenance of the endothelial monolayer.

The Sprouty (SPRY) family of proteins is a highly conserved group of negative feedback loop modulators which control MAPK-signaling in endothelial cells [9, 10]. Our results show a novel cell density-dependent upregulation of SPRY2 in mouse aortic endothelial cells. We further demonstrate that SPRY2 contributes to the establishment of endothelial quiescence and barrier integrity via inhibiting the FGF2-ERK1/2 signaling. Accordingly, ablation of SPRY2 resulted in de-regulated FGF2-ERK1/2 signaling and disturbed endothelial monolayer formation through loss of contact inhibition and barrier integrity.

7.1 SPRY2 expression increases with higher cell density

Results of this thesis reveal a novel mechanism whereby Sprouty2 is upregulated in a cell-density-dependent manner during formation of the endothelial monolayer. SPRY2 exclusively acts as an adaptor protein without any enzymatic activity [127]. Therefore, cells have restricted possibilities to control SPRY2 function: by regulating its abundance [143-145], its localization [10, 123], and/or its post-transcriptional modifications [119, 126, 170]. Here we show, that in primary endothelial cells, SPRY2 is regulated in a previously unknown cell-density dependent fashion: Sparse cell cultures express low SPRY2 protein levels (Figs. 14, 16), which may allow endothelial cell proliferation, migration, and tube formation during angiogenesis and wound closure [7, 10]. In dense cell cultures, SPRY2 expression is highly elevated (Figs. 14, 16), which may inhibit endothelial proliferation and, thus, maintain vascular integrity and quiescence. Indeed, ablation of SPRY2 in confluent cells increases cell proliferation and the permeability of the endothelial monolayer (Fig. 27). In accord with our findings, Zhang et al. (2005) showed in vivo that SPRY2 protein decreased in the vasculature after an injury to the endothelial lining of the carotid artery in rats and then reappeared weeks later after the inner endothelial lining had re-formed [149].

A few studies have shown density dependent effects of SPRY2 in fibroblasts and breast carcinoma cells [157, 171, 172]. However, a direct density-dependent regulation of SPRY2 has not been described. Confluent p38α knock out MEFs showed increased SPRY2 levels when compared to confluent wt MEFs. The authors suggested that p38α mediates growth arrest at confluence via SIAH2 dependent SPRY2 downregulation [172]. We therefore asked whether cell density dependent regulation of SPRY2 is restricted to endothelial cells. However, HBL-100 and Caco2 cells also exhibit a cell density dependent regulation pattern of SPRY2 protein expression. Although both cell lines grow to higher densities than endothelial cells, they exhibit a monolayer like structure and partial contact inhibition (Fig. 17). Therefore, it would be interesting to assess, whether *Spry2* knockout in these cells would promote cancer growth and metastatic potential due to loss of monolayer integrity. Indeed, Sprouty protein expression is distinctly controlled in a number of cancers. In breast cancer cells, *SPRY2* transcription is suppressed by aberrant hypermethylation [173]. McKie et al. have shown SPRY2 downregulation in prostate cancer [174], while others have reported SPRY2 downregulation in liver cancer [131].

7.2 Increased SPRY2 expression at high cell densities – Hypoxia, cell-cell contacts or both?

Several mechanisms may increase SPRY2 protein at high cell density. SPRY2 protein levels steadily increased in endothelial cells growing towards confluency. In the sub-confluent phase, SPRY2 expression correlated with reduced oxygen saturation and increased HIF-1α protein levels. Exogenously applied hypoxia increased SPRY2 protein in both sparse (results not shown) and confluent cells (Fig. 15). Together with data from a previous study demonstrating that hypoxia regulates Sprouty proteins by prolyl hydroxylases [145], these results point to hypoxia as a general post-transcriptional stimulus for SPRY2. In vivo, hypoxia-induced SPRY2 expression may provide a protective homeostatic function when the vasculature is exposed to hypoxia. Endothelium that is subjected to oxygen deprivation maintains cell viability and basic biosynthetic mechanisms, but it displays multiple changes in barrier function, that are relevant to vascular homeostasis [175, 176].

The observation that SPRY2 expression still remains elevated in confluent cells showing normoxic oxygen levels points to another essential mechanism for stabilizing SPRY2 in confluent cultures. We have ruled out the possibility that confluent cells secrete a soluble factor to stimulate SPRY2 expression, instead intact cell-cell contact seem important. Indeed, targeting endothelial cell-cell contacts by Thrombin and TNFα [160, 161] decreased SPRY2 expression in confluent cells (Fig. 19). Accordingly, TNFα downregulated SPRY2 in murine Swiss 3T3 fibroblasts and MLE15 lung epithelial cells. The authors speculated that TNFα modulated SPRY2 translation via p38 MAPK signaling [144]. Therefore, we cannot rule out that TNFα affected SPRY2 protein by signaling events, which might be independent of cell-cell contacts.

N- and VE-cadherins are components of endothelial adherens junctions [56, 163] and interact with cadherins of neighboring cells in a homophilic manner [57]. These adhesive complexes strictly depend on extracellular calcium [59, 162]. We show that Ca^{2+} depletion disrupts cell-cell contacts and rapidly destabilizes SPRY2 protein. Conversely, re-establishing cell-cell contacts stabilizes SPRY2 protein again (Fig. 20). SPRY2 protein levels restores after recalcification at a stage, at which impermeability has not yet completely reestablished. Thus, singular cell-cell contacts are already sufficient to stabilize SPRY2 protein levels. Cadherin clustering-induced signaling events might stabilize SPRY2 levels when cells first touch each other before absolute

confluency is reached and junctions are fully stabilized [177, 178]. Interestingly, the addition of a VE-cadherin binding antibody increases SPRY2 protein levels in confluent but not in sparse cells (Fig. 21A). This antibody is supposed to block VE-cadherin homophilic interactions [164] but it might be possible that the antibody crosslinks adjacent VE-cadherin and thereby induces cadherin signaling events [47, 54]. It might therefore be necessary to increases the blocking antibody concentration to interfere with the homophilic VE-cadherin interactions. Furthermore, it will be indispensable to use a corresponding control antibody. Indeed, when cells were plated in the presence of high concentrations of the VE-cadherin blocking antibody, the SPRY2 protein decreased (preliminary finding; results not shown). When we add soluble recombinant VE-cadherin the opposite, i.e., inhibition of VE-cadherin clustering, may occur. Hereby, the soluble protein might interfere with existing VE-cadherin cell-contacts. However, the SPRY2 downregulation is also observed in sparse cells (Fig. 21B). Taken together, it remains uncertain how VE-cadherin influences SPRY2 expression.

Taddei et al. described reduced *Spry2* mRNA levels in confluent VE-cadherin expressing endothelial cells via inactivation and nuclear exclusion of the *Spry2* transcription factor FoxO1 [179]. This observation is in disagreement with our finding that FoxO1 phosphorylation decreases with higher cell-density (Fig. 18). Dephosphorylated FoxO1 exhibits increased transcriptional activity and predominantly localizes to the nucleus [159, 180]. Surprisingly, its downregulation by siRNA affects neither *Spry2* transcription nor SPRY2 protein expression at high cell density (Fig. 18).

Paik et al. have recently shown that FoxO silencing downregulated *Spry2* in liver but not in lung endothelial cells [148]. An explanation for this observation could be a vascular-bed-specific transcriptional regulation of *Spry2* involving a specific set of transcriptional co-activators. Beside the FoxO binding elements, the *Spry2* promoter contains at least on additional binding element for the ETS-1 transcription factor. Like the FoxOs, the ETS transcription factors are required for proper angiogenesis and endothelial function [181]. However, whether ETS-1 effectively increases *Spry2* expression is not known.

In summary, two independent and consecutive stimuli – transient intrinsic hypoxia and establishment of cell-cell contacts – induce and stabilize SPRY2 protein levels. However the specific cell-cell contact molecule, which stabilizes SPRY2 at high cell densities, remains to be identified.

7.3 Hypoxia in cell cultures – a neglected factor?

Although this study is not the first to show that oxygen saturation in conventional monolayer cell cultures may be considerably lower than in the incubation gas [158], this important fact remains ignored regularly. The emerging pericellular hypoxia likely affects cellular metabolism [182, 183], transcription [184], protein synthesis [185] and viability [186] and thus should be considered for the interpretation of *in vitro* results.
When oxygen concentrations drop below their physiological levels, the cellular energy production is rapidly switched to anaerobic glycolysis [184], and the cell cycle of most cells is arrested to decrease the O_2 demand [187]. Some specialized cells, i.e. vascular endothelial cells (ECs), vascular smooth muscle cells and embryonic fibroblasts increase their proliferation in response to hypoxia [41, 188] and participate in the formation of new microvessels to increase oxygen concentrations in particular tissues [189]. *In vivo*, the physiologic oxygen concentration in different tissues varies from 10-14% in arterial blood, to less than 10% in the myocardium, and to 8-2% in the liver, cartilage or bone marrow [167]. New technics such as real-time measurement of the in-culture-oxygen saturation (Figs. 14, 15) allow monitoring the O_2 consumption of the cultured cells. This parameter then could be used to adapt the oxygen saturation of cultured cells to the physiological oxygen concentration found in the corresponding tissue or organ thereby helping to better simulate the actual *in vivo* situation.

7.4 SPRY2 expression controls monolayer integrity and quiescence via inhibiting FGF2-ERK1/2 signaling

Mechanisms that restore, stabilize, and continue to maintain the endothelial barrier function are the final stage in the morphogenesis of new microvessel formation [3]. The inhibition of cell-cell contact promotes the switch from an angiogenic and proliferative state to a quiescent endothelial cell phenotype. Membrane proteins, in addition to maintaining cell-cell adhesion, also sense cell-cell interactions and transduce this information to intracellular signals [2, 79]. Decoupling of the MAPK pathway is part of the mechanism that arrests growth in confluent endothelial cells [5].
The findings of Vinals and Pouyssegur [5] and the results of this study (Fig. 22A1, A2) demonstrate that FGF2-induced MAPK activity decreased with time in confluent

cells. SPRY2 is a well-known feed-back loop inhibitor of RTK signaling and modulates ERK1/2 activity in different settings [9]. Therefore, we hypothesize that SPRY2 plays a role as a general feedback inhibitor of cell growth that might directly promote cessation of cell growth in the presence of cell-cell contacts.

In confluent cells, SPRY2 expression correlated with decreased ERK1/2 activity (Fig. 22C). Conversely, *Spry2* knockout increased FGF2-induced ERK1/2 signaling in confluent cell cultures (Fig. 24B). The finding that SPRY2 function is affected by cell density is in agreement with previous studies. Kajita et al. have shown that overexpression of SPRY2 inhibited PDGF-induced ERK1/2 activity in dense, but not in sparse NIH 3T3 fibroblast cell cultures [171]. In a similar fashion, SPRY2 function in T47D breast carcinoma cells also depended on cell density [157].

ERK-dependent SPRY2 expression has been reported in many studies [10, 117, 128, 134, 190, 191]. However, it is not known whether this expression pattern depends on cell density. Based on the observation that FGF2 increases SPRY2 expression predominantly in confluent cells (Figs. 22B, C), we assume that FGF2-induced SPRY2 expression might be somehow connected to cell-cell contacts and thereby allow cell-density dependent function of SPRY2. Indeed, preliminary results revealed that increasing cell density possibly dephosphorylates SPRY2 (results not shown). Lao et al. showed that SPRY2 dephosphorylation is a perquisite for ERK inhibition under certain circumstances [130]. At this point however, it is too soon to speculate whether this modification affects SPRY2 function at high cell density.

Although FGF signaling has been identified as a strong pro-angiogenic factor in physiological [84] and pathological situations [192], Murakami et al. [83] have demonstrated that it also plays a key role in the maintenance of vascular integrity, because a loss of FGF results in severe impairment of the endothelial barrier function and eventually to a disintegration of the vasculature. Thus, it would not be favorable for endothelial cells to just block FGF signaling at confluence. Therefore, we propose that SPRY2, as key element embedded in the FGF system, might switch the response of endothelial cells from proliferation and migration to survival and quiescence through control of ERK1/2 activity (Fig. 29).

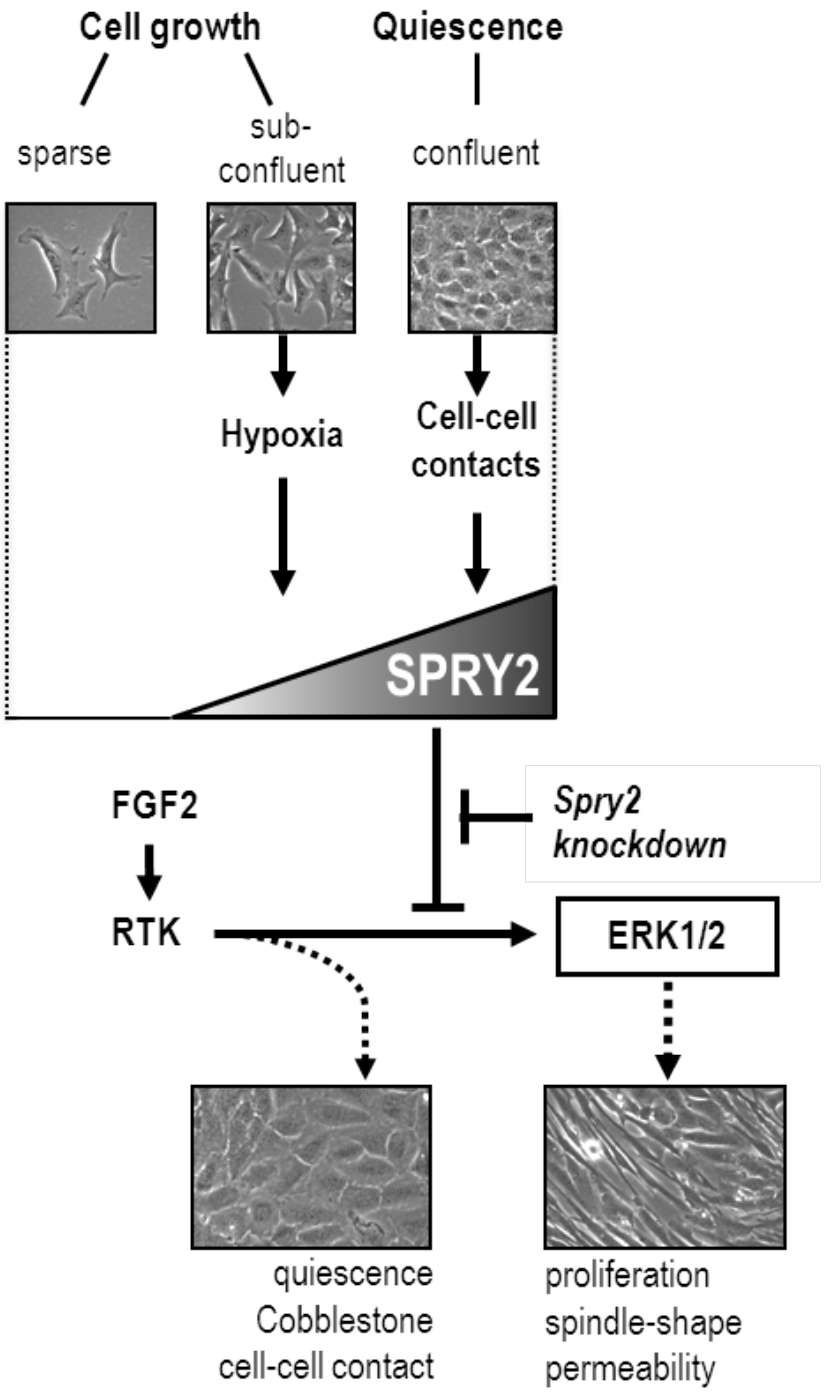

Figure 29. A working model for the regulation of SPRY2-dependent endothelial quiescence and integrity. In wt endothelial cells (*Spry2*$^{fl/fl}$), SPRY2 is upregulated by increasing cell density via transient hypoxia in subconfluent cells and cell-cell contacts in confluent cells. SPRY2 expression allows the endothelial monolayer to retain its integrity and cell quiescence, upon FGF stimulation. In the absence of SPRY2 (*Spry2* knockout), FGF signaling extensively activates ERK1/2. ERK1/2 elicits an endothelial phenotype change from cobble-stone to spindle shape endothelial cells, induces proliferation, and increases permeability.

Indeed, we show that SPRY2 regulates quiescence and integrity of the endothelial monolayer: Whereas the endothelial monolayer remains quiescent in wild type cells, with low mitogenicity, low basal permeability, and the typical cobblestone morphology, the *Spry2*$^{-/-}$ cells fail to form a connected monolayer and exhibit a spindle-shaped morphology with increased proliferation and permeability. The observed phenotype is likely due to deregulated FGF signaling: First, ERK1/2 activity increases considerably in *Spry2*$^{-/-}$ cells during the early phase of monolayer formation and second, pre-incubation of *Spry2*$^{-/-}$ cells with the MAPK inhibitor U0126 is sufficient to restore the wild type-like cobblestone phenotype.

Experimental evidence in several studies suggests that FGF2 activates the VEGF/VEGFR system [193, 194]. Whereas fine-tuned intracellular VEGF-A/VEGFR-2 signaling supports endothelial survival in established mature blood vessels [195], uncontrolled expression of VEGF-A exceeding physiological thresholds leads to the formation of unstable and leaky blood vessels [196] or even hemangiomas [197]. SPRY2 could potentially interfere with this signaling cascade and prevent activation of the VEGF/VEGFR system by FGF in quiescent blood vessels. Sasaki et al. showed that Sprouty4 suppressed VEGF induced ERK activation [142]. Therefore SPRY2 might also interfere with VEGF signaling in a similar fashion.

Spry2 knockout animals display discrete developmental defects that have been attributed to unrestricted FGF signaling [151, 153-155]. Although we observe that *Spry2* knockout markedly affects endothelial quiescence and integrity in vitro, the *Spry2* knockouts described so far exhibit rather mild malformations without an overt vascular phenotype. This discrepancy might be due to redundancies amongst the Sprouty isoforms in in vivo models. Furthermore, exposition of the knock out animals to stress such as severe hypoxia or to high doses of growth factors may hypothetically reveal additional SPRY2 specific phenotypes.

Taken together, cell density (and FGF2)-induced SPRY2 may play a central role in terminating FGF-ERK1/2 signaling and thereby maintaining endothelial monolayer integrity and quiescence.

7.5 SPRY2 expression might be beneficial to treat disease related to dysregulated FGF signaling in the vasculature

The data of the present thesis revealed that high SPRY2 expression levels play a critical role in establishing endothelial monolayer integrity by inhibiting FGF2-induced ERK1/2 signaling. This negative feed-back loop may be important in situations, where endothelial monolayers form, where the regulation of basal permeability must be strict, and where vascular integrity and quiescence must be established and maintained in vivo.

Although necessary to promote tissue repair, FGF2 may also worsen injuries [198] by contributing to the harmful neovascularization of chronic inflammatory diseases such as rheumatoid arthritis [199] and inflammatory bowel disease [200]. SPRY2 expression at sites of chronic inflammation might therefore locally restrict these negative effects of FGF secretion.

Despite having an abundant number of vessels, tumors are usually hypoxic and nutrient-deprived because their disturbed vessel architecture [169]. Such abnormal milieu impairs drug delivery and enhances the metastatic potential. Preclinical and initial clinical studies revealed that tumor vessel normalization is a promising complementary therapeutic approach to treat cancer [20, 201]. We propose that SPRY2 expression may be an option to sequester excessive FGF-signaling and to redirect it from vessel growth to the maintenance of vascular integrity thereby contributing to tumor vessel normalization.

8 CONCLUSION AND KEY POINTS

In conclusion, the data of the present thesis show for the first time that high SPRY2 expression levels play a critical role in endothelial monolayer establishment and maintenance. In wild type MAECs, SPRY2 expression was driven by transient hypoxia and emerging cell-cell contacts in cells growing to high density, whereas expression was reduced in sparse single proliferating cells. We were particularly interested to determine how endothelial cells process signals arising from increasing cell density to allow a switch from a proliferative, migratory phenotype to a quiescent, impermeable monolayer. We therefore compared the ability of primary *Spry2* expressing (*Spry2*$^{fl/fl}$) and *Spry2* knockout (*Spry2*$^{-/-}$) mouse aortic endothelial cells (MAECs) to form a functional endothelial monolayer. *Spry2* knockout MAECs were incapable of forming a functional, impermeable endothelial monolayer in the presence of FGF2 when grown to high cell densities. Dense *Spry2* knockout MAECs showed spindle-like shapes, unrestricted proliferation, and exhibited enhanced signaling by the FGF2 downstream target ERK1/2. Wild type cobblestone monolayer morphology, however, was restored upon inhibiting ERK1/2 activity in *Spry2* knockout cells. The main findings can be summarized in the following key points:

1. SPRY2 expression increases with higher cell densities in mouse aortic endothelial cells.
2. Transient hypoxia increase SPRY2 protein expression during the formation of the endothelial monolayer.
3. Calcium dependent cell-cell contacts stabilize SPRY2 protein at confluence.
4. At high cell-densities, enhanced SPRY2 protein levels correlate with decreased ERK1/2 phosphorylation.
5. Dense *Spry2*$^{-/-}$ cells exhibit increased FGF2-induced ERK1/2 signaling.
6. In the presence of FGF2, dense *Spry2* knockout cells loose contact inhibition and the ability of forming a functional, impermeable monolayer.
7. Inhibition of ERK1/2 in *Spry2* knockout MAECs restores the wild type cobblestone monolayer morphology.

9 LIMITATIONS AND OUTLOOK

The following limitations may restrict the significance of the present study: most of the experiments in this study were performed with MAECs. It is difficult to predict whether the effects of the studied molecules are conserved in other species, e.g. humans. It is unclear whether our data can be extrapolated to other vascular cell types and tissues. Besides, the readouts of the *in vitro* studies performed may not reflect the *in vivo* situation. Therefore, caution should be taken when the data are utilized to interpret in vivo or clinical phenomena.

Additional studies are required to solve many unanswered questions. First, it would be interesting to identify the decisive cell-cell contact molecule(s) which is (are) involved in SPRY2 stabilization at high cell-densities. Future studies might focus on the adherens junction molecule VE-cadherin. Although some results point to an involvement of VE-cadherin in SPRY2 regulation, we were unable to prove the direct connection. The investigation of SPRY2 expression in VE-cadherin knockout endothelial cells would be informative.

Furthermore, potential downstream targets of FGF-induced ERK1/2 signaling need to be investigated to better understand the observed *Spry2* knockout phenotype. It would also be interesting to see whether the expression of the other SPRY isoforms (SPRY1, 3 and 4) is affected by *Spry2* knockout and whether a co-silencing of SPRY1, 3, or 4 would intensify the observed *Spry2* knockout phenotype in MAECs.

Finally, we would like to propose that decreased SPRY2 expression might serve as a prognostic marker for altered vascular permeability and thus, for an increased susceptibility for disease related to defects in the endothelial barrier.

Although the in vivo relevance of our findings remains to be confirmed, our results add to the understanding of how endothelial cells control cell density to switch from a proliferative, migratory phenotype to a quiescent, impermeable monolayer – a process which is crucial not only in the formation of stable and functional blood vessels, but also during organogenesis in general [2, 79, 80].

10 REFERENCES

1. Mader, S.S., *Inquiry into life*. 8th Edition ed. 1997: The MacGraw-Hill Companies.

2. Dejana, E., *Endothelial cell-cell junctions: happy together.* Nat Rev Mol Cell Biol, 2004. **5**(4): p. 261-70.

3. Murakami, M. and M. Simons, *Regulation of vascular integrity.* J Mol Med (Berl), 2009. **87**(6): p. 571-82.

4. Dejana, E., E. Tournier-Lasserve, and B.M. Weinstein, *The control of vascular integrity by endothelial cell junctions: molecular basis and pathological implications.* Dev Cell, 2009. **16**(2): p. 209-21.

5. Vinals, F. and J. Pouyssegur, *Confluence of vascular endothelial cells induces cell cycle exit by inhibiting p42/p44 mitogen-activated protein kinase activity.* Mol Cell Biol, 1999. **19**(4): p. 2763-72.

6. Mailleux, A.A., et al., *Evidence that SPROUTY2 functions as an inhibitor of mouse embryonic lung growth and morphogenesis.* Mech Dev, 2001. **102**(1-2): p. 81-94.

7. Taniguchi, K., et al., *Sprouty2 and Sprouty4 are essential for embryonic morphogenesis and regulation of FGF signaling.* Biochem Biophys Res Commun, 2007. **352**(4): p. 896-902.

8. Mason, J.M., et al., *Sprouty proteins: multifaceted negative-feedback regulators of receptor tyrosine kinase signaling.* Trends Cell Biol, 2006. **16**(1): p. 45-54.

9. Cabrita, M.A. and G. Christofori, *Sprouty proteins, masterminds of receptor tyrosine kinase signaling.* Angiogenesis, 2008. **11**(1): p. 53-62.

10. Impagnatiello, M.A., et al., *Mammalian sprouty-1 and -2 are membrane-anchored phosphoprotein inhibitors of growth factor signaling in endothelial cells.* J Cell Biol, 2001. **152**(5): p. 1087-98.

11. Carmeliet, P., *Angiogenesis in life, disease and medicine.* Nature, 2005. **438**(7070): p. 932-6.

12. Flamme, I., T. Frolich, and W. Risau, *Molecular mechanisms of vasculogenesis and embryonic angiogenesis.* J Cell Physiol, 1997. **173**(2): p. 206-10.

13. Conway, E.M., D. Collen, and P. Carmeliet, *Molecular mechanisms of blood vessel growth.* Cardiovasc Res, 2001. **49**(3): p. 507-21.

14. Bergers, G. and S. Song, *The role of pericytes in blood-vessel formation and maintenance.* Neuro Oncol, 2005. **7**(4): p. 452-64.

15. Swift, M.R. and B.M. Weinstein, *Arterial-venous specification during development.* Circ Res, 2009. **104**(5): p. 576-88.

16. Carmeliet, P. and R.K. Jain, *Molecular mechanisms and clinical applications of angiogenesis.* Nature, 2011. **473**(7347): p. 298-307.

17. Risau, W., *Mechanisms of angiogenesis.* Nature, 1997. **386**(6626): p. 671-4.

18. Semenza, G.L., *Vasculogenesis, angiogenesis, and arteriogenesis: mechanisms of blood vessel formation and remodeling.* J Cell Biochem, 2007. **102**(4): p. 840-7.

19. De Smet, F., et al., *Mechanisms of vessel branching: filopodia on endothelial tip cells lead the way.* Arterioscler Thromb Vasc Biol, 2009. **29**(5): p. 639-49.

20. Mazzone, M., et al., *Heterozygous deficiency of PHD2 restores tumor oxygenation and inhibits metastasis via endothelial normalization.* Cell, 2009. **136**(5): p. 839-51.

21. Carmeliet, P., et al., *Branching morphogenesis and antiangiogenesis candidates: tip cells lead the way.* Nat Rev Clin Oncol, 2009. **6**(6): p. 315-26.

22. Francavilla, C., L. Maddaluno, and U. Cavallaro, *The functional role of cell adhesion molecules in tumor angiogenesis.* Semin Cancer Biol, 2009. **19**(5): p. 298-309.

23. Jain, R.K., *Molecular regulation of vessel maturation.* Nat Med, 2003. **9**(6): p. 685-93.

24. Adams, R.H. and K. Alitalo, *Molecular regulation of angiogenesis and lymphangiogenesis.* Nat Rev Mol Cell Biol, 2007. **8**(6): p. 464-78.

25. Hellberg, C., A. Ostman, and C.H. Heldin, *PDGF and vessel maturation.* Recent Results Cancer Res, 2010. **180**: p. 103-14.

26. Gaengel, K., et al., *Endothelial-mural cell signaling in vascular development and angiogenesis.* Arterioscler Thromb Vasc Biol, 2009. **29**(5): p. 630-8.

27. Armulik, A., A. Abramsson, and C. Betsholtz, *Endothelial/pericyte interactions.* Circ Res, 2005. **97**(6): p. 512-23.

28. Heil, M., et al., *Arteriogenesis versus angiogenesis: similarities and differences.* J Cell Mol Med, 2006. **10**(1): p. 45-55.

29. Heil, M. and W. Schaper, *Insights into pathways of arteriogenesis.* Curr Pharm Biotechnol, 2007. **8**(1): p. 35-42.

30. Eltzschig, H.K. and P. Carmeliet, *Hypoxia and inflammation.* N Engl J Med, 2011. **364**(7): p. 656-65.

31. Schofield, C.J. and P.J. Ratcliffe, *Signalling hypoxia by HIF hydroxylases.* Biochem Biophys Res Commun, 2005. **338**(1): p. 617-26.

32. Kaelin, W.G., Jr. and P.J. Ratcliffe, *Oxygen sensing by metazoans: the central role of the HIF hydroxylase pathway.* Mol Cell, 2008. **30**(4): p. 393-402.

33. Wenger, R.H., D.P. Stiehl, and G. Camenisch, *Integration of oxygen signaling at the consensus HRE.* Sci STKE, 2005. **2005**(306): p. re12.

34. Maes, C., G. Carmeliet, and E. Schipani, *Hypoxia-driven pathways in bone development, regeneration and disease.* Nat Rev Rheumatol, 2012. **8**(6): p. 358-66.

35. Folkman, J., *Angiogenesis: an organizing principle for drug discovery?* Nat Rev Drug Discov, 2007. **6**(4): p. 273-86.

36. Lim, L.S., et al., *Age-related macular degeneration.* Lancet, 2012. **379**(9827): p. 1728-38.

37. Ahn, A., et al., *Therapeutic angiogenesis: a new treatment approach for ischemic heart disease--Part II.* Cardiol Rev, 2008. **16**(5): p. 219-29.

38. Ahn, A., et al., *Therapeutic angiogenesis: a new treatment approach for ischemic heart disease--part I.* Cardiol Rev, 2008. **16**(4): p. 163-71.

39. Humar, R., et al., *Formation of new blood vessels in the heart can be studied in cell cultures.* ALTEX, 2007. **24 Spec No**: p. 35-8.

40. Nicosia, R.F. and A. Ottinetti, *Growth of microvessels in serum-free matrix culture of rat aorta. A quantitative assay of angiogenesis in vitro.* Lab Invest, 1990. **63**(1): p. 115-22.

41. Humar, R., et al., *Hypoxia enhances vascular cell proliferation and angiogenesis in vitro via rapamycin (mTOR)-dependent signaling.* FASEB J, 2002. **16**(8): p. 771-80.

42. Kiefer, F.N., et al., *A versatile in vitro assay for investigating angiogenesis of the heart.* Exp Cell Res, 2004. **300**(2): p. 272-82.

43. Korff, T. and H.G. Augustin, *Integration of endothelial cells in multicellular spheroids prevents apoptosis and induces differentiation.* J Cell Biol, 1998. **143**(5): p. 1341-52.

44. Philippova, M., et al., *Atypical GPI-anchored T-cadherin stimulates angiogenesis in vitro and in vivo.* Arterioscler Thromb Vasc Biol, 2006. **26**(10): p. 2222-30.

45. Korff, T. and H.G. Augustin, *Tensional forces in fibrillar extracellular matrices control directional capillary sprouting.* J Cell Sci, 1999. **112 (Pt 19)**: p. 3249-58.

46. Le Brocq, M., et al., *Endothelial dysfunction: from molecular mechanisms to measurement, clinical implications, and therapeutic opportunities.* Antioxid Redox Signal, 2008. **10**(9): p. 1631-74.

47. Wallez, Y. and P. Huber, *Endothelial adherens and tight junctions in vascular homeostasis, inflammation and angiogenesis.* Biochim Biophys Acta, 2008. **1778**(3): p. 794-809.

48. Vanhoutte, P.M., *Endothelial dysfunction and atherosclerosis.* Eur Heart J, 1997. **18 Suppl E**: p. E19-29.

49. Dorovini-Zis, K., et al., *Formation of a barrier by brain microvessel endothelial cells in culture.* Fed Proc, 1987. **46**(8): p. 2521-2.

50. Rabiet, M.J., et al., *Thrombin-induced increase in endothelial permeability is associated with changes in cell-to-cell junction organization.* Arterioscler Thromb Vasc Biol, 1996. **16**(3): p. 488-96.

51. Del Vecchio, P.J., et al., *Endothelial monolayer permeability to macromolecules.* Fed Proc, 1987. **46**(8): p. 2511-5.

52. Bachetti, T. and L. Morbidelli, *Endothelial cells in culture: a model for studying vascular functions.* Pharmacol Res, 2000. **42**(1): p. 9-19.

53. Harris, E.S. and W.J. Nelson, *VE-cadherin: at the front, center, and sides of endothelial cell organization and function.* Curr Opin Cell Biol, 2010. **22**(5): p. 651-8.

54. Bazzoni, G. and E. Dejana, *Endothelial cell-to-cell junctions: molecular organization and role in vascular homeostasis.* Physiol Rev, 2004. **84**(3): p. 869-901.

55. Harris, T.J. and U. Tepass, *Adherens junctions: from molecules to morphogenesis.* Nat Rev Mol Cell Biol, 2010. **11**(7): p. 502-14.

56. Nyqvist, D., C. Giampietro, and E. Dejana, *Deciphering the functional role of endothelial junctions by using in vivo models.* EMBO Rep, 2008. **9**(8): p. 742-7.

57. Hewat, E.A., et al., *Architecture of the VE-cadherin hexamer.* J Mol Biol, 2007. **365**(3): p. 744-51.

58. Legrand, P., et al., *Self-assembly of the vascular endothelial cadherin ectodomain in a Ca2+-dependent hexameric structure.* J Biol Chem, 2001. **276**(5): p. 3581-8.

59. Chitaev, N.A. and S.M. Troyanovsky, *Adhesive but not lateral E-cadherin complexes require calcium and catenins for their formation.* J Cell Biol, 1998. **142**(3): p. 837-46.

60. Dejana, E., F. Orsenigo, and M.G. Lampugnani, *The role of adherens junctions and VE-cadherin in the control of vascular permeability.* J Cell Sci, 2008. **121**(Pt 13): p. 2115-22.

61. Esser, S., et al., *Vascular endothelial growth factor induces VE-cadherin tyrosine phosphorylation in endothelial cells.* J Cell Sci, 1998. **111 (Pt 13)**: p. 1853-65.

62. Lambeng, N., et al., *Vascular endothelial-cadherin tyrosine phosphorylation in angiogenic and quiescent adult tissues.* Circ Res, 2005. **96**(3): p. 384-91.

63. Morita, K., et al., *Endothelial claudin: claudin-5/TMVCF constitutes tight junction strands in endothelial cells.* J Cell Biol, 1999. **147**(1): p. 185-94.

64. Nitta, T., et al., *Size-selective loosening of the blood-brain barrier in claudin-5-deficient mice.* J Cell Biol, 2003. **161**(3): p. 653-60.

65. Hirase, T., et al., *Occludin as a possible determinant of tight junction permeability in endothelial cells.* J Cell Sci, 1997. **110 (Pt 14)**: p. 1603-13.

66. Liu, Y., et al., *Human junction adhesion molecule regulates tight junction resealing in epithelia.* J Cell Sci, 2000. **113 (Pt 13)**: p. 2363-74.

67. Martin-Padura, I., et al., *Junctional adhesion molecule, a novel member of the immunoglobulin superfamily that distributes at intercellular junctions and modulates monocyte transmigration.* J Cell Biol, 1998. **142**(1): p. 117-27.

68. Ostermann, G., et al., *JAM-1 is a ligand of the beta(2) integrin LFA-1 involved in transendothelial migration of leukocytes.* Nat Immunol, 2002. **3**(2): p. 151-8.

69. Cooke, V.G., M.U. Naik, and U.P. Naik, *Fibroblast growth factor-2 failed to induce angiogenesis in junctional adhesion molecule-A-deficient mice.* Arterioscler Thromb Vasc Biol, 2006. **26**(9): p. 2005-11.

70. Orlova, V.V., et al., *Junctional adhesion molecule-C regulates vascular endothelial permeability by modulating VE-cadherin-mediated cell-cell contacts.* J Exp Med, 2006. **203**(12): p. 2703-14.

71. Lamagna, C., et al., *Dual interaction of JAM-C with JAM-B and alpha(M)beta2 integrin: function in junctional complexes and leukocyte adhesion.* Mol Biol Cell, 2005. **16**(10): p. 4992-5003.

72. Hirata, K., et al., *Cloning of an immunoglobulin family adhesion molecule selectively expressed by endothelial cells.* J Biol Chem, 2001. **276**(19): p. 16223-31.

73. Ishida, T., et al., *Targeted disruption of endothelial cell-selective adhesion molecule inhibits angiogenic processes in vitro and in vivo.* J Biol Chem, 2003. **278**(36): p. 34598-604.

74. Wegmann, F., et al., *ESAM supports neutrophil extravasation, activation of Rho, and VEGF-induced vascular permeability.* J Exp Med, 2006. **203**(7): p. 1671-7.

75. Ogita, H. and Y. Takai, *Nectins and nectin-like molecules: roles in cell adhesion, polarization, movement, and proliferation.* IUBMB Life, 2006. **58**(5-6): p. 334-43.

76. Irie, K., et al., *Roles and modes of action of nectins in cell-cell adhesion.* Semin Cell Dev Biol, 2004. **15**(6): p. 643-56.

77. Reymond, N., et al., *DNAM-1 and PVR regulate monocyte migration through endothelial junctions.* J Exp Med, 2004. **199**(10): p. 1331-41.

78. Lopez, M., et al., *The human poliovirus receptor related 2 protein is a new hematopoietic/endothelial homophilic adhesion molecule.* Blood, 1998. **92**(12): p. 4602-11.

79. Nelson, P.J. and T.O. Daniel, *Emerging targets: molecular mechanisms of cell contact-mediated growth control.* Kidney Int, 2002. **61**(1 Suppl): p. S99-105.

80. Fagotto, F. and B.M. Gumbiner, *Cell contact-dependent signaling.* Dev Biol, 1996. **180**(2): p. 445-54.

81. Caveda, L., et al., *Inhibition of cultured cell growth by vascular endothelial cadherin (cadherin-5/VE-cadherin).* J Clin Invest, 1996. **98**(4): p. 886-93.

82. Grazia Lampugnani, M., et al., *Contact inhibition of VEGF-induced proliferation requires vascular endothelial cadherin, beta-catenin, and the phosphatase DEP-1/CD148.* J Cell Biol, 2003. **161**(4): p. 793-804.

83. Murakami, M., et al., *The FGF system has a key role in regulating vascular integrity.* J Clin Invest, 2008. **118**(10): p. 3355-66.

84. Presta, M., et al., *Fibroblast growth factor/fibroblast growth factor receptor system in angiogenesis.* Cytokine Growth Factor Rev, 2005. **16**(2): p. 159-78.

85. Fukuhara, S., et al., *Angiopoietin-1/Tie2 receptor signaling in vascular quiescence and angiogenesis.* Histol Histopathol, 2010. **25**(3): p. 387-96.

86. Saharinen, P., et al., *Angiopoietins assemble distinct Tie2 signalling complexes in endothelial cell-cell and cell-matrix contacts.* Nat Cell Biol, 2008. **10**(5): p. 527-37.

87. Zhang, J., et al., *Angiopoietin-1/Tie2 signal augments basal Notch signal controlling vascular quiescence by inducing delta-like 4 expression through AKT-mediated activation of beta-catenin.* J Biol Chem, 2011. **286**(10): p. 8055-66.

88. Fiedler, U. and H.G. Augustin, *Angiopoietins: a link between angiogenesis and inflammation.* Trends Immunol, 2006. **27**(12): p. 552-8.

89. Augustin, H.G., et al., *Control of vascular morphogenesis and homeostasis through the angiopoietin-Tie system.* Nat Rev Mol Cell Biol, 2009. **10**(3): p. 165-77.

90. Hartsock, A. and W.J. Nelson, *Adherens and tight junctions: structure, function and connections to the actin cytoskeleton.* Biochim Biophys Acta, 2008. **1778**(3): p. 660-9.

91. Bogatcheva, N.V. and A.D. Verin, *The role of cytoskeleton in the regulation of vascular endothelial barrier function.* Microvasc Res, 2008. **76**(3): p. 202-7.

92. Vandenbroucke, E., et al., *Regulation of endothelial junctional permeability.* Ann N Y Acad Sci, 2008. **1123**: p. 134-45.

93. Simionescu, N., M. Simionescu, and G.E. Palade, *Open junctions in the endothelium of the postcapillary venules of the diaphragm.* J Cell Biol, 1978. **79**(1): p. 27-44.

94. Hackett, P.H. and R.C. Roach, *High altitude cerebral edema.* High Alt Med Biol, 2004. **5**(2): p. 136-46.

95. Severinghaus, J.W., *Hypothesis: angiogenesis cytokines in high altitude cerebral oedema.* Acta Anaesthesiol Scand Suppl, 1995. **107**: p. 177-8.

96. Schoch, H.J., S. Fischer, and H.H. Marti, *Hypoxia-induced vascular endothelial growth factor expression causes vascular leakage in the brain.* Brain, 2002. **125**(Pt 11): p. 2549-57.

97. Pate, M., et al., *Endothelial cell biology: role in the inflammatory response.* Adv Clin Chem, 2010. **52**: p. 109-30.

98. Sander, M., B. Chavoshan, and R.G. Victor, *A large blood pressure-raising effect of nitric oxide synthase inhibition in humans.* Hypertension, 1999. **33**(4): p. 937-42.

99. Pollock, D.M., *Endothelin, angiotensin, and oxidative stress in hypertension.* Hypertension, 2005. **45**(4): p. 477-80.

100. Duran, W.N., J.W. Breslin, and F.A. Sanchez, *The NO cascade, eNOS location, and microvascular permeability.* Cardiovasc Res, 2010. **87**(2): p. 254-61.

101. Maugeri, N., et al., *Translational mini-review series on immunology of vascular disease: mechanisms of vascular inflammation and remodelling in systemic vasculitis.* Clin Exp Immunol, 2009. **156**(3): p. 395-404.

102. Brem, S., et al., *Prolonged tumor dormancy by prevention of neovascularization in the vitreous.* Cancer Res, 1976. **36**(8): p. 2807-12.

103. Holmgren, L., M.S. O'Reilly, and J. Folkman, *Dormancy of micrometastases: balanced proliferation and apoptosis in the presence of angiogenesis suppression.* Nat Med, 1995. **1**(2): p. 149-53.

104. Weis, S.M. and D.A. Cheresh, *Pathophysiological consequences of VEGF-induced vascular permeability.* Nature, 2005. **437**(7058): p. 497-504.

105. Goel, S., et al., *Normalization of the vasculature for treatment of cancer and other diseases.* Physiol Rev, 2011. **91**(3): p. 1071-121.

106. Harris, A.L., *Hypoxia--a key regulatory factor in tumour growth.* Nat Rev Cancer, 2002. **2**(1): p. 38-47.

107. Morikawa, S., et al., *Abnormalities in pericytes on blood vessels and endothelial sprouts in tumors.* Am J Pathol, 2002. **160**(3): p. 985-1000.

108. De Bock, K., et al., *Endothelial oxygen sensors regulate tumor vessel abnormalization by instructing phalanx endothelial cells.* J Mol Med (Berl), 2009. **87**(6): p. 561-9.

109. Hacohen, N., et al., *sprouty encodes a novel antagonist of FGF signaling that patterns apical branching of the Drosophila airways.* Cell, 1998. **92**(2): p. 253-63.

110. Casci, T., J. Vinos, and M. Freeman, *Sprouty, an intracellular inhibitor of Ras signaling.* Cell, 1999. **96**(5): p. 655-65.

111. Minowada, G., et al., *Vertebrate Sprouty genes are induced by FGF signaling and can cause chondrodysplasia when overexpressed.* Development, 1999. **126**(20): p. 4465-75.

112. de Maximy, A.A., et al., *Cloning and expression pattern of a mouse homologue of drosophila sprouty in the mouse embryo.* Mech Dev, 1999. **81**(1-2): p. 213-6.

113. Chambers, D., et al., *Differential display of genes expressed at the midbrain - hindbrain junction identifies sprouty2: an FGF8-inducible member of a family of intracellular FGF antagonists.* Mol Cell Neurosci, 2000. **15**(1): p. 22-35.

114. Tefft, J.D., et al., *Conserved function of mSpry-2, a murine homolog of Drosophila sprouty, which negatively modulates respiratory organogenesis.* Curr Biol, 1999. **9**(4): p. 219-22.

115. Furthauer, M., et al., *sprouty4 acts in vivo as a feedback-induced antagonist of FGF signaling in zebrafish.* Development, 2001. **128**(12): p. 2175-86.

116. Nutt, S.L., et al., *Xenopus Sprouty2 inhibits FGF-mediated gastrulation movements but does not affect mesoderm induction and patterning.* Genes Dev, 2001. **15**(9): p. 1152-66.

117. Gross, I., et al., *Mammalian sprouty proteins inhibit cell growth and differentiation by preventing ras activation.* J Biol Chem, 2001. **276**(49): p. 46460-8.

118. Yusoff, P., et al., *Sprouty2 inhibits the Ras/MAP kinase pathway by inhibiting the activation of Raf.* J Biol Chem, 2002. **277**(5): p. 3195-201.

119. Mason, J.M., et al., *Tyrosine phosphorylation of Sprouty proteins regulates their ability to inhibit growth factor signaling: a dual feedback loop.* Mol Biol Cell, 2004. **15**(5): p. 2176-88.

120. Hanafusa, H., et al., *Shp2, an SH2-containing protein-tyrosine phosphatase, positively regulates receptor tyrosine kinase signaling by dephosphorylating and inactivating the inhibitor Sprouty.* J Biol Chem, 2004. **279**(22): p. 22992-5.

121. Jarvis, L.A., et al., *Sprouty proteins are in vivo targets of Corkscrew/SHP-2 tyrosine phosphatases.* Development, 2006. **133**(6): p. 1133-42.

122. Li, X., et al., *FRS2-dependent SRC activation is required for fibroblast growth factor receptor-induced phosphorylation of Sprouty and suppression of ERK activity.* J Cell Sci, 2004. **117**(Pt 25): p. 6007-17.

123. Lim, J., et al., *Sprouty proteins are targeted to membrane ruffles upon growth factor receptor tyrosine kinase activation. Identification of a novel translocation domain.* J Biol Chem, 2000. **275**(42): p. 32837-45.

124. Lim, J., et al., *The cysteine-rich sprouty translocation domain targets mitogen-activated protein kinase inhibitory proteins to phosphatidylinositol 4,5-bisphosphate in plasma membranes.* Mol Cell Biol, 2002. **22**(22): p. 7953-66.

125. Yigzaw, Y., et al., *The C terminus of sprouty is important for modulation of cellular migration and proliferation.* J Biol Chem, 2001. **276**(25): p. 22742-7.

126. Hanafusa, H., et al., *Sprouty1 and Sprouty2 provide a control mechanism for the Ras/MAPK signalling pathway.* Nat Cell Biol, 2002. **4**(11): p. 850-8.

127. Guy, G.R., et al., *Sprouty proteins: modified modulators, matchmakers or missing links?* J Endocrinol, 2009. **203**(2): p. 191-202.

128. Sasaki, A., et al., *Identification of a dominant negative mutant of Sprouty that potentiates fibroblast growth factor- but not epidermal growth factor-induced ERK activation.* J Biol Chem, 2001. **276**(39): p. 36804-8.

129. Rubin, C., et al., *Phosphorylation of carboxyl-terminal tyrosines modulates the specificity of Sprouty-2 inhibition of different signaling pathways.* J Biol Chem, 2005. **280**(10): p. 9735-44.

130. Lao, D.H., et al., *Direct binding of PP2A to Sprouty2 and phosphorylation changes are a prerequisite for ERK inhibition downstream of fibroblast growth factor receptor stimulation.* J Biol Chem, 2007. **282**(12): p. 9117-26.

131. Lao, D.H., et al., *A Src homology 3-binding sequence on the C terminus of Sprouty2 is necessary for inhibition of the Ras/ERK pathway downstream of fibroblast growth factor receptor stimulation.* J Biol Chem, 2006. **281**(40): p. 29993-30000.

132. Martinez, N., et al., *Sprouty2 binds Grb2 at two different proline-rich regions, and the mechanism of ERK inhibition is independent of this interaction.* Cell Signal, 2007. **19**(11): p. 2277-85.

133. Ozaki, K., et al., *Efficient suppression of FGF-2-induced ERK activation by the cooperative interaction among mammalian Sprouty isoforms.* J Cell Sci, 2005. **118**(Pt 24): p. 5861-71.

134. Abe, M. and M.C. Naski, *Regulation of sprouty expression by PLCgamma and calcium-dependent signals.* Biochem Biophys Res Commun, 2004. **323**(3): p. 1040-7.

135. Rubin, C., et al., *Sprouty fine-tunes EGF signaling through interlinked positive and negative feedback loops.* Curr Biol, 2003. **13**(4): p. 297-307.

136. Wong, E.S., et al., *Sprouty2 attenuates epidermal growth factor receptor ubiquitylation and endocytosis, and consequently enhances Ras/ERK signalling.* EMBO J, 2002. **21**(18): p. 4796-808.

137. Egan, J.E., et al., *The bimodal regulation of epidermal growth factor signaling by human Sprouty proteins.* Proc Natl Acad Sci U S A, 2002. **99**(9): p. 6041-6.

138. Haglund, K., et al., *Sprouty2 acts at the Cbl/CIN85 interface to inhibit epidermal growth factor receptor downregulation.* EMBO Rep, 2005. **6**(7): p. 635-41.

139. Kim, H.J., L.J. Taylor, and D. Bar-Sagi, *Spatial regulation of EGFR signaling by Sprouty2.* Curr Biol, 2007. **17**(5): p. 455-61.

140. Takahashi, T., et al., *A single autophosphorylation site on KDR/Flk-1 is essential for VEGF-A-dependent activation of PLC-gamma and DNA synthesis in vascular endothelial cells.* EMBO J, 2001. **20**(11): p. 2768-78.

141. Coultas, L., K. Chawengsaksophak, and J. Rossant, *Endothelial cells and VEGF in vascular development.* Nature, 2005. **438**(7070): p. 937-45.

142. Sasaki, A., et al., *Mammalian Sprouty4 suppresses Ras-independent ERK activation by binding to Raf1.* Nat Cell Biol, 2003. **5**(5): p. 427-32.

143. Ding, W., et al., *Sprouty2 downregulation plays a pivotal role in mediating crosstalk between TGF-beta1 signaling and EGF as well as FGF receptor tyrosine kinase-ERK pathways in mesenchymal cells.* J Cell Physiol, 2007. **212**(3): p. 796-806.

144. Ding, W. and D. Warburton, *Down-regulation of Sprouty2 via p38 MAPK plays a key role in the induction of cellular apoptosis by tumor necrosis factor-alpha.* Biochem Biophys Res Commun, 2008. **375**(3): p. 460-4.

145. Anderson, K., et al., *Regulation of cellular levels of Sprouty2 protein by prolyl hydroxylase domain and von Hippel-Lindau proteins.* J Biol Chem, 2011. **286**(49): p. 42027-36.

146. Glienke, J., et al., *Differential gene expression by endothelial cells in distinct angiogenic states.* Eur J Biochem, 2000. **267**(9): p. 2820-30.

147. Lee, S.H., et al., *Inhibition of angiogenesis by a mouse sprouty protein.* J Biol Chem, 2001. **276**(6): p. 4128-33.

148. Paik, J.H., et al., *FoxOs are lineage-restricted redundant tumor suppressors and regulate endothelial cell homeostasis.* Cell, 2007. **128**(2): p. 309-23.

149. Zhang, C., et al., *Regulation of vascular smooth muscle cell proliferation and migration by human sprouty 2.* Arterioscler Thromb Vasc Biol, 2005. **25**(3): p. 533-8.

150. Taniguchi, K., et al., *Suppression of Sproutys has a therapeutic effect for a mouse model of ischemia by enhancing angiogenesis.* PLoS One, 2009. **4**(5): p. e5467.

151. Shim, K., et al., *Sprouty2, a mouse deafness gene, regulates cell fate decisions in the auditory sensory epithelium by antagonizing FGF signaling.* Dev Cell, 2005. **8**(4): p. 553-64.

152. Taketomi, T., et al., *Loss of mammalian Sprouty2 leads to enteric neuronal hyperplasia and esophageal achalasia.* Nat Neurosci, 2005. **8**(7): p. 855-7.

153. Matsumura, K., et al., *Sprouty2 controls proliferation of palate mesenchymal cells via fibroblast growth factor signaling.* Biochem Biophys Res Commun, 2011. **404**(4): p. 1076-82.

154. Klein, O.D., et al., *Sprouty genes control diastema tooth development via bidirectional antagonism of epithelial-mesenchymal FGF signaling.* Dev Cell, 2006. **11**(2): p. 181-90.

155. Peterkova, R., et al., *Revitalization of a diastemal tooth primordium in Spry2 null mice results from increased proliferation and decreased apoptosis.* J Exp Zool B Mol Dev Evol, 2009. **312B**(4): p. 292-308.

156. Miyamoto, R., et al., *Loss of Sprouty2 partially rescues renal hypoplasia and stomach hypoganglionosis but not intestinal aganglionosis in Ret Y1062F mutant mice.* Dev Biol, 2011. **349**(2): p. 160-8.

157. Cabrita, M.A., et al., *A functional interaction between sprouty proteins and caveolin-1.* J Biol Chem, 2006. **281**(39): p. 29201-12.

158. Metzen, E., et al., *Pericellular PO2 and O2 consumption in monolayer cell cultures.* Respir Physiol, 1995. **100**(2): p. 101-6.

159. Brunet, A., et al., *Akt promotes cell survival by phosphorylating and inhibiting a Forkhead transcription factor.* Cell, 1999. **96**(6): p. 857-68.

160. Aird, W.C., *The role of the endothelium in severe sepsis and multiple organ dysfunction syndrome.* Blood, 2003. **101**(10): p. 3765-77.

161. Seybold, J., et al., *Tumor necrosis factor-alpha-dependent expression of phosphodiesterase 2: role in endothelial hyperpermeability.* Blood, 2005. **105**(9): p. 3569-76.

162. Schnittler, H.J., B. Puschel, and D. Drenckhahn, *Role of cadherins and plakoglobin in interendothelial adhesion under resting conditions and shear stress.* Am J Physiol, 1997. **273**(5 Pt 2): p. H2396-405.

163. Lampugnani, M.G., et al., *The molecular organization of endothelial cell to cell junctions: differential association of plakoglobin, beta-catenin, and alpha-catenin with vascular endothelial cadherin (VE-cadherin).* J Cell Biol, 1995. **129**(1): p. 203-17.

164. Gotsch, U., et al., *VE-cadherin antibody accelerates neutrophil recruitment in vivo.* J Cell Sci, 1997. **110 (Pt 5)**: p. 583-8.

165. Yeh, W.L., et al., *Inhibition of hypoxia-induced increase of blood-brain barrier permeability by YC-1 through the antagonism of HIF-1alpha accumulation and VEGF expression.* Mol Pharmacol, 2007. **72**(2): p. 440-9.

166. Harten, S.K., et al., *Regulation of renal epithelial tight junctions by the von Hippel-Lindau tumor suppressor gene involves occludin and claudin 1 and is independent of E-cadherin.* Mol Biol Cell, 2009. **20**(3): p. 1089-101.

167. Fong, G.H., *Mechanisms of adaptive angiogenesis to tissue hypoxia.* Angiogenesis, 2008. **11**(2): p. 121-40.

168. Carmeliet, P., *Angiogenesis in health and disease.* Nat Med, 2003. **9**(6): p. 653-60.

169. Carmeliet, P. and R.K. Jain, *Angiogenesis in cancer and other diseases.* Nature, 2000. **407**(6801): p. 249-57.

170. Fong, C.W., et al., *Tyrosine phosphorylation of Sprouty2 enhances its interaction with c-Cbl and is crucial for its function.* J Biol Chem, 2003. **278**(35): p. 33456-64.

171. Kajita, M., et al., *Regulation of platelet-derived growth factor-induced Ras signaling by poliovirus receptor Necl-5 and negative growth regulator Sprouty2.* Genes Cells, 2007. **12**(3): p. 345-57.

172. Swat, A., et al., *Cell density-dependent inhibition of epidermal growth factor receptor signaling by p38alpha mitogen-activated protein kinase via Sprouty2 downregulation.* Mol Cell Biol, 2009. **29**(12): p. 3332-43.

173. Lo, T.L., et al., *The ras/mitogen-activated protein kinase pathway inhibitor and likely tumor suppressor proteins, sprouty 1 and sprouty 2 are deregulated in breast cancer.* Cancer Res, 2004. **64**(17): p. 6127-36.

174. McKie, A.B., et al., *Epigenetic inactivation of the human sprouty2 (hSPRY2) homologue in prostate cancer.* Oncogene, 2005. **24**(13): p. 2166-74.

175. Pinsky, D.J., et al., *Hypoxia and modification of the endothelium: implications for regulation of vascular homeostatic properties.* Semin Cell Biol, 1995. **6**(5): p. 283-94.

176. Yan, S.F., et al., *Hypoxia-induced modulation of endothelial cell properties: regulation of barrier function and expression of interleukin-6.* Kidney Int, 1997. **51**(2): p. 419-25.

177. Dejana, E., et al., *Organization and signaling of endothelial cell-to-cell junctions in various regions of the blood and lymphatic vascular trees.* Cell Tissue Res, 2009. **335**(1): p. 17-25.

178. Nelson, C.M., et al., *Emergent patterns of growth controlled by multicellular form and mechanics.* Proc Natl Acad Sci U S A, 2005. **102**(33): p. 11594-9.

179. Taddei, A., et al., *Endothelial adherens junctions control tight junctions by VE-cadherin-mediated upregulation of claudin-5.* Nat Cell Biol, 2008. **10**(8): p. 923-34.

180. Zhang, X., et al., *Phosphorylation of serine 256 suppresses transactivation by FKHR (FOXO1) by multiple mechanisms. Direct and indirect effects on nuclear/cytoplasmic shuttling and DNA binding.* J Biol Chem, 2002. **277**(47): p. 45276-84.

181. Dejana, E., A. Taddei, and A.M. Randi, *Foxs and Ets in the transcriptional regulation of endothelial cell differentiation and angiogenesis.* Biochim Biophys Acta, 2007. **1775**(2): p. 298-312.

182. Dickman, K.G. and L.J. Mandel, *Glycolytic and oxidative metabolism in primary renal proximal tubule cultures.* Am J Physiol, 1989. **257**(2 Pt 1): p. C333-40.

183. Webster, K.A., *Regulation of glycolytic enzyme RNA transcriptional rates by oxygen availability in skeletal muscle cells.* Mol Cell Biochem, 1987. **77**(1): p. 19-28.

184. Semenza, G.L., et al., *Transcriptional regulation of genes encoding glycolytic enzymes by hypoxia-inducible factor 1.* J Biol Chem, 1994. **269**(38): p. 23757-63.

185. Holzer, C. and P. Maier, *Maintenance of periportal and pericentral oxygen tensions in primary rat hepatocyte cultures: influence on cellular DNA and protein content monitored by flow cytometry.* J Cell Physiol, 1987. **133**(2): p. 297-304.

186. Balin, A.K., A.J. Fisher, and D.M. Carter, *Oxygen modulates growth of human cells at physiologic partial pressures.* J Exp Med, 1984. **160**(1): p. 152-66.

187. Green, S.L., R.A. Freiberg, and A.J. Giaccia, *p21(Cip1) and p27(Kip1) regulate cell cycle reentry after hypoxic stress but are not necessary for hypoxia-induced arrest.* Mol Cell Biol, 2001. **21**(4): p. 1196-206.

188. Li, W., et al., *Hypoxia-induced endothelial proliferation requires both mTORC1 and mTORC2.* Circ Res, 2007. **100**(1): p. 79-87.

189. Hickey, M.M. and M.C. Simon, *Regulation of angiogenesis by hypoxia and hypoxia-inducible factors.* Curr Top Dev Biol, 2006. **76**: p. 217-57.

190. Ozaki, K., et al., *ERK pathway positively regulates the expression of Sprouty genes.* Biochem Biophys Res Commun, 2001. **285**(5): p. 1084-8.

191. Jiang, Z.L., et al., *Fibroblast growth factor-2 regulation of Sprouty and NR4A genes in bovine ovarian granulosa cells.* J Cell Physiol, 2011. **226**(7): p. 1820-7.

192. Folkman, J., et al., *Isolation of a tumor factor responsible for angiogenesis.* J Exp Med, 1971. **133**(2): p. 275-88.

193. Tille, J.C., et al., *Vascular endothelial growth factor (VEGF) receptor-2 antagonists inhibit VEGF- and basic fibroblast growth factor-induced angiogenesis in vivo and in vitro.* J Pharmacol Exp Ther, 2001. **299**(3): p. 1073-85.

194. Seghezzi, G., et al., *Fibroblast growth factor-2 (FGF-2) induces vascular endothelial growth factor (VEGF) expression in the endothelial cells of forming capillaries: an autocrine mechanism contributing to angiogenesis.* J Cell Biol, 1998. **141**(7): p. 1659-73.

195. Lee, S., et al., *Autocrine VEGF signaling is required for vascular homeostasis.* Cell, 2007. **130**(4): p. 691-703.

196. Fong, G.H., *Regulation of angiogenesis by oxygen sensing mechanisms.* J Mol Med (Berl), 2009. **87**(6): p. 549-60.

197. Ozawa, C.R., et al., *Microenvironmental VEGF concentration, not total dose, determines a threshold between normal and aberrant angiogenesis.* J Clin Invest, 2004. **113**(4): p. 516-27.

198. Meij, J.T., et al., *Exacerbation of myocardial injury in transgenic mice overexpressing FGF-2 is T cell dependent.* Am J Physiol Heart Circ Physiol, 2002. **282**(2): p. H547-55.

199. Gudbjornsson, B., R. Christofferson, and A. Larsson, *Synovial concentrations of the angiogenic peptides bFGF and VEGF do not discriminate rheumatoid arthritis from other forms of inflammatory arthritis.* Scand J Clin Lab Invest, 2004. **64**(1): p. 9-15.

200. Kanazawa, S., et al., *VEGF, basic-FGF, and TGF-beta in Crohn's disease and ulcerative colitis: a novel mechanism of chronic intestinal inflammation.* Am J Gastroenterol, 2001. **96**(3): p. 822-8.

201. Carmeliet, P. and R.K. Jain, *Principles and mechanisms of vessel normalization for cancer and other angiogenic diseases.* Nat Rev Drug Discov, 2011. **10**(6): p. 417-27.

11 ABBREVIATIONS

AJ = Adherens Junction
ANG2 = Angiotensin 2
BBB = Blood Brain Barrier
C = Confluent
CBL = Casitas B-lineage Lymphoma proto-oncogene product
CO_2 = Carbon Dioxide
CRD = Cysteine-Rich Domain
DAG = Diacylglycerol
DLL4 = Delta like ligand 4
DMEM = Dulbecco's Minimal Essential Medium
DSPRY = Drosophila Sprouty
EC = Endothelial Cell
EGF = Epidermal Growth Factor
EGFR = Epidermal Growth Factor Receptor
EGTA = Ethylene Glycol Tetraacetic Acid
EMT = Epithelial-to-Mesenchymal Transition
eNOS = Endothelial Nitric Oxide Synthase
ERK1/2 = Extracellular signal-Regulated Kinase 1/2
ESAM = Endothelial cell Selective Adhesion Molecule
FCS = Fetal Calf Serum
FGF = Fibroblast Growth Factor
FGFR = Fibroblast Growth Factor Receptor
GDNF = Glial-Derived Growth Factor
GRB2 = Growth factor Receptor-Bound protein 2
HACE = High Altitude Cerebral Edema
HIF-1α = Hypoxia inducible Factor alpha
HMVEC = Human Microvascular Endothelial Cell
HRE = Hypoxia Response Element
HT = Human Thrombin
HUVEC = Human Umbilical Endothelial Cell
IL-1 = Interleukin-1

IP_3 = Inositol (1,4,5)-Trisphosphate
JAM-A = Junctional Adhesion Molecule A
KO = knockout
LDL = Low-Density Lipoprotein
MAEC = Mouse Aortic Endothelial Cell
MAPK = Mitogen-Activated Protein Kinase
MEK = MAPK and ERK kinase
MLC = Myosin light chain
MLCK = Myosin light chain kinase
MMP = Matrix Metalloproteinases
NO = Nitric Oxide
NOS = Nitric Oxide Synthase
O_2 = Oxygen
PC = Pericyte
PDGF = Platelet-Derived Growth Factor
PHD = Prolyl Hydroxylase Domain-containing protein
PIGF = Placental Growth Factor
PIP_2 = Phosphatidylinositol (4,5)-Bisphosphate
PI3K = Phosphatidylinositol-3-kinase
PKA = Protein Kinase A
PKC = Protein Kinase C
PLCγ = Phospholipase C gamma
PP2A = Protein Phosphatase 2A
PVC = Perivascular Cell
p44/p42 = ERK1/2
RBD = Raf1-Binding Domain
RHOA = Rho kinase A
ROCK = RhoA kinase
RTK = Receptor Tyrosine Kinase
SC = Sub Confluent
Ser = Serine
SHP2 = SH2-domain containing protein tyrosine Phosphatase 2
SIAH2 = Seven-In-Absentia Homolog 2
SOS1 = Son of Sevenless 1

SP = Sparse

SPRY2 = Sprouty2

TGFβ = Tumor Growth Factor beta

Thr = Threonine

TJ = Tight Junction

TNFα = Tumor Necrosis Factor alpha

VEGF = Vascular Endothelial Growth Factor

VEGFR = Vascular Endothelial Growth Factor Receptor

VHL = von Hippel-Lindau protein

VSMC = vascular smooth muscle cell

(Y) = Tyrosine

ZO-1 = Zonula Occludens 1 (Tight junction protein 1)

12 CURRICULUM VITAE

CONTACT INFORMATION

Name: Peier Martin Anton

Address: Division of Internal Medicine
University Hospital Zürich
Gloriastrasse 30
8091 Zürich

Phone: +41 44 634 56 02

E-mail: martin.peier@usz.ch

PERSONAL INFORMATION

Date of Birth: September 25th, 1983

Place of Birth: Bern

Nationality: Swiss

Sex: male

PROFESSIONAL EXPERIENCE

2007 – 2012 Ph.D. Thesis in the group of Prof. Edouard Battegay, Division of Internal Medicine, University Hospital Zurich, Switzerland, Title: “Sprouty2 expression controls endothelial monolayer integrity and quiescence”

2005-2007 Master thesis in the group of Prof. Thomas Seebeck, Institute of Cell Biology, University of Bern, Switzerland, Title: “The regulatory subunit of *trypanosomal PKA* “.

2002-2005 Internships in Immunology, Biochemistry, Molecular Biology, Molecular Parasitology, Microscopy and Bioinformatics, University of Bern

EDUCATION

2005-2006 University of Bern, Master Studies in Cell Biology
Degree: Master in Biology

2002-2005 University of Bern, Undergraduate studies in Biology
Degree: Vordiplom

1995-2002 Gymnasium Burgdorf
Degree: Kantonale Maturität, Major: Biology and Chemistry

LANGUAGE SKILLS

German	(native language)
English	(working language)
French	(basic skills)

COMPUTER SKILLS

MS Office (Word, Excel, Power-Point), Adobe Acrobat, Adobe Photoshop, Adobe Illustrator, EndNote, ImageJ, GraphPad Prism

ADDITIONAL COURSES

Scientific Writing, E-Science and Web publishing

AWARDS DURING THE PhD

2011 1st poster prize at the 7th ***ZIHP*** Symposium in Zürich

PUBLICATIONS

Martin Peier, Thomas Walpen, Gerhard Christofori, Edouard Battegay, Rok Humar. Sprouty2 expression controls endothelial monolayer integrity and quiescence. In revision, Angiogenesis 2012.

Thomas Walpen, Martin Peier, Elvira Haas, Ina Kalus, Jürg Schwaller, Edouard Battegay, Rok Humar. Loss of Pim1 imposes a hyperadhesive phenotype on endothelial cells. Cell Physiol Biochem 2012;30:1083-1096.